M o n o g r a p h

urn:lsid:zoobank.org:pub:8009DD3B-53B0-45C9-921E-58D04C9C0B48

New species, revision, and phylogeny of *Ronzotherium* Aymard, 1854 (Perissodactyla, Rhinocerotidae)

Jérémy TISSIER [1,*], Pierre-Olivier ANTOINE [2] & Damien BECKER [3]

[1,3] Route de Fontenais 21, JURASSICA Museum, 2900 Porrentruy, Switzerland & Chemin du musée 4, Université de Fribourg, Department of Geosciences, 1700 Fribourg, Switzerland.
[2] Place Eugène Bataillon, Institut des sciences de l'évolution de Montpellier-CNRS-IRD-RPHE, Université de Montpellier, 34095 Montpellier, France.

*Corresponding author: jeremy.tissier123@gmail.com
[2] Email: pierre-olivier.antoine@umontpellier.fr
[3] Email: damien.becker@jurassica.ch

[1] urn:lsid:zoobank.org:author:7418361D-FAA0-4D7D-AE4A-80B5C9288B31
[2] urn:lsid:zoobank.org:author:61FBD377-963B-4530-A4BC-0AB4CBCAD967
[3] urn:lsid:zoobank.org:author:E1D8E6B2-6F92-4B0B-A772-4F5C561851DB

Abstract. *Ronzotherium* is one of the earliest Rhinocerotidae in Europe, which first appeared just after the Eocene/Oligocene transition (Grande Coupure), and became extinct at the end of the Oligocene. It is a large-sized rhinocerotid, with a special position in the phylogeny of this group, as being one of the earliest-branching true Rhinocerotidae. However, its intra-generic systematics has never been tested through computational phylogenetic methods and it is basically unknown. Its taxonomical history has gone through numerous complications, and thus we aim to provide here a complete revision of this genus, through phylogenetic methods. After a re-examination of all type specimens (five supposed species) as well as of most well-preserved specimens from all over Europe and ranging through the complete Oligocene epoch, we performed a parsimony analysis to test the position of some problematic specimens. According to our results, five species can be distinguished, *Ronzotherium velaunum* (type species), *R. filholi*, *R. elongatum* and *R. romani* as well as a new species: *R. heissigi* sp. nov. We also drastically re-interpret its anatomy and show that the 'short-limbed' "*Diaceratherium*" *massiliae*, described from Southern France, can be considered as a junior synonym of *R. romani*. Finally, we exclude the Asian species "*Ronzotherium*" *orientale* and "*Ronzotherium*" *brevirostre* from *Ronzotherium* and we consider *R. kochi* as a junior synonym of *R. filholi*.

Keywords. Europe, taxonomy, Oligocene, Grande Coupure, phylogeny.

Introduction

The genus *Ronzotherium* Aymard, 1854 is the most typical rhinocerotoid in the Oligocene of Europe. It was a hornless, medium- to large-sized rhinoceros, that notably appeared during the Grande Coupure

event, and survived until the latest Oligocene (Heissig 1969; Brunet 1979). The Grande Coupure event, first termed by Stehlin (1909), refers to an extinction and possibly migration-related event, occurring just after the Eocene/Oligocene boundary in Western Europe. *Ronzotherium* is one of the markers of this event, as one of the earliest European rhinocerotids, along with *Epiaceratherium* Abel, 1910 (Brunet 1979; Uhlig 1999a, 1999b; Becker 2009). It is also of particular interest for the evolution of the Rhinocerotidae because of its systematic position as one of the earliest-branching rhinocerotids (e.g., Cerdeño 1995), and shows some relatively primitive characters compared with more derived rhinocerotids such as the presence of two well-developed upper incisors, and very poorly molarised premolars (Brunet 1979).

Regrettably, the taxonomical history of this genus is quite confused, and it remains a poorly studied taxon, despite its phylogenetic and biogeographical significance. The genus *Ronzotherium* was first named after the hill of Ronzon by the French paleontologist Aymard in 1854, from material found in his hometown of Le Puy-en-Velay, which gave its name to *R. velaunum* (Aymard in Pictet, 1853). This locality of Ronzon is significant for the study of Western European Oligocene faunas because it has been dated from MP21 (earliest Oligocene) and is very rich, preserving numerous vertebrate and invertebrate taxa. Yet, it was Filhol (1881) who first illustrated and described most of the mammalian taxa from Ronzon, including *R. velaunum*, almost 30 years after its first mention. This probably explains why no new material was attributed to this genus until Osborn (1900) wrongly referred a lower jaw from Brons (Cantal, France) to *Ronzotherium gaudryi* Osborn, 1900. This species is now attributed to the genus *Eggysodon* Roman, 1910 (Rhinocerotoidea, Eggysodontidae Breuning, 1923), like several others that have also been erroneously attributed to *Ronzotherium* such as *Eggysodon osborni* (Schlosser, 1902) or *Eggysodon reichenaui* (Deninger, 1903), notably because of the presence of upper and lower canines. Because of these complications and the absence of explicit definition of *Ronzotherium* by Aymard (1854), Roman (1912a) advocated that the name "*Ronzotherium*" should be forgotten and replaced by *Aceratherium*, but the name nonetheless persisted.

By complete chance, Osborn (1900) also named in the same publication a new species *Acerotherium filholi* Osborn, 1900 based on material from the Phosphorites du Quercy, it now indeed belongs to *Ronzotherium*. Later, this species was also discovered in several localities of Switzerland (Stehlin 1903; Jenny 1905) and France (Roman 1912a), although it was also confused with *Diaceratherium* (e.g., Roman 1912a: pl. V figs 4–5, even though Roman admitted his doubts on this attribution).

Almost thirty years after the work of Roman (1912a), the Hungarian palaeontologist Miklós Kretzoi dedicated him a new species, *Ronzotherium romani* Kretzoi, 1940, based on his illustration of a lower incisor from La Ferté-Alais (Roman 1912a: fig. 17). Even though this species was only named in a footnote of the paper (Kretzoi 1940), without either a proper diagnosis or direct observation, the species remained valid and was accepted by subsequent authors. In particular, several specimens were attributed to this taxon by Heissig (1969), after an almost exhaustive revision of this genus.

In that work, Heissig considered *R. romani* as a subspecies of *R. filholi*, along with a new subspecies, *Ronzotherium filholi elongatum* Heissig, 1969. This large-scale work brought a significant clarification of the genus *Ronzotherium* by identifying numerous specimens and delivered the first and only (handmade) phylogenetic representation of this genus. Yet, this revision remained incomplete, since only dental and mandibular remains were considered. Ten years later, Brunet (1979) also conducted a large-scale revision of this genus in his PhD thesis, focusing on the material from Villebramar (France), which delivered numerous specimens of *R. filholi*, including one well-preserved skull (the third only known for this genus to have ever been described). Based on his observations, he refuted the existence of *R. elongatum* that he considered a junior synonym of *R. filholi* and he reconsidered *R. romani* as a species. Contrary to Heissig (1969), Brunet (1979) considered the evolution of *Ronzotherium* as fully

anagenetic: *R. velaunum* evolved into *R. filholi*, which evolved into *R. romani*. However, this hypothesis is not based on any phylogenetic evidence, and is only supported by stratigraphy, following a then-popular model of phyletic gradualism.

Finally, even though *Ronzotherium* is mostly a Western European taxon, several non-Western European species have been attributed to this genus, notably *Ronzotherium kochi* Kretzoi, 1940 from Romania or *Ronzotherium brevirostre* (Beliayeva, 1954) from Mongolia (Dashzeveg 1991; = "*R.*" *orientale* according to Antoine *et al*. 2003). However, they have only been partly revised, and remain very poorly known.

Thus, we propose here a quasi-exhaustive revision of this genus, aiming at elucidating its systematics by using methods of computational phylogenetics, at the population level. Using populations (i.e., ronzothere remains from a single locality) helps understanding the evolutionary history of the genus by taking into consideration the type morphology, as well as the intraspecific variability. After considering this variability, we tested the position of this genus within a larger-scale phylogeny.

Our results, based on direct observation of every type and most major localities of *Ronzotherium* permit us to re-identify several specimens, and they support the validity of five Western European species: the type species *Ronzotherium velaunum* (Aymard in Pictet, 1853), *Ronzotherium filholi* (Osborn, 1900), *Ronzotherium romani* Kretzoi, 1940, *Ronzotherium elongatum* Heissig, 1969 and *Ronzotherium heissigi* sp. nov. Based on the phylogenetic results, each species can now be properly diagnosed and described. This complete revision allows us to discuss the evolution of *Ronzotherium* altogether, and we suggest that cingulum may have played a central role in the persistence of *R. romani* until the end of the Oligocene epoch. We also tentatively investigate the relation between age, geography, and body mass, and suggest that there is no correlation between the evolution of the body mass and these parameters.

Material and methods

Institutional abbreviations

The specimens discussed in this study are deposited in the following institutions:

AIX = Muséum d'histoire naturelle d'Aix-en-Provence (France)
BSPG = Bayerische Staatssammlung für Paläontologie und Geologie, Munich (Germany)
FSL = Collections de la Faculté des Sciences de Lyon (France)
MBT = Muzeul de Paleontologie-Stratigrafie, Universitatea Babeș-Bolyai, Cluj-Napoca (Romania)
MGL = Musée cantonal de géologie de Lausanne (Switzerland)
MHNB41 = Muséum d'histoire naturelle de Blois (France)
MHNM = Muséum d'histoire naturelle de Marseille (France)
MNHN = Muséum national d'histoire naturelle, Paris (France)
MJSN = Jurassica Museum of Porrentruy (Switzerland)
NMB = Naturhistorisches Museum Basel (Switzerland)
NMBE = Naturhistorisches Museum der Burgergemeinde Bern (Switzerland)
NMO = Naturmuseum Olten (Switzerland)
SMNS = Staatliches Museum für Naturkunde Stuttgart (Germany)
PUY = Musée Crozatier, Le Puy-en-Velay (France)
TLM = Muséum d'histoire naturelle de Toulouse (France)
UM = Université de Montpellier (France)

Surface scanning

Numerous specimens were scanned with a structured-light surface scanner (Artec Space Spider, Artec Group) and the 3D models have been reconstructed using the Artec Studio 13 Professional software.

Some of these 3D models are presented in the figures of this study, with texture (e.g., Fig. 3A), or without (e.g., Fig. 3B–D). In most cases, representing 3D models without the texture enhances the contrast and shadows to distinguish articulation surfaces.

Anatomy and anatomical abbreviations

The characters described follow the terminology of Antoine (2002). The estimation of the body mass follows the equations for Rhinocerotidae of Fortelius & Kappelman (1993: appendix 1) based on cranial, dental, humeral, radial, femoral and tibial measurements, as well as the best predictors for the equation of Tsubamoto (2014) based on astragalar measurements: Li1, Ar1 and Ar3.

Dental abbreviations

Cc   = calcaneus
d/D = lower/upper decidual tooth
i/I   = lower/upper incisor
m/M = lower/upper molar
Mc   = metacarpal
Mt   = metatarsal
p/P   = lower/upper premolar

Dental measurements are provided in Supp. file 1, and postcranial measurements are provided in Supp. file 2, for all species of *Ronzotherium*.

Phylogeny

The taxonomical sampling includes all the specimens from the type localities of Ronzon for *Ronzotherium velaunum* and La Ferté-Alais for *R. romani* as well as the holotype and 'cotype' of *R. filholi* designated by Osborn (1900) from the Phosphorites du Quercy, the holotype of *R. kochi* from Cluj-Napoca and the holotype of *R. filholi elongatum* from Pernes. The species "*R.*" *brevirostre* (= "*R.*" *orientale* according to Antoine *et al*. 2003) was excluded from the analysis because of the very scarce remains preserved (only a few fragmentary lower jaws are known). From the few observable characters and their dimensions, we suggest that this species should be excluded from *Ronzotherium* (presence of well-developed i1, of an isolated entoconid on p3–4 and of a keel below the symphysis in specimens illustrated by Dashzeveg 1991).

The other ronzothere terminals were chosen according to the completeness of the remains, and to their age, to represent as much as possible the morphological diversity through time. Therefore, we included specimens from Kleinblauen (MP21; Switzerland), Villebramar (MP22; France), Vendèze (MP24, France), Poillat (MP24, Switzerland), Bumbach (MP25, Switzerland), St-Henri/St-André/Les-Milles (= 'Marseille'; MP26, France), Gaimersheim (MP27, Germany), Rickenbach (MP29, Switzerland) as well as Lamothe-Capdeville (late early Oligocene, France) and 'Auvergne' (early Oligocene, France).

To test the monophyly of *Ronzotherium* and to understand its systematic position within the early Rhinocerotidae, we included a branching group (see Antoine 2002), comprising some of the earliest known Rhinocerotidae: the Late Eocene North American taxa *Teletaceras radinskyi* Hanson, 1989, *Penetrigonias dakotensis* (Peterson, 1920), *Trigonias osborni* Lucas, 1900 and representatives of *Epiaceratherium* Abel, 1910, comprising the Asian *E. naduongense* Böhme, Aiglstorfer, Antoine, Appel, Havlik, Métais, Laq, Schneider, Setzer, Tappert, Dang, Uhl & Prieto, 2013 and the European *E. bolcense* Abel, 1910, *E. magnum* Uhlig, 1999 and *E. delemontense* (Becker & Antoine, 2013), according to Tissier *et al.* (2020). We also included rhinocerotids ranging from the Oligocene to the earliest Miocene: *Molassitherium albigense* (Roman, 1912), *Mesaceratherium gaimersheimense* Heissig, 1969, *M. welcommi* Antoine & Downing, 2010 and *M. paulhiacense* (Richard, 1937), *Pleuroceros pleuroceros* (Duvernoy, 1853) and *P. blanfordi* Lydekker, 1884, *Protaceratherium minutum* Abel, 1910, *Subhyracodon occidentalis* (Leidy, 1850), *Diceratherium armatum* Marsh, 1875 and *Diaceratherium tomerdingense* Dietrich, 1931. Finally, we used *Uintaceras radinskyi* Holbrook & Lucas, 1997 from the late Middle Eocene of North America as outgroup of our study, because it is either considered as the

closest sister group to Rhinocerotidae (Prothero 2005), or as belonging to another rhinocerotoid family (Wang *et al.* 2016; Tissier *et al.* 2018).

The characters matrix is based on the matrix from Antoine (2002), and is provided in Supp. file 3. All characters except 72, 94, 102, 103, 140, 187 and 190 were considered to form morphoclines and were ordered ('additive') during the parsimony analysis. Six new characters were added:

283: p3, lingual branch of the paralophid: 0, developed; 1, reduced
284: p3–4, anterolingual cingulum: 0, stopping at the anterior valley or absent; 1, joining metaconid
285: P2, metacone fold: 0, strong; 1, weak or absent
286: P3–4, metacone fold: 0, strong; 1, weak or absent
287: M1–2, parastyle: 0, long; 1, short
288: I1, shape: 0, spatulate; 1, conical and pointed; 2, chisel (ordered)

We modified characters 2 and 3 from the original matrix of Antoine (2002) as follows:

2: Maxilla: foramen infraorbitalis: 0, above P1–2; 1, above P3; 2, above P4; 3, above molars
3: Nasal notch: 0, above P1–2; 1, above P3; 2, above P4–M1

Parsimony analyses were computed with the software PAUP* ver. 4.0a (build 167) (Swofford 2002). We used the heuristic search algorithm, with a random addition sequence of 1000 replicates and held 100 trees at each step, with a TBR swapping algorithm with no reconnection limit and swapping on all trees.

The analyses were performed by incrementing the new taxa, to test the reliability of the nodes and their behaviour to the addition of new terminals. When terminals not representing a type specimen were systematically found together in the most parsimonious tree (or strict consensus), even after the addition of new terminals, we decided to merge them together into a single terminal, thus representing the same species. When originally distinct, the scores of these terminals were considered as polymorphism after merging. The taxonomic sampling of the first analysis included only ronzotheres and the outgroup (*Uintaceras radinskyi*). The detailed protocol of the terminals addition and mergings and their results are reported in Table 1. The final resulting consensus tree is presented in the Results. In addition, a 100 bootstrap replicates were performed, retaining groups with frequency over 50% and decay index (Bremer) was calculated with the script for PAUP created by TreeRot ver. 3 (Sorenson & Franzosan 2007).

The results of these analyses are further discussed in the Results section below.

Systematics and comparison
The systematics provided here directly stem from our phylogenetic results. Emended diagnoses are provided and are also based on this phylogeny. All type specimens of each species of *Ronzotherium* are described in the Systematics section. In addition to these type specimens, all specimens from Ronzon assigned to *Ronzotherium velaunum* (type species of the genus) are described and illustrated, mostly for the first time. Postcranial remains from the Phosphorites du Quercy are tentatively attributed to *Ronzotherium filholi* and are also described and illustrated for the first time. These specimens provide complementary morphological comparisons of the postcranial anatomy of *Ronzotherium*. The holotype of *Ronzotherium kochi* Kretzoi, 1940, now synonymised with *Ronzotherium filholi*, is also illustrated, due to the scarcity of illustrations of this specimen in the literature. Recently found specimens from Poillat (Jura Canton, Switzerland) attributed to *Ronzotherium romani* are also described and illustrated for the first time. Moreover, we provide illustrations and descriptions of unpublished postcranial remains from Gaimersheim (Germany) which we refer to *R. romani*, and which unambiguously support its synonymy with *Diaceratherium massiliae* Ménouret & Guérin, 2009. For this reason, we also illustrate and describe all other known postcranial remains attributed to *R. romani*, i.e., those from the localities of 'Marseille' and Rickenbach. To support this synonymy and discriminate *R. romani* from *Diaceratherium*, we also compare these postcranial remains with other species of *Ronzotherium*, and with species of *Diaceratherium*. Finally, recently restored specimens from Bumbach attributed to *R. heissigi* sp. nov. are also illustrated and described for the first time. A list of comparative material used in this study is provided in the Appendix.

Table 1 (continued on next page). Terminals used during each parsimony analysis and their results. Names in bold correspond to terminals that frequently appear as sister groups and could be merged into a single terminal. Abbreviations: RI = retention index; CI = consistency index.

Taxa added	Terminals merged	Number of trees found	Results from the strict consensus for *Ronzotherium*	CI/RI
–	–	2	(*R. filholi*, Villebramar) (***R. elongatum*, Kleinblauen**) (Poillat (**'Marseille' (Rickenbach (*R. romani*, Gaimersheim**))))	0.67/0.50
Teletaceras radinskyi	–	1	(*R. kochi* (*R. filholi*, Villebramar) (Poillat ((Vendèze (Lamothe (Auvergne, Bumbach))) ((***R. elongatum*, Kleinblauen**) (**'Marseille'** (Rickenbach (***R. romani*, Gaimersheim**))))))	0.65/0.48
Penetrigonias dakotensis	–	8	(***R. elongatum*, Kleinblauen**) (Poillat (**'Marseille' (Rickenbach (*R. romani*, Gaimersheim**))))	0.63/0.50
–	***R. elongatum*, Kleinblauen**	4	(Poillat (**'Marseille' (Rickenbach (*R. romani*, Gaimersheim**))))	0.64/0.50
Trigonias osborni	–	19	(**'Marseille', Rickenbach, *R. romani*, Gaimersheim**)	0.61/0.49
–	***R. romani*, Rickenbach, Gaimersheim, 'Marseille'**	2	(***R. filholi*, Villebramar**) (**Auvergne, Bumbach**)	0.67/0.52
Epiaceratherium naduongense	–	2	Identical	0.64/0.51
Epiaceratherium bolcense	–	1	(*R. velaunum* (*R. elongatum* (*R. romani* ((Vendèze, Lamothe) ((***R. filholi*, Villebramar**) ((*R. kochi*, Poillat) ((**Auvergne, Bumbach**))))))))	0.62/0.50
–	**Auvergne, Bumbach (= *R*. indet.)**	24	–	0.63/0.50
Epiaceratherium magnum	–	23	–	0.60/0.51
Subhyracodon occidentalis	–	2	(*R. elongatum* (***R. filholi*, Villebramar**) ((***R. romani*, Poillat**)(Vendèze (***R*. indet.**, Lamothe)))	0.56/0.48
Epiaceratherium delemontense	–	2	Identical	0.56/0.50
Molassitherium albigense	–	5	((***R. romani*, Poillat**) (**Vendèze (*R*. indet., Lamothe**)))	0.53/0.49
Diceratherium armatum	–	2	(*R. elongatum* (***R. filholi,* Villebramar**) ((***R. romani*, Poillat**)(Vendèze (***R*. indet., Lamothe**)))	0.49/0.48
–	***R. romani*, Poillat**	1	((*R. elongatum* (***R. filholi*, Villebramar**)) (*R. romani* (**Vendèze (Lamothe, *R*. indet.**))))	0.50/0.49

Table 1 (continued). Terminals used during each parsimony analysis and their results. Names in bold correspond to terminals that frequently appear as sister groups and could be merged into a single terminal. Abbreviations: RI = retention index; CI = consistency index.

Taxa added	Terminals merged	Number of trees found	Results from the strict consensus for *Ronzotherium*	CI/RI
Mesaceratherium gaimersheimense	–	2	(*R. velaunum* (((*R. elongatum* (**R. filholi**, **Villebramar**)) (*R. romani* (**Vendèze (Lamothe, R. indet.**)))))	0.48/0.47
Pleuroceros pleuroceros	–	6	(((*R. elongatum* (**R. filholi**, **Villebramar**)) (*R. romani* (**Vendèze (Lamothe, R. indet.**))))	0.46/0.47
–	**R. filholi, Villebramar**	6	((*R. elongatum*, *R. filholi*) (*R. romani* (**Vendèze (Lamothe, R. indet.**))))	0.47/0.46
–	**R. indet., Vendèze, Lamothe (= R. sp. nov.)**	14	(*R. romani*, *R.* sp. nov.)	0.48/0.44
Diaceratherium tomerdingense	–	4	(*R. velaunum*, *R. elongatum* ((*R. romani*, *R.* sp. nov.)(*R. filholi*, *R. kochi*)))	0.46/0.43
Pleuroceros blanfordi	–	1	(*R. velaunum* (*R. elongatum* ((*R. romani*, *R.* sp. nov.)(*R. filholi*, *R. kochi*)))	0.45/0.44
Mesaceratherium welcommi	–	1	Identical	0.42/0.44
Protaceratherium minutum	–	1	Identical	0.41/0.44
Mesaceratherium paulhiacense	–	2	Identical	0.40/0.44

Species delimitation

Throughout this paper, we will consider that all specimens from a single locality represent a small portion of a population, and we use these units as terminals in the phylogenetic analysis. Therefore, several terminals in our tree can belong to a single species. We use the "Diagnosable and Monophyly" version of the "Phylogenetic Species Concept" (PSC3 in Mayden 1997) of species to define species a posteriori, after the parsimony analysis. With this concept, a species is defined as "the smallest diagnosable cluster of individual organisms forming a monophyletic group within which there is a parental pattern of ancestry and descent" (McKitrick & Zink 1988). Under the "Unified Species Concept" proposed by de Queiroz (2005, 2007), this would correspond to a species defined by two properties: diagnosability and monophyly, which is near the maximum number of properties obtainable by palaeontological data, since reproductive isolation, ecology, behaviour, and genetic data are mostly unavailable. Furthermore, if one of these diagnosable and monophyletic clusters includes the holotype of any species, we consider that the terminals of this clade do belong to that species. If several holotype specimens of different species are grouped within a same clade and cannot be differentiated, we consider them as synonyms following the taxonomical rule of priority. Finally, to avoid the multiplication of poorly diagnosed species, we favour the most inclusive clades as species, for practical reasons. Indeed, any terminal which has even just one autapomorphy could be considered as a new species, as it is diagnosable, but applying this rule would imply that we know the full extent of intraspecific variability, which is not the case, and would also make species practically unusable.

Results

Phylogeny

Several terminals have been merged, in agreement with the results of the parsimony analyses. From the first analyses, the holotype of *Ronzotherium filholi elongatum* was always found as sister group to the specimens from Kleinblauen. They have thus been merged quite early into a single terminal representing *R. elongatum*. Similarly, the specimens from 'Marseille' (= St-Henri, St-André and Les Milles), Gaimersheim, and Rickenbach were always found together with the specimens of *Ronzotherium romani* from the type locality of La Ferté-Alais, although after the addition of *Trigonias osborni*, their topology slightly differed, resulting in an unresolved polytomy in the strict consensus. Yet, they still remained together as a clade and were thus also merged in a single terminal, which supports the former identifications of these specimens by other authors (i.e., Heissig 1969 for Gaimersheim; Ménouret & Guérin 2009 for Marseille; Mennecart *et al*. 2012 for Rickenbach). Furthermore, this also highlights the synonymy of *Ronzotherium romani* with *Diaceratherium massiliae* Ménouret & Guérin, 2009, that we further detail in the Systematic palaeontology section.

After these two fusions, the specimens from Bumbach and Auvergne were systematically found as sister groups. They were thus merged, representing an indeterminate species of *Ronzotherium*. After that, and the addition of new terminals, two clades occurred systematically: one including *Ronzotherium romani* and the specimens from Poillat, and another comprising the specimen from Vendèze as sister group to '*Ronzotherium* indet.' + the specimen from Lamothe-Capdeville. This former clade was thus merged into a single terminal, representing *R. romani*, and a new clade then became predominant, comprising the holotype of *Ronzotherium filholi* and the specimens from Villebramar. These were thus merged, as was also supported by the identification of these specimens from Villebramar as *R. filholi* by Brunet (1979), after which the specimens from Vendèze and Lamothe-Capdeville were merged with the '*Ronzotherium* indet.' documenting a new species: *Ronzotherium heissigi* sp. nov.

The identification of a new species from the localities of Bumbach, Auvergne, Vendèze, and Lamothe-Capdeville is supported by eight unambiguous autapomorphies, including mandibular, dental and postcranial characters (see Fig. 1). *Ronzotherium romani* further differs from this new species by seven unambiguous autapomorphies. The specimens from Bumbach were originally assigned to *Ronzotherium elongatum* by Heissig (1969), an assumption which is not supported by our analyses, as these samples are never found as sister groups and *R. elongatum* notably differs by its strong and continuous cingulum on the cheek teeth. Likewise, the specimens from 'Auvergne' (exact locality unknown) were attributed to *R. velaunum* by the same author, which is not supported by our analyses. However, both Heissig (1969) and Brunet (1979) referred to the specimens from Lamothe-Capdeville (described by Roman 1912a) as *R. romani*, whereas the specimen from Vendèze was identified as *R. velaunum* by Heissig (1969) and as *R. romani* by Brunet (1979). Here, we show that these specimens both belong to the same species, *R. heissigi* sp. nov., which is furthermore the sister species to *R. romani*, which could explain such previous discrepancies.

The final tree is presented in Fig. 1 and results from the strict consensus tree of two equally most parsimonious trees of 704 steps with a retention index (RI) of 0.44 and a consistency index (CI) of 0.40. According to our results, *Ronzotherium* is monophyletic and is the closest sister group to the Rhinocerotinae, which include *Mesaceratherium* Heissig, 1969, *Molassitherium* Becker & Antoine, 2013, *Subhyracodon* Brandt, 1878, *Diceratherium* Marsh, 1875, *Diaceratherium* Dietrich,1931, *Protaceratherium* Abel, 1910 and *Pleuroceros* Roger, 1898. At the base of the tree, four genera are placed as stem Rhinocerotidae. Within those, *Epiaceratherium* Abel, 1910 is the most basal and is monophyletic, followed by the American *Trigonias* Lucas, 1900, *Teletaceras* Hanson, 1989 and *Penetrigonias* Tanner & Martin, 1976. The nodes are overall quite poorly supported, either by Bremer values or bootstrap, which indicates high levels of homoplasy.
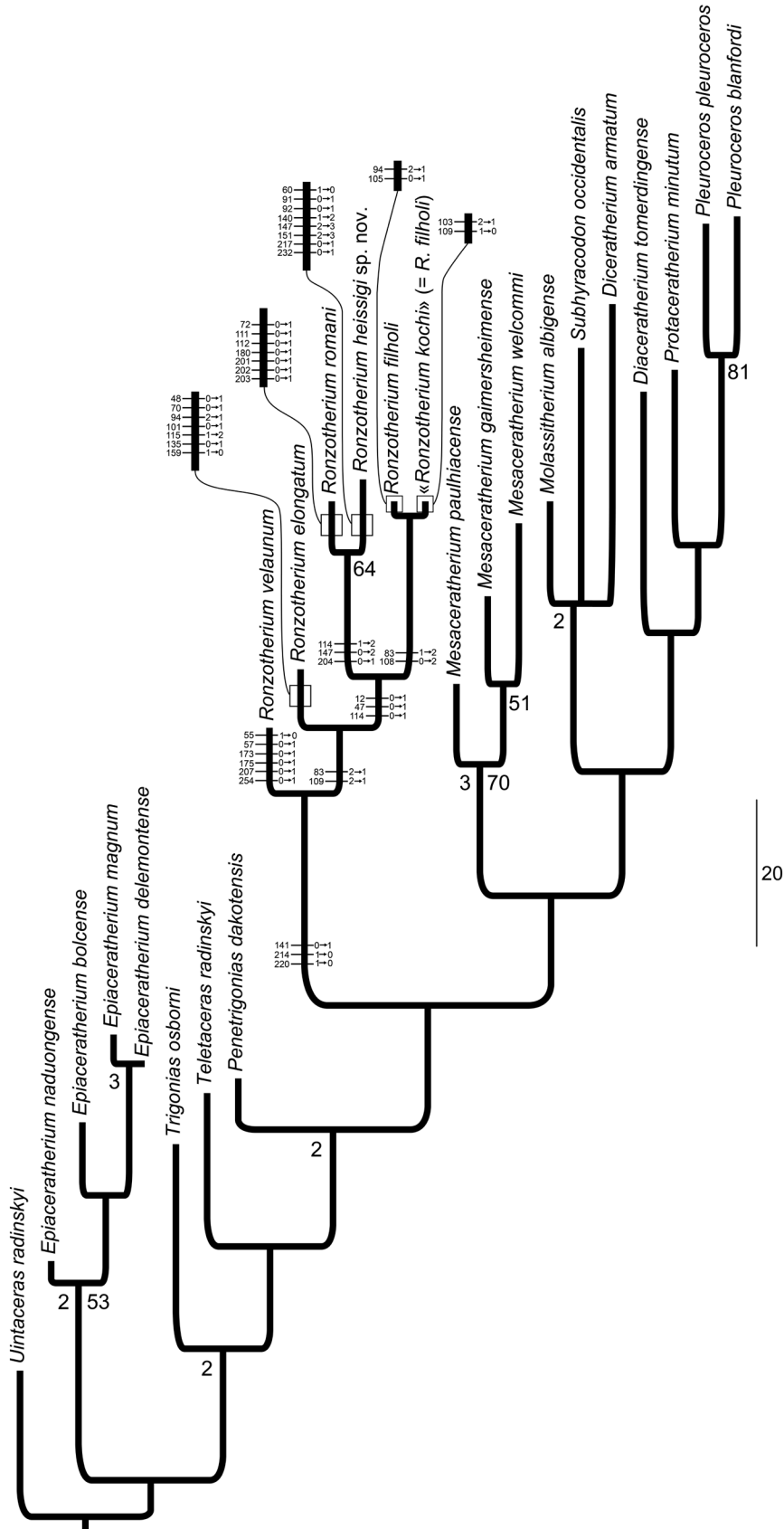
Fig. 1. Strict consensus of two equiparsimonious trees, inferred from a cladistic analysis of 288 morphological characters (length = 704 steps, RI = 0.44, CI = 0.40) and 24 rhinocerotid taxa. Numbers at nodes at the left of branches are decay index above 1, while numbers on the right of branches are bootstrap values above 50. Unambiguous synapomorphies of species of *Ronzotherium* Aymard, 1854 are reported on branches, with character numbers on the left and characters states changes on the right. Branch lengths are proportional to the number of transformations with ACCTRAN optimisation, the scale represents 20 steps.

Based on these results, *Ronzotherium* could comprise six species: *R. velaunum*, *R. elongatum*, *R. romani*, *R. heissigi* sp. nov., *R. filholi* and *R. kochi*. However, *R. filholi* and *R. kochi* only differ from each other by four unambiguous autapomorphies (two for each species), which is very poor to differentiate them. Thus, we suggest that they should actually be synonymized, pending more material from *R. kochi* is discovered, as it is currently only represented by a single maxilla with P2–M3.

Systematic palaeontology

Order Perissodactyla Owen, 1848
Superfamily Rhinocerotoidea Owen, 1845
Family Rhinocerotidae Gray, 1821

Genus ***Ronzotherium*** Aymard, 1854

Type species

Ronzotherium velaunum (Aymard in Pictet, 1853)

Other species

Ronzotherium filholi (Osborn, 1900); *Ronzotherium romani* Kretzoi, 1940; *Ronzotherium elongatum* Heissig, 1969; *Ronzotherium heissigi* sp. nov.

Emended diagnosis

These are large-sized hornless rhinocerotoids with two pointed upper incisors (I1 and I2) but only one large tusk-shaped lower incisor (i2) and without canines. The crown of the i1 is reduced. The dorsal profile of the skull is concave. The nasal incision is short and opening above P1–3. The anterior border of the orbit is above the molars and the infraorbital foramen is above P3–4. The processus posttympanicus and paraoccipitalis are fused at their base. The upper premolars are not molarised and the hypocone is always connected or completely fused to the protocone on P3–4. The upper molars are simple, with poorly developed crochet and antecrochet and the crista is always absent. The posterior part of the ectoloph of the upper molars is straight. The M3 is quadrangular in occlusal view. The ectoloph and metaloph are fused into an ectometaloph on M3, and there is no metastyle, but a posterior groove remains. The entoconid is very poorly developed on the lower premolars, or completely absent, and the opening of the posterior valley is wide and U-shaped. The lower d1 is usually absent. The ectolophid groove of the lower molars is developed until the neck. The distal articulation of the pyramidal for the lunate is symmetrical in medial view, the indentation on the medial side of the magnum is absent and the posterior tuberosity of the magnum is short. The collum tali of the astragalus is high.

Stratigraphical distribution

Late Eocene (?) to latest Oligocene.

Geographical distribution

Europe.

Ronzotherium velaunum (Aymard in Pictet, 1853)
Figs 2–7

Acerotherium velaunum Aymard in Pictet, 1853: 296.
Ronzotherium cuvieri Aymard, 1856: 233.

Rhinoceros velaunus – Aymard in Pictet 1853: 298.

Rhinocéros à incisives (*Ronzotherium*) – Aymard 1854: 675.

Ronzotherium velaunum – Aymard 1856: 233. — Filhol 1881: 3. — Osborn 1900: 232–237, 241, fig. 3. — Deninger 1903: 94–95. — Stehlin 1909: 509. — Abel 1910: 4–6, 8–9, 18, 33. — Roman 1912a: 4–5, 8, 10. — Kafka 1913: 5, 47, fig. 40a. — Airaghi 1925: 25. — Heissig 1969: figs 6a, 8c, 9a, 10a, 11, 25a (from Ronzon). — Brunet 1977: 16, 23; 1979: 102–104, 152–153, table 51, pls XV, XIXa–f. — Brunet *et al*. 1977: 109–112. — Jehenne & Brunet 1992: 202–203. — Uhlig 1996: 140–142. — Ménouret & Guérin 2009: 293–327. — Becker 2009: 495, 500.

Ronzotherium cuvieri (?) – Filhol 1881: 3.

Acerotherium velaunum – Filhol 1881: 75–78, figs 69–86, 88. — Mermier 1895: 176, 180, 186. — Roman 1910: 1558–1560; 1912a: 7, 27, 42–45, 56, 78, fig. 13, pl. II figs 2, 2a. — Gignoux 1928: 147, 149, 151.

Acerotherium cuvieri – Filhol 1881: fig. 87, 89–90. — Airaghi 1925: 26, 29.

? *Ronzotherium* cf. *velaunum* – Schlossser 1902: 112–113, pl. V figs 23, 25.

Rhinoceros velaunus – Roman 1912a: 45.

? *Ronzotherium velaunum* – Kafka 1913: 48–50, figs 40b, 41. — Kretzoi 1940: 89–92, 97–98, figs 1–2. — Lavocat 1951: 115. — Balme 2000: 153. — Costeur & Guérin 2001: 77.

Rhinoceros velaunum – Airaghi 1925: 32–33, 40–41.

Ronzotherium cf. *velaunum* – Heissig 1978: 249.

Non *Ronzotherium filholi* – Lavocat 1951: 116, pl. 19 fig. 3, pl. 26 fig. 1 (from Vendèze).

Non *Ronzotherium velaunum* – Heissig 1969: figs 5, 6b–d, 7, 8a–b, d–g, 9b–c, 10b–d, 25b (from 'Auvergne', Mouillac, Vendèze, St-Henri, St-André, Marseille, Les Milles).

Historical diagnoses

The first diagnosis of the species was provided by Heissig (1969, translated by the authors): "type species of the genus *Ronzotherium* with almost parallel i2 facing forward; i1 absent, I1 and I2 large. Lower jaw branches at an acute angle to each other. Upper molars broad, with long postfossette, narrow, slightly curved medisinus, thick and far forward paracone and mostly weak or missing lingual cingulum; M3 with sharp, narrow ectoloph edge behind the metacone. Upper premolars with straight or barely curved, parallel, originally slightly inclined transverse lophs and strongly waved lingual cingulum, slowly reduced; reduction begins at P4. P2 semimolariform to molariform, P3 and P4 premolariform to submolariform, but with relatively far apart inner lophs. Lower molars broad with weak labial cingulum; lower premolars with long talonid, mostly groove-shaped talonid pit and sharp, deep external groove. The entoconid lies far back, the cingulum is weak. The p1 is single rooted or missing."

An emended diagnosis was provided by Brunet (1979, translated by the authors): "Stratigraphically the most ancient and primitive species of its kind. Skull: unknown. Mandible: posterior border of the symphysis just ahead of the d1, its lower surface presents a hull; very strong occlusion between i1 and i2. Decidual teeth: the upper milk premolars are unknown; the inferiors have a strongly curved hypolophid; d1 is biradiculate; the first lobe of d2 is strong with a long lingual branch of the paralophid, the 'metaconid' is not individualized; the anterior lobe of d3 is strong with a very long anterior branch of the paralophid. Definitive dentition: probable presence of i1. Upper premolars with a short postfossette, located above the posterior cingulum; strong lingual cingulum, barely waved. Upper molars with strong lingual cingulum, complete or disappearing only at the level of the hypocone. Lower premolars and molars: more or less large with a strong labial cingulum, more or less complete; the very notched talonid fossae on the labial side of the hypolophid are flatter, more horizontal, and lingually higher than in *R. filholi*; the trigonid fossae also open higher, above the anterolingual cingulum; premolars with long paralophid, without protoconid fold; P2 not reduced, with a strong anterolabial groove. Appendicular skeleton: tetradactyl hand with a gracile McV, reduced but complete; on the dorsal side of the hand, the

lunate articulates with the magnum; on the pyramidal, the ulnar facet is more laterally widened and the lower facet for the lunate higher and larger than in *R. filholi*; likewise, the magnum carries a much longer and higher facet for the McII."

Emended diagnosis

Type species of the genus with a posterior border of the symphysis located anterior to p2 and without lingual groove for the sulcus mylohyoideus on the corpus mandibulae. The metacone fold is present on M1–2. The d1 is absent in the juvenile, and the entoconid is constricted on decidual lower milk teeth. The cingula are poorly developed on upper and lower cheek teeth and discontinuous. The postero-proximal and anteroproximal facets for the lunate are in contact on the scaphoid and the fibula facet is oblique on the astragalus. The trapezium facet is absent on the McII.

Type material

Lectotype
FRANCE • right hemimandible still partly in sediment with poorly preserved p2–m3 and broken symphysis; Haute-Loire, near Le Puy-en-Velay, hill of Ronzon; PUY.2004.6.1765.RON.

Additional material
FRANCE • 1 broken mandible in several pieces, with i2 and p2–m3 on the left side and i2 and p2–(m1) on the right side; same collection data as for lectotype; PUY.2004.6.1766.RON • 1 juvenile mandible, still partly in sediment, with d2–d4 and erupting m1 on both sides and a small di1; same collection data as for lectotype; PUY.2004.7.1.RON • 1 broken ectoloph of P2?; same collection data as for lectotype; PUY.2004.6.1551.RON • 1 isolated P3; same collection data as for lectotype; PUY.2004.6.1767.RON • 1 isolated M1; same collection data as for lectotype; TLM.PAL.2010.0.122 • 1 cast of an isolated lower molar; same collection data as for lectotype; PUY.2004.6.841.RON • 1 distal part of humerus; same collection data as for lectotype; PUY.2004.6.262.RON • 1 complete scaphoid; same collection data as for lectotype; MNHN.F.RZN.503 • 1 lunate partly unextracted from sediment; same collection data as for lectotype; PUY.2004.6.1901.RON • 1 pyramidal, still in sediment; same collection data as for lectotype; MNHN.F.RZN.504 • 1 pyramidal; same collection data as for lectotype; MNHN.F.RZN.502 • 1 pisiforms, still in sediment; same collection data as for lectotype; MNHN.F.RZN.505 • 1 pisiforms, still in sediment; same collection data as for lectotype; PUY.2004.6.1901.RON • 1 magnum, still in sediment; same collection data as for lectotype; PUY.2004.6.907.RON • 1 magnum; same collection data as for lectotype; PUY.2004.6.263.RON • 1 broken anterior part of unciform; same collection data as for lectotype; PUY.2004.6.1480.RON • 2 distal parts of femora; same collection data as for lectotype; PUY.2004.6.266.RON, PUY.2004.6.267.RON • 2 proximal parts of tibiae; same collection data as for lectotype; PUY.2004.6.260.RON, PUY.2004.6.261.RON • 1 ectocuneiform, still partly in sediment; same collection data as for lectotype; PUY.2004.6.577.RON • 1 cuboid, still in sediment; same collection data as for lectotype; PUY.2004.6.1309.RON • 1 cuboid; same collection data as for lectotype; PUY.2004.6.268.RON • 1 astragalus, still preserved in sediment; same collection data as for lectotype; PUY.2004.6.1770.RON • 1 central metapodial, still in sediment; same collection data as for lectotype; PUY.2004.6.840.RON • 1 lateral phalanx, still in sediment; same collection data as for lectotype; PUY.2004.6.604.RON.

Type horizon and locality

Hill of Ronzon, near Le Puy-en-Velay (Haute-Loire, France), MP21 (early Oligocene).

Stratigraphical distribution

MP21 (early Oligocene).

Geographical distribution

France: Ronzon, Lagny-Torigny, Ruch. Germany: Haag 2, Möhren 20.

Description

MANDIBLES. Three mandibles of *R. velaunum* from Ronzon are preserved. The lectotype mandible PUY.2004.6.1765.RON is a right hemimandible with p2–m3 (Fig. 2A–D). The posterior part of the specimen and the symphysis are broken, and the left side is still in sediment. The base of the corpus mandibulae is straight and low, with a constant height below the teeth neck. The ramus is vertical, and the coronoid process is well developed and high. The mandible PUY.2004.6.1766.RON is badly preserved and in several pieces (Fig. 2E–J). The symphysis as well as both branches are preserved, with i2, the root of d1 and p2–m3 on the left side, and only i2 and p2–m1 on the right side. It was recently prepared and new characters can now be observed: the angle between the symphysis and the corpus is low, the symphysis is rather narrow and its posterior borders is in front of p2, the foramen mentale is below p2 and there is no lingual groove of the sulcus mylohyoideus. The last mandible PUY.2004.7.1.RON belonged to a juvenile individual and is still partly preserved in sediment (Fig. 2K–O). It bears d2–d4 and erupting m1 on both sides as well as a small di1 on the right side. There is apparently no dp1. The posterior border of the symphysis is anterior to d2. No lingual groove of the sulcus mylohyoideus is visible.

UPPER DENTITION. Very few upper teeth are preserved in this locality (Fig. 3): an ectoloph of a left P2 (PUY.2004.6.1551.RON), a P3 (PUY.2004.6.1767.RON) and an M1 (TLM.PAL.2010.0.122). However, Filhol (1881) noted the existence of an upper maxilla that he could not have accessed during his study and was supposedly in Pichot-Dumazel's collection. Unfortunately, this maxilla remains unknown. The P2 and P3 have strong paracone and metacone folds and very thin discontinuous labial cingulum. Their crown is low. The lingual cingulum is strong and continuous on P3. The P3 is three-rooted and few characters can be observed, as it is very worn. Its postfossette is narrow and the protocone and hypocone were probably not separated. The M1 has four roots and is also much worn. Labial cingulum is almost completely absent. Lingual cingulum is strong and continuous under the protocone and disappears under the hypocone. The paracone fold is strong and the metacone fold is present but very thin. The parastyle is strong and there is no mesostyle. The protocone does not seem constricted. The posterior profile of the ectoloph is slightly concave.

LOWER DENTITION. The definitive anterior dentition is only represented by two i2 from the mandible PUY.2004.6.1766.RON. They are straight and horizontal. The roots are wider than the crown, and the crown shows a clear and large wear-facet, which means that I1 and i2 could contact each other. The transverse outline of the crown is in the shape of a medially pinched drop. The neck is not marked and the enamel is very thin. The lower cheek teeth are two-rooted and low-crowned. There is no cement. The premolar row is short compared to the molar row ($0.42 < Lp3–4/Lm1–3 < 0.50$). A weak labial cingulum is sometimes present on the lower cheek teeth, but a lingual cingulum is always absent. Vertical external rugosities are present on the ectolophid of p2–3. The ectolophid groove is developed and does not vanish before the neck. In occlusal view, the trigonid is very angular and forms a right dihedron which becomes more acute with wear, while the talonid is rounded. The talonid basin of the lower premolars is poorly developed: the entoconid is completely absent and the hypoconid is low. The hypolophid vanishes before the posterolingual border of the premolars, the posterior valley is therefore very wide and U-shaped. On the contrary, the anterior valley is narrow, and both valleys open very high above the neck. The metaconid is the largest and most developed cusp on lower premolars. On p3, the metaconid bears an anterior crest, almost closing the anterior valley. The paralophid of premolars has two branches, a labial branch, and a high and long anterior branch, parallel to the protolophid. The molars greatly differ from the premolars by the much stronger development of the entoconid, which is also slightly constricted. The opening of the anterior valley is higher than the posterior one.
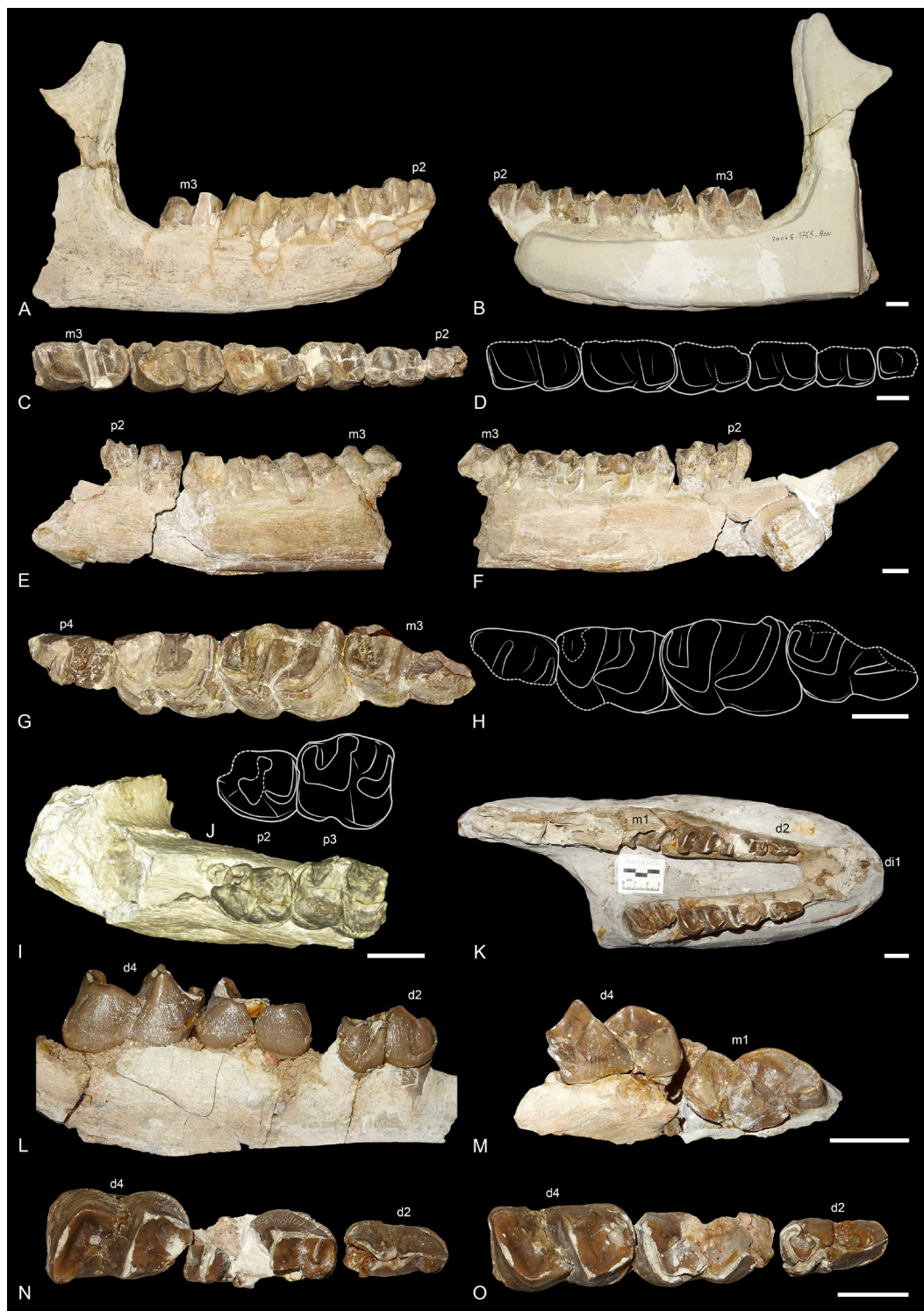
Fig. 2. *Ronzotherium velaunum* (Aymard in Pictet, 1853) from Ronzon (earliest Oligocene, France). – **A–D**. Lectotype right hemimandible PUY.2004.6.1765.RON with p2–m3. **A**. Lateral view. **B**. Medial view. **C**. Occlusal view. **D**. Drawing of the occlusal view. – **E–J**. Broken left hemimandible PUY.2004.6.1766. RON with i2 and p2–m3. **E**. Lateral view. **F**. Medial view. **G**. p4–m3 in occlusal view. **H**. Drawing of p4–m3. **I**. Symphysis with p2–3 in occlusal view. **J**. Drawing of p2–3. – **K–O**. Juvenile mandible PUY.2004.7.1.RON. **K**. di1, d2–d4 and erupting m1 in occlusal view. **L**. Right d2–4 in labial view. **M**. Left d4–m1 in lingual view. **N**. Left d2–4 in occlusal view. **O**. Right d2–4 in occlusal view. Scale bars: 2 cm.

DECIDUAL DENTITION. Only the lower decidual dentition is known from Ronzon, from the juvenile mandible PUY.2004.7.1.RON (Fig. 2K–O). The di1 is very small and has a conical crown. There does not seem to be a d1 in the juveniles. However, d2–4 are well developed. The metaconid and entoconid are slightly constricted, especially on d4. There is neither a protoconid fold nor a vertical external rugosity. The lingual and labial cingulum are absent. The ectolophid fold is strong on d2 but there is no anterior groove on the ectolophid. The paralophid is double on d2–3 and simple on d4. On d2, the posterior valley is almost closed by the extension of the entoconid, but still narrowly open. There is no lingual groove of the entoconid on d3. The d4 is very molariform.

HUMERUS. One distal fragment of humerus is preserved (PUY.2004.6.262.RON, Fig. 4A–C). The fossa olecrani is high but not very deep. The distal articulation is well constricted and there is no scar on the trochlea. The distal gutter on the epicondyle is also absent. Medial and lateral epicondyles are poorly developed and the lateral epicondylar crest is weakly extended laterally.
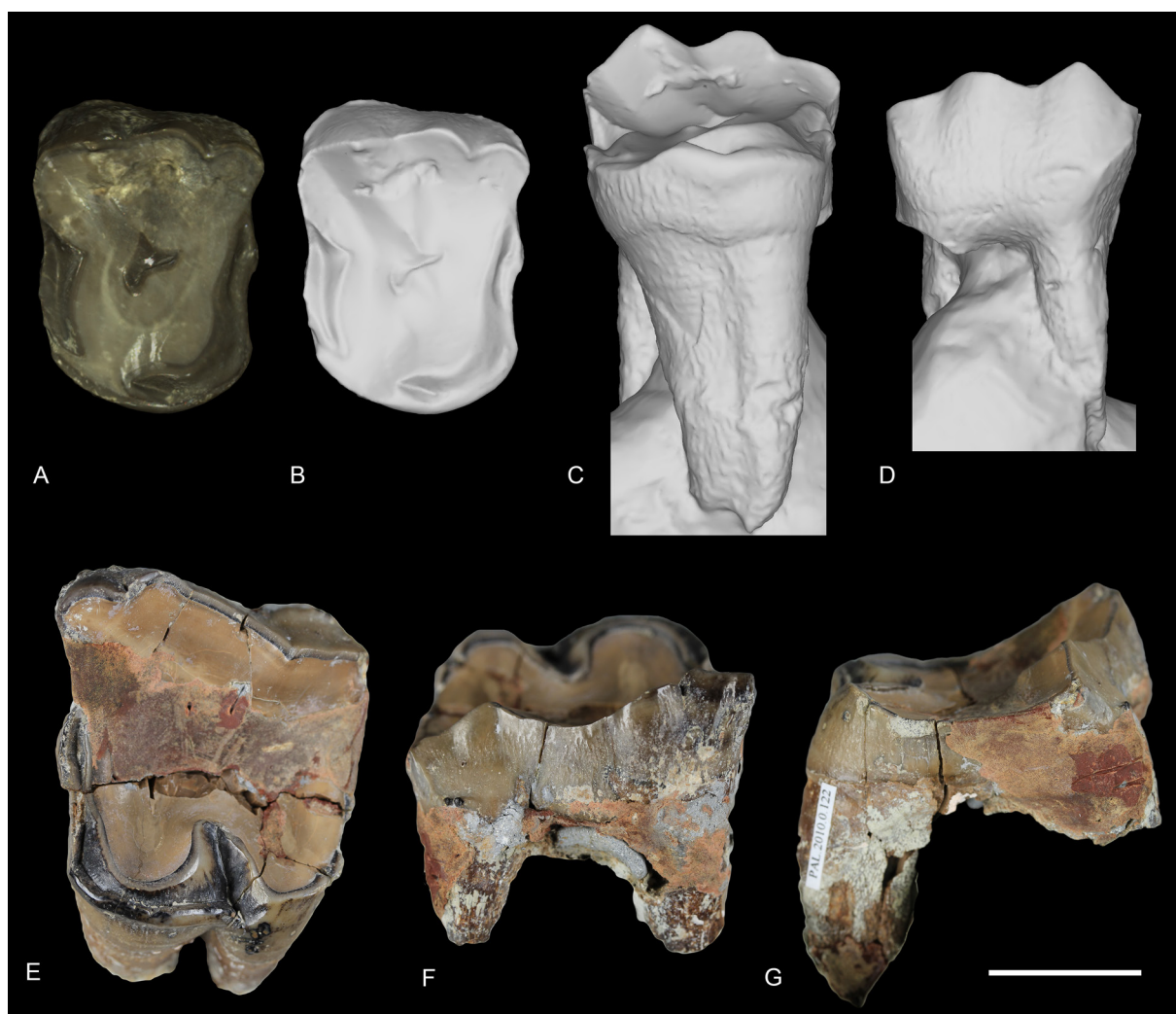

Fig. 3. *Ronzotherium velaunum* (Aymard in Pictet, 1853) from Ronzon (earliest Oligocene, France). – **A–D**. 3D surface scans of P3 PUY.2004.6.1767.RON. **A**. With texture in occlusal view. **B**. Without texture in occlusal view. **C**. Without texture in lingual view. **D**. Without texture in labial view. – **E–F**. M1 TLM.PAL.2010.0.122. **E**. Occlusal view. **F**. Labial view. **G**. Lateral view. Scale bar: 2 cm.

Fig. 4. *Ronzotherium velaunum* (Aymard in Pictet, 1853) from Ronzon (earliest Oligocene, France). – **A–C**. Left distal humerus PUY.2004.6.262.RON. **A**. Anterior view. **B**. Posterior view. **C**. Distal view. – **D–G**. Right scaphoid MNHN.F.RZN.503. **D**. Medial view. **E**. Lateral view. **F**. Proximal view. **G**. Distal view. – **H–J**. Right lunate PUY.2004.6.1901.RON. **H**. Anterior view. **I**. Lateral view. **J**. Proximal view. – **K–M**. Right pyramidal MNHN.F.RZN.502. **K**. Lateral view. **L**. Medial view. **M**. Posterior view. – **N**. Left pyramidal MNHN.F.RZN.504, distal view. Abbreviations: adl = anterodistal facet for the lunate; apl = anteroproximal facet for the lunate; l = lunate; le = lateral epicondyle; lec = lateral epicondylar crest; m = magnum; me = medial epicondyle; of = olecranon fossa; p = pyramidal; pi = pisiform; ppl = postero-proximal facet for the lunate; pt = posterior tuberosity; r = radius; s = scaphoid; td = trapezoid; tm = trapezium; u = ulna; un = unciform. Articular surfaces highlighted in white. Scale bars: 2 cm.

SCAPHOID. The scaphoid MNHN.F.RZN.503 (Fig. 4D–G) is well preserved. The anterior height is equal to the posterior one. The postero-proximal articulation with the lunate bone is not visible but may have been present on the eroded proximo-lateral tuberosity and fused with the anteroproximal facet. The proximal facet for the radius is very concave and fuses anteriorly with the anteroproximal facet for the lunate bone. The anterodistal facet for the lunate is poorly distinguished. The three distal articular facets are concave in lateral view. The trapezium facet is rather large and triangular. The trapezoid facet is the largest and has a prominent dorso-medial extension. The magnum facet is concave in lateral view.

LUNATE. The lunate bone PUY.2004.6.1901.RON (Fig. 4H–J) is still mostly concealed in the sedimentary block. Only the proximal, dorsal and lateral sides are visible. It is an overall large and robust bone. The posterior tuberosity is almost as wide as the proximal facet for the radius. Two articular facets are visible on the lateral side, both corresponding to the pyramidal bone. The proximal facet is small while the distal one is large, flat and circular. On the medial side, two well separated articular facets can be distinguished and correspond to the scaphoid, which implies the presence of a postero-proximal facet for the lunate on the scaphoid, that is not visible on the scaphoid MNHN.F.RZN.503.

PYRAMIDAL. Two pyramidals are preserved (MNHN.F.RZN.502, Fig. 4K–M and MNHN.RZN.504, Fig. 4N). There are two proximal articulation facets: a large one for the ulna, and a smaller one, elongated and band-like for the pisiform. The medio-distal articulation for the lunate is symmetrical and the distal facet for the unciform is triangular.

PISIFORM. The pisiform MNHN.RZN.505 is still in articulation with the pyramidal MNHN.RZN.504. Another unnumbered pisiform is preserved on the sedimentary bloc of the lunate bone PUY.2004.6.1901. RON. The pisiform is very small, and neither flattened nor elongated. It bears a large proximal articular facet for the radius. The distal end is roughly conical and rounded.

UNCIFORM. Only the dorsal part of the left unciform PUY.2004.6.1480.RON is preserved, the posterior tuberosity is missing (Fig. 5F–G). There are two proximal facets: a large one, dorso-ventrally convex for the pyramidal, and smaller one, flattened and arrowhead-shaped for the lunate. They form an angle of 120–130° in dorsal view. The posterior expansion of the pyramidal facet is very short and wide. The three distal facets, for the magnum, McIII and McIV, are partially covered in sediment. The lateral McV facet is broken but was probably distinct from the pyramidal facet.

MAGNUM. Two magnums are preserved. PUY.2004.6.907.RON is still in a sedimentary bloc, while PUY.2004.6.263.RON is subcomplete and fully extracted (Fig. 5A–E). It is a rather tall bone, the proximodistal height is almost equal to the dorsoventral length, but it is very compressed transversally. In anterior view, the anterior border of the scaphoid facet is nearly straight. The lunate facet is very long dorsoventrally, and very convex proximally. There are two medial facets below the scaphoid facet: a proximal one for the trapezoid and a distal one for the McII. The former is trapezoidal while the latter is curved. There is no indentation between these two facets. The distal facet for the McIII is large and deeply concave dorsoventrally. The unciform facet on the lateral side is not preserved. The posterior tuberosity of the magnum is long, thin and curved.

FEMUR. There are two distal ends of left femora in Ronzon (PUY.2004.6.266.RON, Fig. 6A–D, I and PUY.2004.6.267.RON, Fig. 6E–H, J). In anterior view, the medial lip of the trochlea is prominent. The groove between the two trochlea is not very deep and the proximal border of the trochlea is almost straight. In lateral view, the medial lip of the trochlea is strongly forward compared to the diaphysis. In posterior view, the two condyles are similar in size and widely separated by the intercondylar fossa.
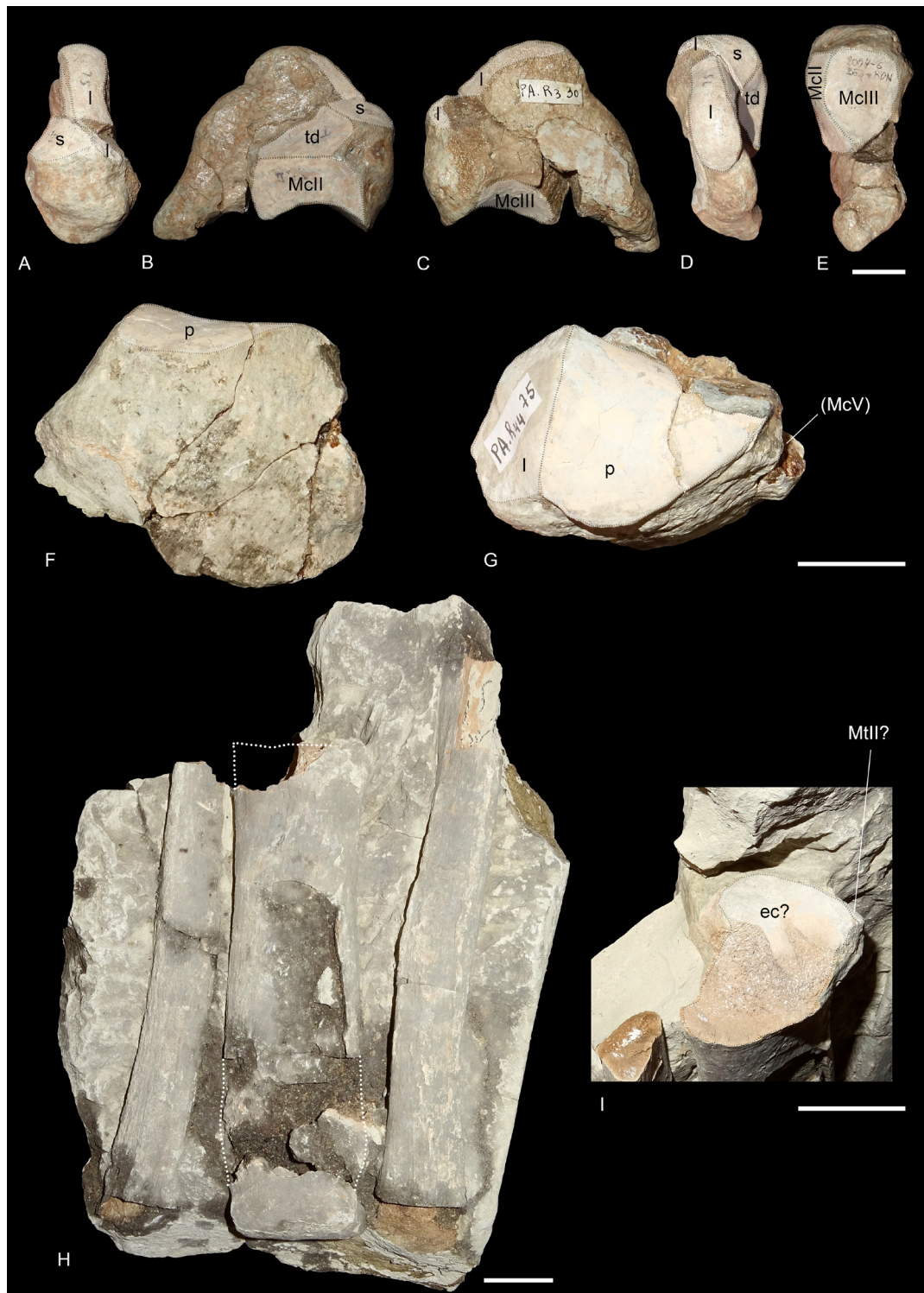
Fig. 5. *Ronzotherium velaunum* (Aymard in Pictet, 1853) from Ronzon (earliest Oligocene, France). – **A–E**. Left magnum PUY.2004.6.263.RON. **A**. Anterior view. **B**. Medial view. **C**. Lateral view. **D**. Proximal view. **E**. Distal view. – **F–G**. Left unciform PUY.2004.6.1480.RON. **F**. Anterior view. **G**. Proximal view. – **H–I**. Central metapodial PUY.2004.6.840.RON (possibly a MtIII) on sedimentary block, along with two probable ribs on its right and left. **H**. Anterior view. **I**. Close-up view of the proximal extremity. Abbreviations: ec = ectocuneiform; l = lunate; p = pyramidal; s = scaphoid; td = trapezoid. Articular surfaces highlighted in white. Scale bars: 2 cm.

The supracondylar fossa is shallow. In distal view, the articular surfaces of the trochlea and the condyles are connected medially and laterally.

TIBIA. Two proximal ends of left tibias (PUY.2004.6.260.RON and PUY.2004.6.261.RON) could belong to the same individuals as the femora (Fig. 6K–P). In proximal view, it is wider than long. The tibial tuberosity is weakly developed and is laterally displaced. It is separated from the medial tuberosity by a wide groove. The cranial intercondylar area is deep and wide, the central one very small and the caudal one is deep and slender. The lateral condyle is oval, and wider than long, while the medial one is almost rectangular and longer than wide. In anterior view, the medial tuberosity is higher than the lateral one. In lateral view, the groove for the extensor is wide and shallow and the tibial fossa rather deep. The tibia and fibula were completely independent, there is no contact mark along the diaphysis, only a high articular facet below the lateral condyle.

ASTRAGALUS. Only the anterior face of the astragalus (PUY.2004.6.1770.RON) is visible, the other side is still in sediment, but it is complete (Fig. 7A–D). The transverse diameter/height (TD/H) ratio is slightly above 1, but below 1.2, whereas the anteroposterior diameter/height (APD/H) ratio is below 0.65. On the lateral side, the fibula facet is slightly oblique and flat. The collum tali is very high. There are two distal articular facets: the navicular facet is large and slightly concave transversally, while the facet for the cuboid is small and flat. In distal view, the trochlea is very oblique compared to the distal articulation. The medio distal tubercle is well developed.

CUBOID. Two cuboids are preserved: one is still partially in sediment (PUY.2004.6.1309.RON) but the other is subcomplete (PUY.2004.6.268.RON, Fig. 7I–M). The proximal articular surface is triangular. There are two distinct surfaces, for the astragalus and the calcaneus, distinguished by a shallow groove. The calcanear one is the largest. In anterior view, the bone is rectangular and higher than wide. In lateral view, the lateral groove for the tendons is very deep. The posterior apophysis is wide and stout, and extends more distally than the distal articular facet. The distal articulation surface for the MtIV is almost a right triangle with rounded edges.

ECTOCUNEIFORM. The right ectocuneiform PUY.2004.6.577.RON is still partially in sediment, the proximal side is not visible (Fig. 7E–H). The distal articular facet for the MtIII is crescent-shaped. The posterolateral process is rather short and medially oriented. The medial side is straight and bears three facets: one dorsal and band-shaped for the mesocuneiform, and two distal, oval-shaped for the MtII. The lateral side is curved and the two articulations postero-proximal and anterodistal for the cuboid are separated by a deep groove.

METAPODIAL. A central metapodial (PUY.2004.6.840.RON) is also preserved from Ronzon, still in sediment, and only the dorsal side is visible (Fig. 5H–I). The proximal articulation is very incomplete, but it is nonetheless rather dorsoventrally flat, which would indicate a MtIII rather than a McIII, as also suggested by Brunet (1979). There is a small anteroproximal facet for the MtII, the posterior one, if present is hidden by sediment. The diaphysis gets slightly wider towards the distal end. The median keel of the distal articulation is smooth.

LOST MATERIAL. The scaphoid and pyramidal thought as lost by Brunet (1979) and figured by Filhol (1881) are now in fact in the collections of MNHN (Paris, France) (MNHN.F.RZN.502, MNHN.F.RZN.503 and MNHN.F.RZN.504). However, the calcaneum, MtIV and McV, figured by Filhol (1881: pl. 13), are indeed lost and could not be found either in the Musée Crozatier (Le Puy-en-Velay, France) or in the MNHN.

Fig. 6. *Ronzotherium velaunum* (Aymard in Pictet, 1853) from Ronzon (earliest Oligocene, France). – **A–D, I**. Left distal femur PUY.2004.6.266.RON. **A**. Anterior view. **B**. Posterior view. **C**. Lateral view. **D**. Medial view. **I**. Distal view. – **E–H, J**. Left distal femur PUY.2004.6.267.RON. **E**. Anterior view. **F**. Posterior view. **G**. Lateral view. **H**. Medial view. **J**. Distal view. – **K, M–N**. Left proximal tibia PUY.2004.6.261.RON. **K**. Proximal view. **M**. Anterior view. **N**. Posterior view. – **L, O–P.** Left proximal tibia PUY.2004.6.260.RON. **L**. Proximal view. **O**. Anterior view. **P**. Posterior view. Abbreviations: aia = anterior intercondylar area; icf = intercondylar fossa; lc = lateral condyle; ll = lateral lip of the trochlea; mc = medial condyle; ml = medial lip of the trochlea; pia = posterior intercondylar area; tt = tibial tuberosity. Articular surfaces highlighted in white. Scale bar: 2 cm.
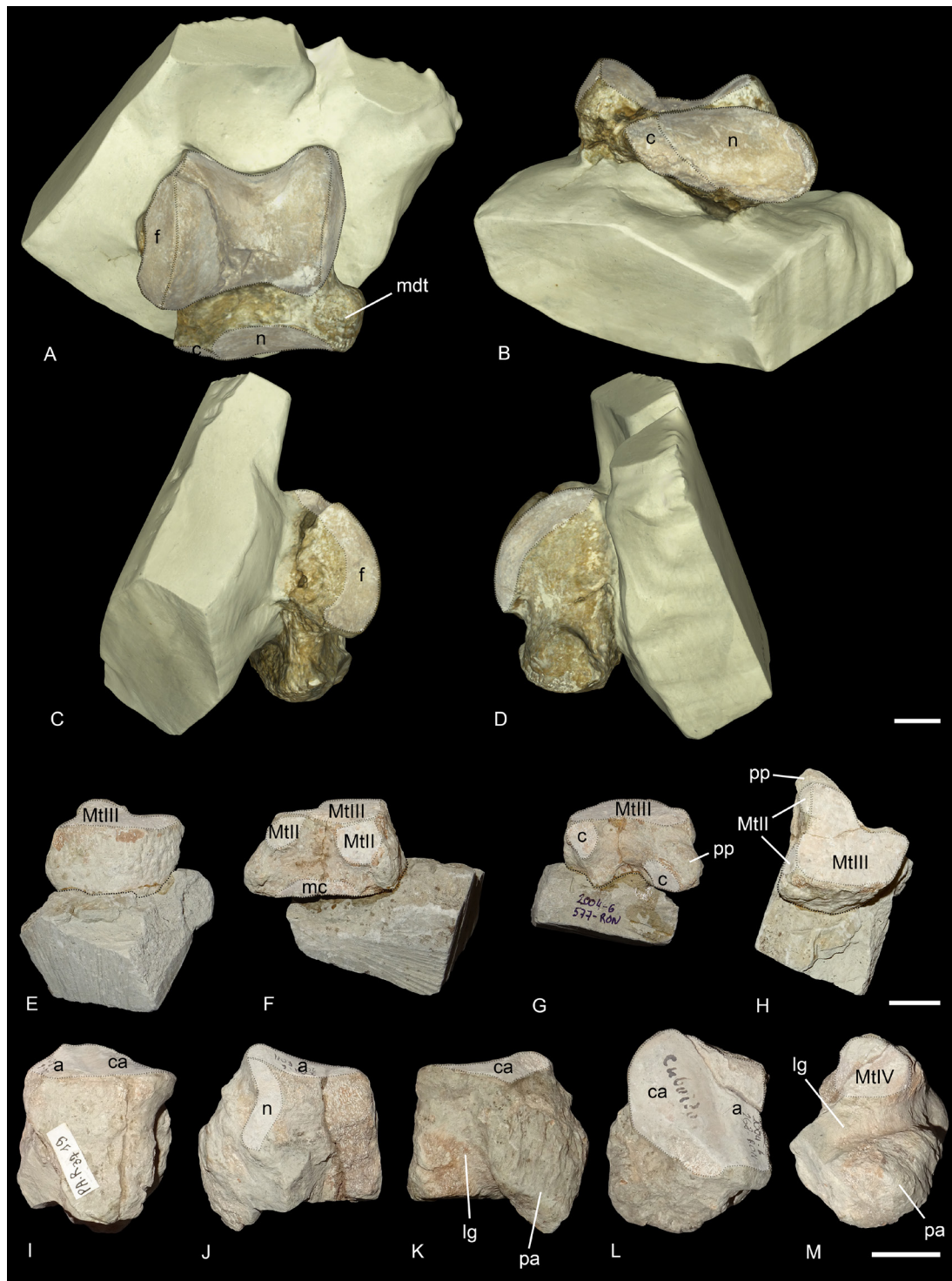
Fig. 7. *Ronzotherium velaunum* (Aymard in Pictet, 1853) from Ronzon (earliest Oligocene, France). – **A–D**. Right astragalus PUY.2004.6.1770.RON. **A**. Anterior view. **B**. Distal view. **C**. Lateral view. **D**. Medial view. – **E–H**. Right ectocuneiform PUY.2004.6.577.RON. **E**. Anterior view. **F**. Medial view. **G**. Posterior view. **H**. With distal border towards the top, and distal view. – **I–M**. Left cuboid PUY.2004.6.268.RON. **I**. Anterior view. **J**. Medial view. **K**. Lateral view. **L**. Proximal view. **M**. Distal view. Abbreviations: a = astragalus; c = cuboid; ca = calcaneus; f = fibula; lg = lateral groove; mc = mesocuneiform; mdt = medio-distal tubercle; n = navicular; pa = posterior apophysis; pp = posterolateral process. Articular surfaces highlighted in white. Scale bars: 2 cm.

Ronzotherium elongatum Heissig, 1969
Figs 8–10

Ronzotherium filholi elongatum Heissig, 1969: 46–55, 68, 71, 116, 119, fig. 18d (from Pernes and
   Kleinblauen).

Rhinoceros filholi – Jenny 1905: 125.
Aceratherium filholi – Jenny 1905: 125. — Roman 1910: 1559 (from Pernes and Kleinblauen); 1912a:
   17, 27, 45–50, 57–58, figs 14.1, 15, 18, pl. V figs 1–2 (from Pernes and Kleinblauen); 1912b: 360–
   364, fig. 2. — Stehlin 1914: 185 (from Kleinblauen). — Gignoux 1928: 148, 151, fig. 3 (from Pernes
   and Kleinblauen).
Praeaceratherium filholi – Spillmann 1969: figs 11, 13, 16.
Ronzotherium filholi – Brunet 1979: 105, table 2 (from Pernes and Kleinblauen). — Becker 2003:
   212–213, 230–231, 234, 256, pl. II fig. a–d (from Kleinblauen); 2009: 490, 493–495, fig. 4h–l, table
   1 (from Kleinblauen). — Ménouret & Guérin 2009: 296 (from Pernes and Kleinblauen).

Non *Ronzotherium filholi elongatum* – Heissig 1969: 46–55, figs 16–17, 18a–c, 19 (from Villebramar,
   Bumbach, Montans, Cournon).

Historical diagnosis

From Heissig (1969), translated by the authors: "A subspecies of *Ronzotherium filholi* with the
following characteristics: corpus mandibulae low, very slender, fossa masseterica deeply concave,
foramen mandibulae at about the level of the teeth neck, strongly enlarged, symphysis long, flat forward;
i2 still shearing towards I1, i1 present; angle of jaw branches very pointed; upper molars elongated
with very broad medisinus, extremely short post-fossette and strong lingual cingulum; upper P3 and
P4 premolariform to semimolariform, P2 molariform, protocone and hypocone widely separated, all
upper premolars strongly widened, inside slightly rounded, metaloph curved and S-shaped, often with
complicated folds, hypostyle missing; lower molars with strong labial cingulum and relatively long
anterolingual cingulum, relatively long, narrow and conspicuously low, talonid pit unclear or notched;
lower premolars, especially p3 often lengthened to the front, protoconid fold strong, metalophid strongly
backwards, labial cingulum strong, p2 strongly narrowed, p1 single-rooted."

However, this diagnosis is not only based on the type material, but also on referred material from other
localities, such as Villebramar or Bumbach that we refer to other species. We thus propose an emended
diagnosis.

Emended diagnosis

The paraoccipital process is poorly developed. The roots of the upper cheek teeth are lingually fused,
P2 is molariform with a lingual bridge connecting the protocone and hypocone, the protocone and
hypocone form a lingual wall on P3 and P4, with a well-marked lingual groove above the cingulum,
especially on P4. Upper premolars usually bear a simple crochet, the protocone is slightly constricted,
the metaloph curved and S-shaped and the hypostyle missing. The protocone is usually constricted on
upper molars and the lingual cingulum is strong and continuous, except under the hypocone of M1–2
and the protocone of M2. The labial cingulum of the lower molars is always present and continuous.

Differs from *Ronzotherium filholi* by the presence of a processus postorbitalis on the zygomatic arch and
by its poorly developed processus paraoccipitalis.

Type material

Holotype

FRANCE • two-parts well preserved skull with almost complete cheek teeth rows, the two parts are joined together by plaster, which does not reflect the original morphology; Vaucluse, Pernes-les-Fontaines; probably MP23; FSL-9601.

Additional material

No other material is known from this locality.

Type horizon and locality

Pernes (= Pernes-les-Fontaines, Vaucluse, France), probably dated from MP23. The 'sands and green sandstones of the Valette-de-Pernes' in which this skull was found, have been dated from MP23 in Murs, another locality 20 km from Pernes.

Stratigraphical distribution

Early Oligocene.

Geographical distribution

France: Pernes. Switzerland: Kleinblauen.

Description

Skull. The skull was originally described by Roman (1912a, 1912b), who attributed it to *Ronzotherium filholi*. It is heavily reconstructed in plaster, especially the frontals and parietals, but it is nonetheless possible to identify the original bony material (Figs 8–9). The nasals are very fragmentary, the anterior part is broken. The lateral apophysis is not preserved. The infraorbital foramen opens above P4. The posterior border of the nasal incision is above P3 and the anterior border of the orbit is above the middle of M1. The lachrymal process is well developed and there is a large postorbital process of the frontals above the orbit. Only the anterior parts of the jugal bones are preserved, and the anterior base of the zygomatic arch is high above the teeth neck. The postorbital process of the zygomatic arch is large and on the jugal. The squamosals are not preserved. The dorsal profile of the skull is difficult to interpret, because of the heavy reconstruction, yet it was probably concave, though not as much as suggested by the reconstruction. The area between the temporal and nuchal crests is very concave. The external auditory pseudomeatus is ventrally open, between the postglenoid and posttympanic apophyses. The nuchal tubercle is well-developed. From the preserved part of the parietal bone, we can observe a wide parietal crest. The occipital crest is concave. In ventral view, the anterior part of the zygomatic arch does not strongly diverge from the maxilla. The vomer is badly preserved. The articular tubercle of the squamosal is smooth and tranversally straight. The postglenoid apophysis is rounded and convex anteriorly, and anteroposteriorly elongated. The foramen nervi hypoglossi is in the middle of the condylar fossa. There is a strong and high sagittal crest on the basilar process of the basioccipital. In occipital view, the paraoccipital and posttympanic processes are fused. The posttympanic process is well-developed and the paraoccipital process is partly broken. The foramen magnum is circular. There is neither a median crest nor a medial truncation on the occipital condyles.

Upper cheek teeth. No anterior teeth are preserved on the skull, only the cheek teeth (Figs 8B–C, 9B–C, 10C–D). The three molars are well preserved on both sides, but the ectolophs of P3–4 are missing, whereas P2 is well preserved and P1 is absent on both sides. There is, however, a single broken root still preserved on the left side which means that this tooth was present in the juvenile at least. The premolar series is short compared to the molar series (LP3–4/LM1–3 = 0.48). There are no enamel folds and the cement is absent. The crown of the cheek teeth is low.
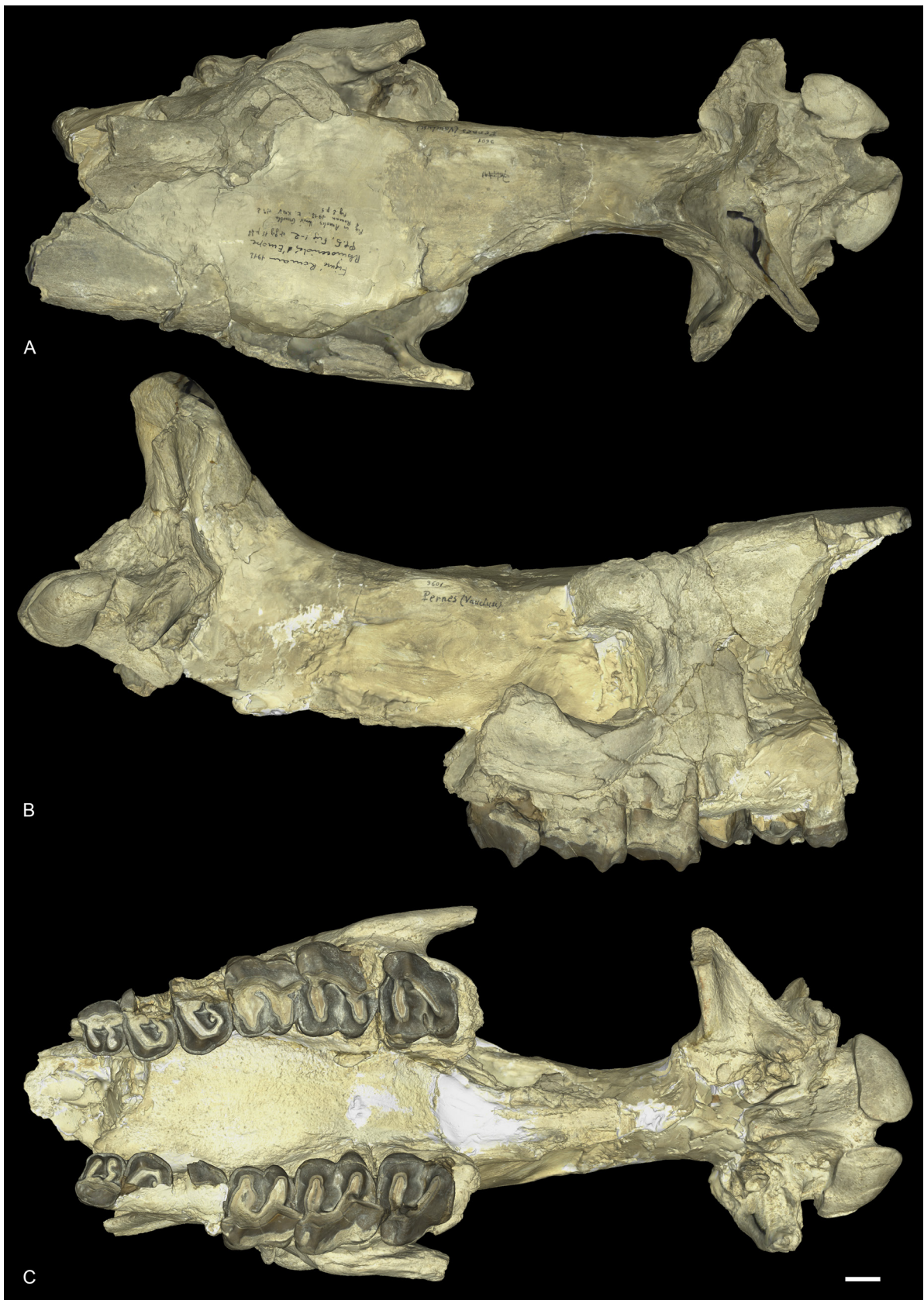
Fig. 8. *Ronzotherium elongatum* Heissig, 1969 from Pernes (early Oligocene?). Skull FSL-9601. **A**. Dorsal view. **B**. Right lateral view. **C**. Ventral view. Scale bar: 2 cm.
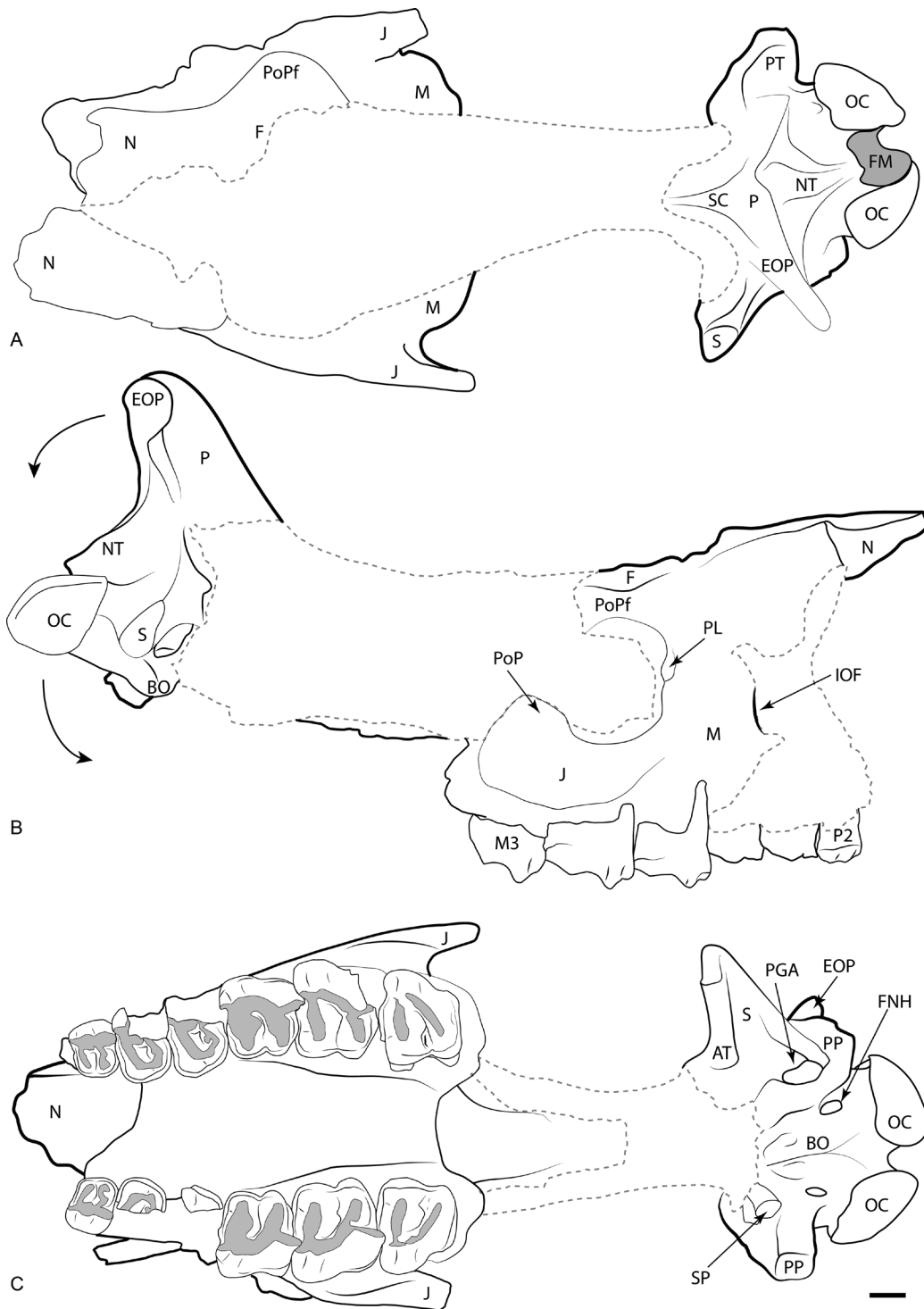
Fig. 9. *Ronzotherium elongatum* Heissig, 1969 from Pernes (early Oligocene?). Drawing of the skull FSL-9601. **A**. Dorsal view. **B**. Right lateral view. **C**. Ventral view. The arrows indicate the hypothetical position of the posterior part of the skull. Abbreviations: AT = articular tubercle; BO = basioccipital; EOP = external occipital process; F = frontal; FM = foramen magnum; FNH = foramen nervi hypoglossi; IOF = infraorbital foramen; J = jugal; M = maxilla; N = nasal; NT = nuchal tubercle; OC = occipital condyle; P = parietal; PGA = postglenoid apophysis; PL = processus lacrimalis; PoP = postorbital process; PoPf = postorbital process of the frontal; PP = paraoccipital process; PT = posttympanic; S = squamosal; SC = sagittal crest; SP = styloid process. Scale bar: 2 cm.
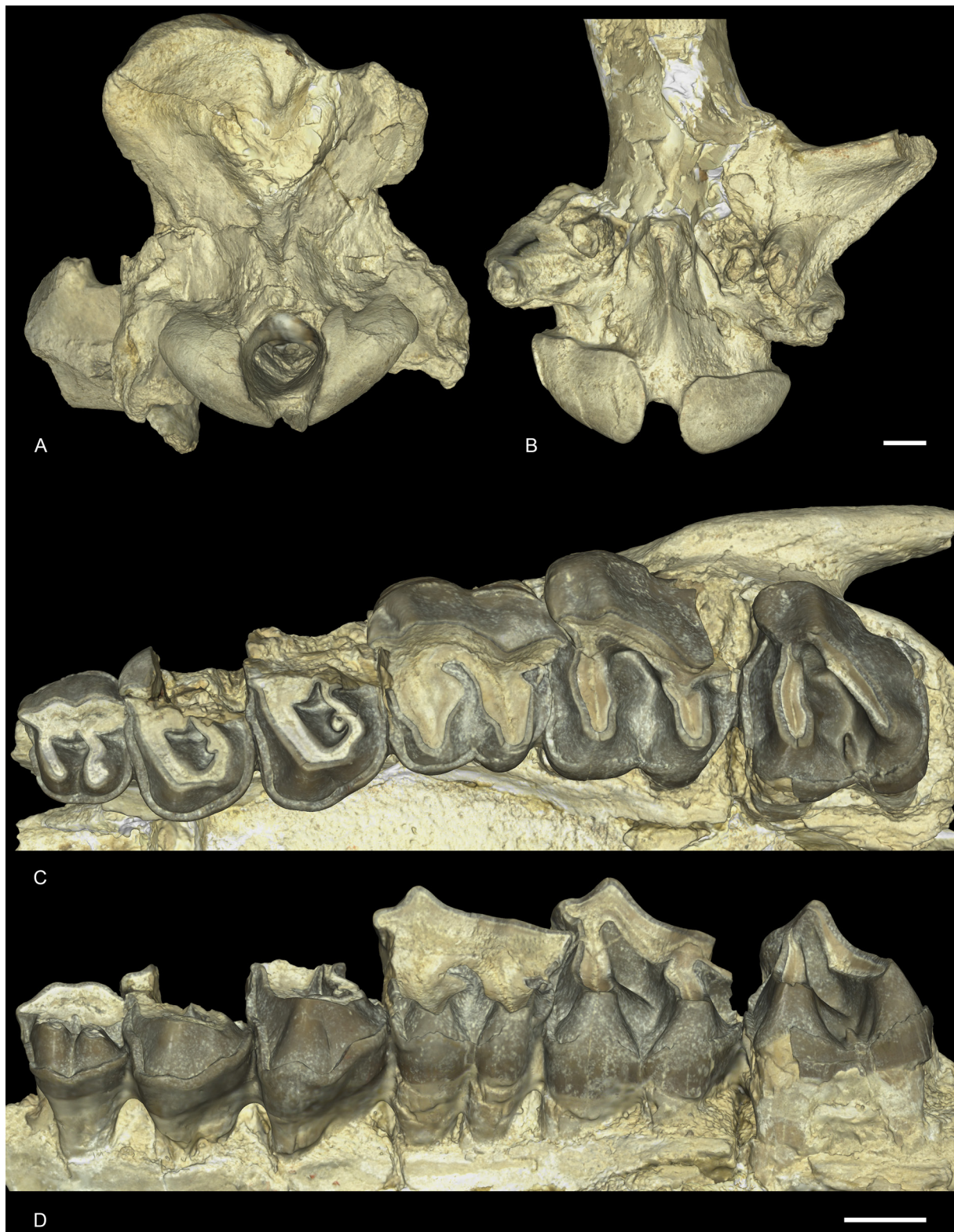
Fig. 10. *Ronzotherium elongatum* Heissig, 1969 from Pernes (early Oligocene?). – **A–B**. Skull FSL-9601. **A**. Posterior view. **B**. Close-up view of the posterior part in ventral view. – **C–D**. Left P2–M3 of the skull FSL-9601. **C**. Occlusal view. **D**. Lingual view. Scale bars: 2 cm.

The labial cingulum is strong and continuous on P2, but the ectolophs are broken on P3–4 so we cannot determine whether it was present or absent. The lingual cingulum is very strong and continuous on P2–4 and is rippled in lingual view, especially on P4. There is a short but well-defined crochet on P3–4. It is simple, directed towards the protocone and completely missing on P2. The metaloph is not constricted and the postfossette is narrow. The antecrochet is always absent. The protocone and hypocone of P2 are connected by a low bridge and are rather equal in size. The protoloph of P2 is directed slightly postero-lingually while the metaloph is S-shaped and transverse. They are both joining the ectoloph. The paracone and metacone folds of P2 are present and wide. The medifossette is always absent on premolars and the protocone is never constricted. The protocone and hypocone of P3–4 form a lingual wall, and a lingual groove is present. The metaloph of P3–4 is S-shaped and directed postero-lingually. The protoloph and metaloph of P3–4 are connected to the ectoloph.

The labial cingulum is strong under the metastyle of M1–2 and the parastyle of M1 but is absent otherwise. The lingual cingulum is also strong and almost completely continuous on all upper molars. It is only fainted under the hypocone of M1 and the protocone of M2. The anterior and posterior cingulum are continuous. The antecrochet is present, but poorly defined and only appears effectively on the protoloph with very strong wear. The crochet, crista and medifossette are always absent on upper molars. The protocone is always weakly constricted. The paracone fold is strong and there is neither a metacone fold nor a mesostyle. The metastyle and metaloph are long and the posterior part of the ectoloph is straight. The hypocone is never constricted and the anterior groove of the metaloph is very shallow or absent. The postfossette is short, but deep, below the posterior cingulum. The ectoloph and metaloph of M3 are completely fused, and the posterior groove is very shallow. It is quadrangular in occlusal view. The protoloph is transverse. There is a small crest in the median valley of the left M3, that seem to have been broken on the right one. It may be caused by individual variation and is completely absent on other molars.

Remark

This species is the most recently one erected, though it was originally considered a subspecies of *R. filholi*. Brunet (1979) and subsequent authors considered it as a junior synonym of *R. filholi*. Based on our comparative work and our phylogeny, we consider it as a valid species.

<div align="center">

Ronzotherium filholi (Osborn, 1900)
Figs 11–14

</div>

Aceratherium filholi Osborn, 1900: 240–243, figs 7, 8a.
Badactherium latidens Croizet, 1841: 79 (nomen nudum).
Rhinoceros brivatensis Bravard, 1843: 408–410 (nomen oblitum).
Rhinoceros incisivus Blainville, 1846: pl. XII (Ongulogrades, 'Auvergne') (misidentification).
Rhinoceros minutus Thomas, 1867: 239 (misidentification).
Rhinoceros tetradactylus Filhol, 1877: 126 (misidentification).
Rhinoceros lemanensis Lydekker, 1886: 153 (from Caylux) (misidentification).
Praeaceratherium minus Koch, 1911: 377–379, 385–387 (misidentification).
Paracaenopus kochi Kretzoi, 1940: 92.
Ronzotherium filholi elongatum Heissig, 1969: 46–55, figs 16–17, 18a–c, 19 (from Villebramar) (misidentification).

Ronzotherium velaunum – Aymard 1856: 235. — Boada-Saña *et al*. 2007: 6.
Rhinoceros brivatensis – Aymard 1856: 235.
Badactherium latidens – Landesque 1888: 21, 27.

Rhinoceros latidens – Landesque 1888: 27.
Aceratherium lemanense – Pavlov 1892: 184, pl. V, fig. 7 (from Quercy).
Ronzotherium filholi – Deninger 1903: 95. — Wood 1929: 2 (= "*Praeaceratherium minus*" = *Paracenopus*). — Lavocat 1951: 116–118 (from Bournoncle). — Brunet & Guth 1968: 573–575, pl. I. — Heissig 1969: 38. — Brunet 1970: 2535; 1979: 105–152, 159–161, figs 8, 9a, c, e, 10a, 11–14, 16b, pls IX–XIV, XVIa, XIXm–n, XX–XXV. — Santafé Llopis 1978: 44. — Antoine 2002: 32. — Becker 2003: 231, pl. IIh (from Bressaucourt); 2009: 493–495, fig. 4g (from Bressaucourt).
Praeaceratherium filholi – Abel 1910: 18–20, 44–45.
Acerotherium filholi – Roman 1910: 1559 (from Quercy and Puylaurens); 1912a: 5, 27, 45, 51–53, fig. 16a (from Quercy, Villebramar and Puylaurens).
Praeaceratherium filholi – Koch 1911: 377–379, 385–386. — Wood 1927: 232/72.
Acerotherium lemanense – Roman 1912a: 60–61 (from Montans).
Aceratherium filholi– Stehlin 1914: 185 (from Bressaucourt).
Paracaenopus filholi – Breuning 1924: 7, 17–20, figs ?6, 7.
? *Aceratherium filnoli* [sic] – Crusafont Pairó 1967: 116.
Ronzotherium filholi filholi – Heissig 1969: 39–46, figs 12–15, 25c–d, 26a–b.
Ronzotherium kochi – Heissig 1969: 36–37. — Adrover *et al*. 1983: 126. — Codrea & Şuraru 1989: 322. — Guérin 1989: 4. — Uhlig 1999a: 477–479. — Codrea 2000: 38–42, fig. 8.
Epiaceratherium ? *kochi* – Brunet 1979: 158.
Allacerops kochi – Russell *et al*. 1982: 58.
"*Ronzotherium*" *kochi* – Radulescu & Samson 1989: 302.
Epiaceratherium sp. – Becker 2009 (= *Ronzotherium kochi*).

Non *Ronzotherium filholi* – Lavocat 1951: 116, pl. 19 fig. 3, pl. 26 fig. 1 (from Vendèze) (misidentification).
Non *Ronzotherium filholi* – Brunet 1979: 105, 134 (from Pernes, Kleinblauen and Bumbach) (misidentification).
Non *Ronzotherium filholi* – Becker 2003: 230–233, pl. IIa–f (from Kleinblauen and Bumbach) (misidentification).
Non *Ronzotherium filholi* – Becker 2009: 493–495, fig. 4h–l (from Kleinblauen) (misidentification).

Historical diagnosis

(From Osborn 1900): "Large upper premolars, simple, unlike molars, with incompletely formed crests; upper molars with internal cingulum and strong protoconule [= paracone] fold, small antecrochet, no crochet; depression in posterior face of metaloph of third molar; third and fourth lower premolars with depressed and incomplete posterior crests. Measurements: P2–M3=224."

However, this diagnosis could refer to several species of *Ronzotherium* since these characters are mostly synapomorphies of the genus. Therefore, we emend the diagnosis based on the type specimens from the Phosphorites du Quercy. Other emended diagnoses were provided by Heissig (1969) and Brunet (1979), but they were not only based on the type material, but also on referred material from other localities. We emend here the diagnosis based on our phylogenetic analysis.

Emended diagnosis

The coronoid process of the mandible is rather weak. The upper premolars are large, simple, non-molariform, with incompletely formed protoloph and metaloph, and labial cingulum always present; P2 molariform, protocone and hypocone usually fused on P3–4, strong, simple and continuous lingual cingulum, usually without ridges; crista sometimes present on P3; metaloph of P2–4 discontinuous; upper molars with strong and continuous lingual cingulum except under the hypocone of M1, almost no labial cingulum, small antecrochet, no crochet, and a posterior groove on the ectometaloph of M3; lower cheek teeth with strong and continuous labial cingulum and lingual cingulum in the opening of the posterior valley; d/p1 usually present and two-rooted, the paraconid of p2 is developed; the magnum facet of the McII is straight; high proximal articulation of the fibula with the tibia; the expansion of the calcaneus facet is wide and low on the astragalus; proximal border of the anterior side of the MtIII straight and intermediate reliefs of the metapodials low and smooth.

It differs from *R. velaunum* by the deep median constriction of the distal humeral articulation and from *R. elongatum* by its close frontoparietal crests, its straight occipital crest and its poorly developed processus posttympanicus and its constricted metaloph on P3–4 (hypocone not connected to the ectoloph).

It further differs from *R. elongatum* and *R. romani* by its sharp angle at the anterior tip of the zygomatic process and the higher posterior side of the scaphoid compared to its anterior side.

Type material

    Holotype
FRANCE • maxilla fragment with right and left cheek teeth rows with P2–M3; Quercy Phosphorites (southwestern France); MNHN.F.QU7232.

    Paratypes
FRANCE • 1 left mandible fragment; Quercy; MNHN.F.QU7202 • 1 right mandible fragment; Quercy; MNHN.F.QU7201.

Osborn (1900) designated a left mandible fragment (MNHN.F.QU7202) also from Quercy as "cotype", which was followed by Heissig (1969), who also added its right counterpart (MNHN.F.QU7201) from the same individual. These two hemimandibles should be regarded as paratypes. The upper and lower anterior dentition are unknown.

    Additional material
Old collections from Quercy are preserved in almost every large European institution, including, but not limited to the MNHN, TLM or NMB, but are problematic because the exact age and locality are unknown. The specimens examined from these collections that we mention in the text are:

FRANCE – **Quercy** • 1 right maxillary fragment with P1-2; MNHN.F.QU16445 • 1 left hemimandible with m1-3; MNHN.F.QU17193 • 1 right scaphoid; NMB-QV-275 • 1 right lunate; NMB-QE-440 • 1 left pyramidal; NMB-QE-433 • 1 left magnum; NMB-QE-472 • 1 left cuboid; NMB-QE-362. – **Bournoncle-Saint-Pierre** • 1 astragalus; MNHN.LIM7.

ROMANIA – **Cluj-Napoca** • 1 right maxilla with P2–M3; MBT 1509.

GERMANY – **Espenhain** • 1 left radius; BSPG-2008-I-44. – **Möhren 4** • 1 left D4; BSPG-1966-XXXIII-47 •1 left MtIV; BSPG-1971-V. – **Möhren 7** • 1 left P1; BSPG-1969-XXIV-151 • 1 left P3; BSPG-1969-XXIV-150 •1 right p3/4; BSPG-1969-XXIV-71 • 1 fragment of left lower molar; BSPG-1969-XXIV-152 • 1 right distal ulna; BSPG-1969-XXIV • 1 right proximal McIII; BSPG-1969-XXIV • 1 fragmentary astragalus; BSPG-1969-XXIV-183 • 1 right MtII; BSPG-1969-XXIV-73 • 1 left MtIII; BSPG-1969-XXIV-156. – **Möhren 11** • 1 right calcaneum; BSPG-1971-V-11.

Type horizon and locality
Unknown horizon and locality in the Phosphorites du Quercy.

Stratigraphical distribution
Possibly restricted to the early Oligocene.

Geographical distribution
France: Phosphorites du Quercy, Bournoncle Saint-Pierre, Villebramar, Penchenat (= Moulinet?), Puylaurens. Germany: Möhren 4, 7/16, 19, 20, Burgmagerbein 8, Ronheim 1, Grafenmühle 6. Romania: Cluj-Napoca. Spain: Montalbán. Switzerland: Bressaucourt.
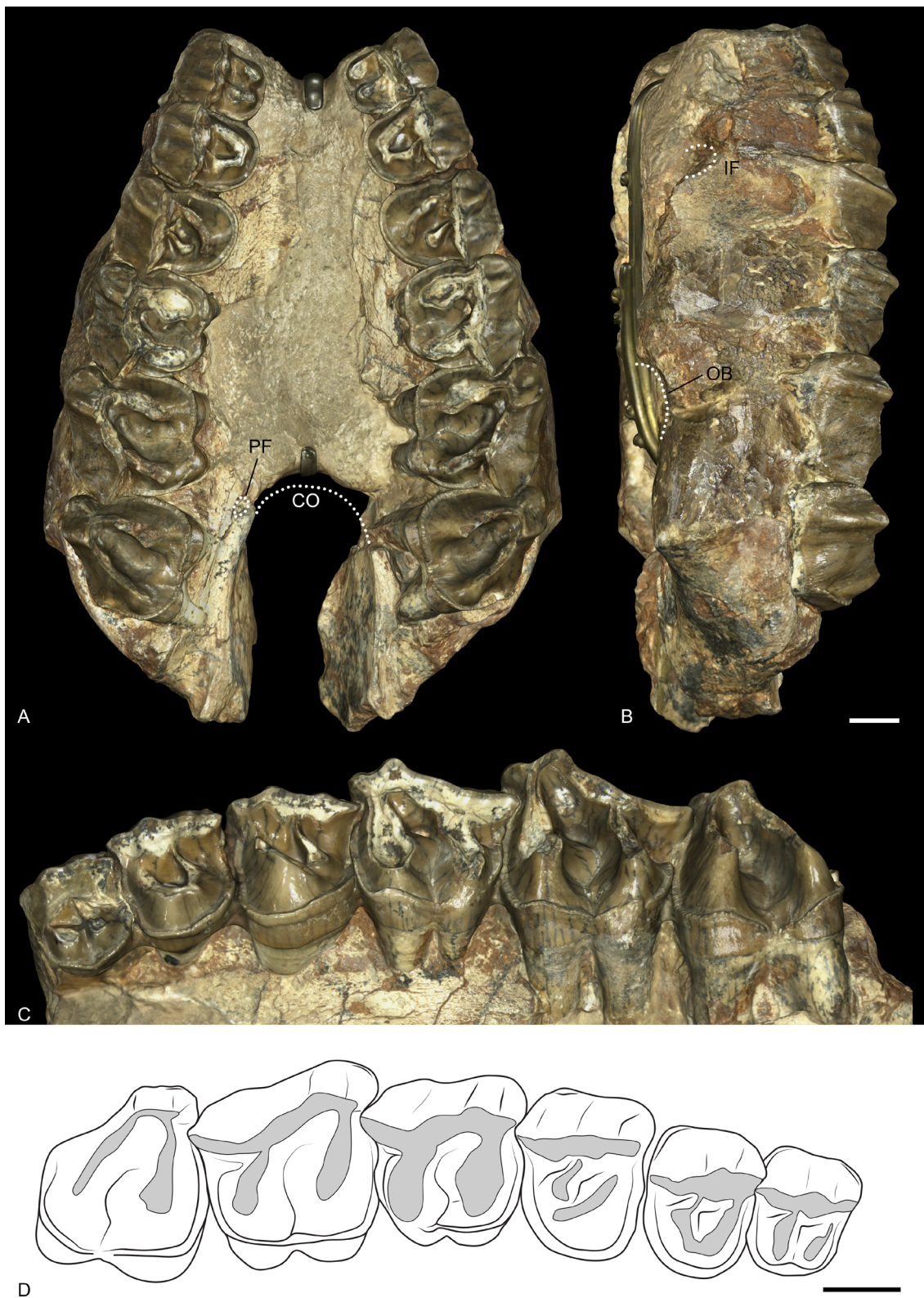
Fig. 11. *Ronzotherium filholi* (Osborn, 1900) from the Phosphorites du Quercy (early Oligocene?, France). Holotype maxilla MNHN.F.QU7232 with P2–M3. **A**. Occlusal view. **B**. Right lateral view. **C**. Left lingual view. **D**. Drawing of the right toothrow with P2–M3 in occlusal view. Abbreviations: CO = choanae opening; IF = infraorbital foramen; OB = orbital border; PF = palatine foramen. Scale bars: 2 cm.

Description

MAXILLA. The right and left maxillae of the holotype MNHN.F.QU7232 are well preserved, and bear P2–M3 on both sides (Fig. 11). The anterior border of the choanae opens approximately at the level of M2 and the palatine foramen is at the level of the anterior border of M3. The infraorbital foramen (still preserved via the infraorbital canal) is located above the anterior border of P4. The anterior border of the orbit is between M2 and M1. The zygomatic arches are broken but the anterior border was above M2 and was high above the teeth neck. The retromolar space behind M3 is short.

Fig. 12. *Ronzotherium filholi* (Osborn, 1900) from the Phosphorites du Quercy (early Oligocene?, France). Paratype left hemimandible MNHN.F.QU7202 with p3–m3. **A**. Lateral view. **B**. Occlusal view. **C**. Medial view. Scale bar: 2 cm.

31

Mandibles. The paratype hemimandibles MNHN.F.QU7202 and MNHN.F.QU7201 are incomplete, the symphysis and the two rami are not preserved (Fig. 12). The foramen mentale was anterior to p3. The base of the corpus mandibulae is straight and the lingual groove is present, though extremely shallow, and barely visible. The foramen mandibulare is located below the teeth neck line. Because of the fragmentary condition of the specimen, no other characters can be observed. From another mandible from Quercy (MNHN.F.QU17193), we can observe that the posterior border of the mandible and the foramen mentale were both located at the level of p2, lingually and labially.

Upper dentition. The cheek teeth have no cement and the crown is low (Fig. 11). The LP3–4/LM1–2 ratio is equal to 0.51, i.e., the premolar row is long compared to the molar row.

The first premolar is not preserved on the holotype MNHN.F.QU7232. Only one P1 was found among the numerous isolated teeth of *Ronzotherium* from Quercy in the MNHN collection, on a maxilla fragment with P2 (MNHN.F.QU16445). It has three roots, two labial and a lingual one. The paracone is the largest cusp, and the paracone and metacone folds are strong. The protocone is extremely weak, and fuses with the strong and continuous lingual cingulum. The protocone connects lingually to the hypocone by a small bridge. The protoloph is very weak and does not fully connect to the paracone. The metaloph is complete and connects the well-developed hypocone to the metacone. The parastyle is weak. The anterolingual cingulum is present. The labial cingulum is strong under the parastyle and the metacone but absent under the paracone.

All upper premolars (P2–4) on the holotype have a very strong and continuous lingual cingulum, which extends anteriorly and posteriorly. The labial cingulum is only present under the parastyle and metastyle, and completely absent under the paracone and metacone. The paracone fold is rather strong and the metacone fold is weak. There is no constriction of the protocone. They have no crista, crochet or antecrochet and the postfossette is narrow. They all bear three roots.

The protocone and hypocone of P2 are equal and connected by a low lingual bridge. The protoloph is weak and directed towards the parastyle, not the paracone, and does not fully connect to the ectoloph. The metaloph is continuous and postero-lingually directed.

On P3, the hypocone is very weak and very poorly differentiated from the protocone by a shallow lingual groove. The protoloph is straight, connected to the parastyle and well developed. The metaloph is thinner, transverse and S-shaped.

The protocone and hypocone of P4 are completely fused, and the protoloph is L-shaped. The metaloph is very weak and it is completely separated from the protocone/hypocone. It is S-shaped, short and connects to the ectoloph between the paracone and the metacone.

Upper molars have four roots. The lingual cingulum is strong and continuous, except under the hypocone of M1, where it is completely fainted. The labial cingulum is almost completely absent except for a few traces either under the parastyle or the metastyle. The paracone fold is strong and the metacone fold is absent. There is a broad and weak mesostyle on the ectoloph of M1. The crochet, crista and medifossette are completely absent and there is no protocone constriction. The posterior part of the ectoloph is straight.

The M1 is square. The antecrochet is broad and distinguished by a postero-lingual groove on the protoloph. The postfossette is very short and shallow. The metaloph and protoloph are transverse. The posterior cingulum is high and continuous.

The M2 differs from M1 by its larger size, the more oblique lophs, a shorter metaloph, and the metacone more lingual. There is no lingual groove of the protocone. The mesostyle is very weak and disappears at the base of the crown.

The M3 is quadrangular but bears no metacone. The metaloph and ectoloph are fused into an ectometaloph. The protocone is not constricted and the protoloph is transverse. The posterior groove on the ectometaloph is present.

LOWER DENTITION. The p1, p2 and anterior dentition are unknown from the paratypes MNHN.F.QU7202 and MNHN.F.QU7201, and from the other mandibles from Quercy (Fig. 12).

Other lower cheek teeth (p3–m3) are double-rooted, low-crowned, and have no cement. The labial cingulum is strong and almost completely continuous, it only vanishes under the ectolophid groove and it is very weak overall on m1. The lingual cingulum is present at the opening of the anterior and posterior valleys. The ectolophid groove is developed until the neck. In occlusal view, the trigonid is very angular and forms a right dihedron while the talonid is rounded. The metaconid of p3 bears a weak anterior crest that is almost joining the anterior branch of the paralophid. There are no vertical rugosities on p3. The talonid of p3–4 is poorly developed and the entoconid is almost completely absent. The hypolophid is very low and the posterior valley is U-shaped in lingual view. The anterior valley opens much higher above the neck than the posterior one. The metaconid of premolars is very large and slightly constricted. The anterior branch of the paralophid is long on molars and premolars. The entoconid of molars is strongly developed and slightly constricted.

POSTCRANIALS. The postcranial remains from the Quercy collection can only be hardly associated with the cranial remains for several reasons. First, almost all specimens belong to 'old' collections, i.e., the exact localities were not specified, and specimens were mixed together and could belong to several loci. Furthermore, the Quercy localities range in age from the early Eocene to the early Miocene, and thus cannot be precisely dated. Therefore, only a few well-preserved postcranial remains are tentatively attributed to ?*R. filholi* and described here.

SCAPHOID. The scaphoid NMB-QV-275 is very well preserved, except for the distal part of the anterior apophysis, which is partly broken (Fig. 13A–D). The posterior height is slightly reduced compared to the anterior. The proximal articulation for the radius is large, and very concave anteroposteriorly. It is lozenge-shaped in proximal view, and very developed laterally. Below and anterior to this proximal facet is the thin and elongated anteroproximal facet for the lunate, which is completely fused to the postero-proximal one. The anteroproximal one is horizontal while the posterior is oblique. The anterodistal facet for the lunate is separated from the proximal ones by a wide groove. This facet is long and low, but hardly distinguishable from the distal magnum facet just below. This distal facet for the magnum is very concave in lateral view and separated from the large medio-distal facet for the trapezoid by a high ridge. The latter is also very concave in lateral view, but very convex mesio-laterally, and bears a large extension on the medial side. The trapezium facet is not reduced and separated from the trapezoid facet by a ridge. It is quite flat and oval-shaped.

LUNATE. The lunate NMB-QE-440 is very poorly preserved and the posterior part is broken (Fig. 13E–I). In anterior view, the distal border is very acute. Three facets are visible in medial view, two small ones are for the scaphoid, while the most distal one, for the magnum, is thin and elongated until the posterior border. On the lateral side, the two facets for the pyramidal are separated by a deep groove. The distal facet is larger than the proximal one. In distal view, the unciform facet is large, almost rectangular and anteroposteriorly concave.

PYRAMIDAL. The pyramidal NMB-QE-433 is perfectly preserved (Fig. 13J–N). The proximal articulation for the ulna is very large, concave anteroposteriorly and convex transversally. The postero-proximal facet for the pisiform is long and drop-shaped. On the medial side, there are two large facets for the lunate, separated by a deep groove. The distal one is symmetrical and slightly curved towards the posterior side. In distal view, the facet for the unciform is triangular and concave anteroposteriorly.

MAGNUM. The magnum NMB-QE-472 is well preserved and complete (Fig. 13O–S). The anterior side is pentagonal, and the proximal apophysis is very high. In anterior view, the anterior border of the scaphoid facet is slightly concave while the distal border is almost completely straight. On the lateral
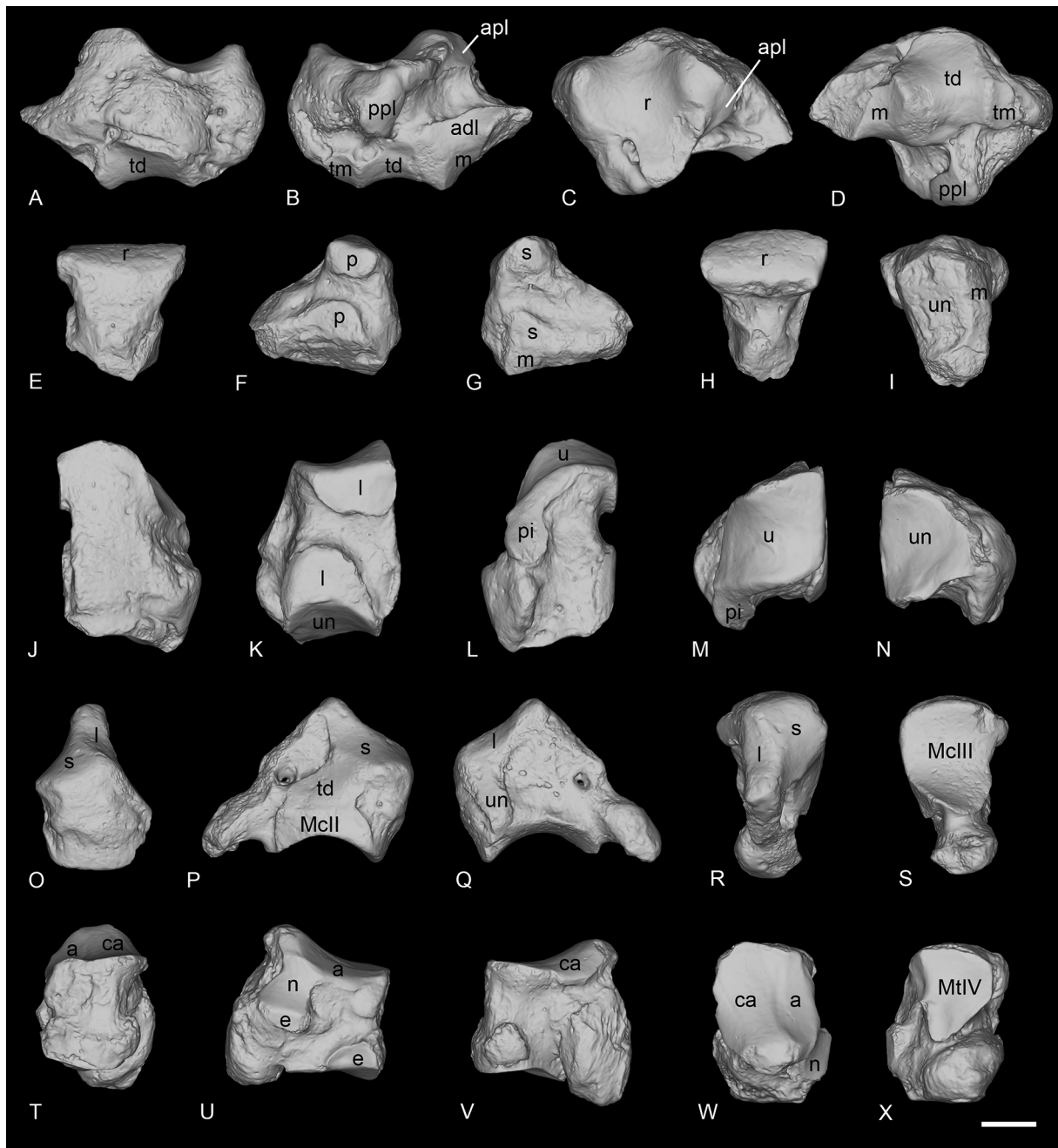
Fig. 13. ?*Ronzotherium filholi* (Osborn, 1900) from the Phosphorites du Quercy (early Oligocene?, France). – **A–D**. Right scaphoid NMB-QV-275. **A**. Medial view. **B**. Lateral view. **C**. Proximal view. **D**. Distal view. – **E–I**. Right lunate NMB-QE-440. **E**. Anterior view. **F**. Lateral view. **G**. Medial view. **H**. Proximal view. **I**. Distal view. – **J–N**. Left pyramidal NMB-QE-433. **J**. Anterior view. **K**. Medial view. **L**. Posterior view. **M**. Proximal view. **N**. Distal view. – **O–S**. Left magnum NMB-QE-472. **O**. Anterior view. **P**. Medial view. **Q**. Lateral view. **R**. Proximal view. **S**. Distal view. – **T–X**. Left cuboid NMB-QE-362. **T**. Anterior view. **U**. Medial view. **V**. Lateral view. **W**. Proximal view. **X**. Distal view. Abbreviations: a = astragalus; adl = anterodistal facet for the lunate; apl = anteroproximal facet for the lunate; ca = calcaneus; e = ectocuneiform; l = lunate; m = magnum; n = navicular; p = pyramidal; pi = pisiform; ppl = postero-proximal facet for the lunate; r = radius; s = scaphoid; td = trapezoid; tm = trapezium; u = ulna; un = unciform. Scale bar: 2 cm.
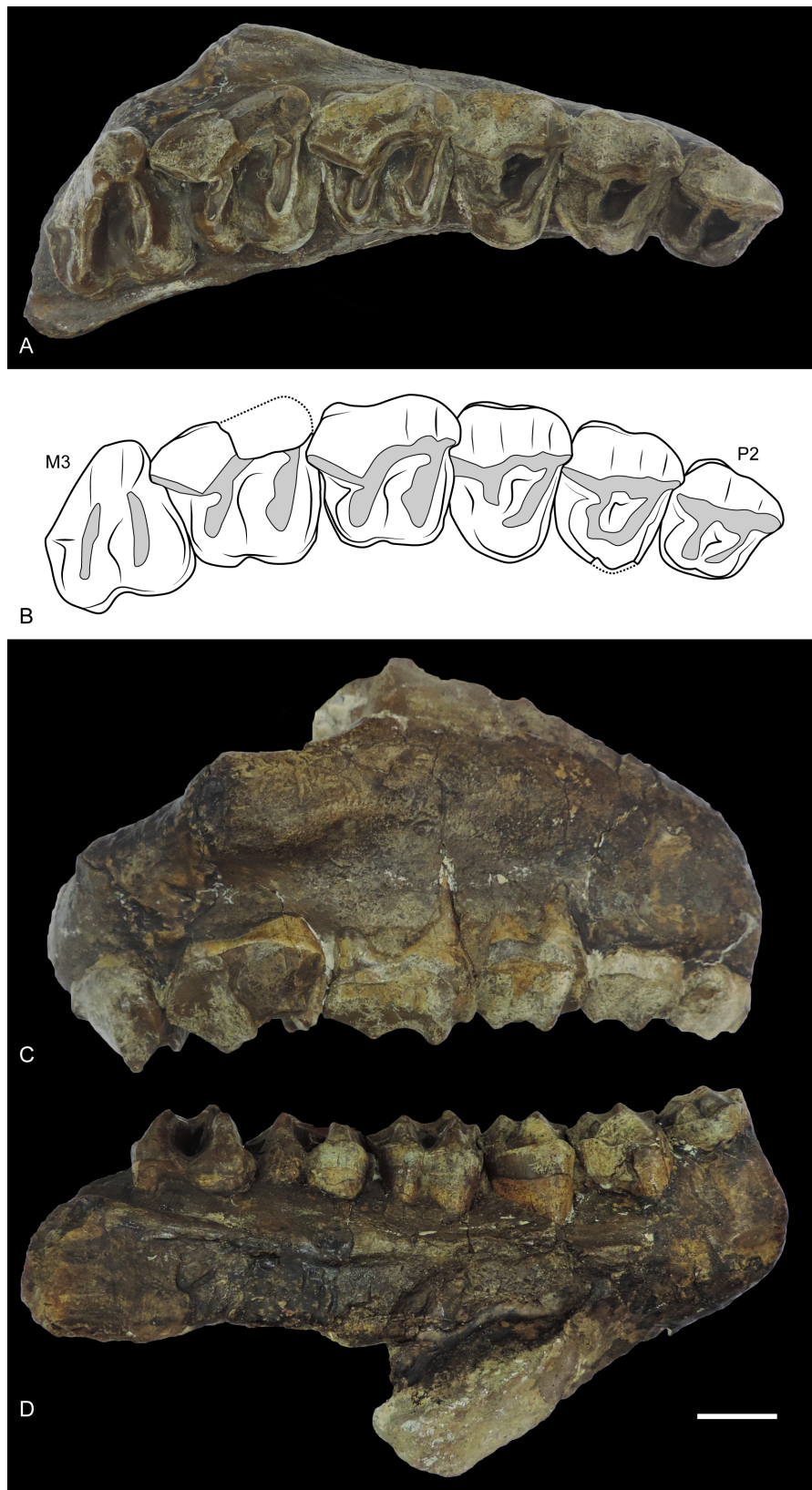
Fig. 14. *Ronzotherium filholi* (Osborn, 1900), senior synonym of *R. kochi* Kretzoi, 1940, from Valea Popii, Cluj-Napoca (earliest Oligocene, Romania). Right maxilla MBT 1509 with P2–M3. **A**. Occlusal view. **B**. Drawing of P2–M3. **C**. Maxilla in lateral view. **D**. Maxilla in medial view. Scale bar: 2 cm.

side, the lunate and unciform facets are fused and form a unique L-shaped facet, occupying all the anterolateral part of the proximal apophysis. Distally, it contacts the distal facet for the McIII. This latter is very concave anteroposteriorly. The posterior tuberosity is very short and curved. In medial view, the distal McII facet and the medial facet for the trapezoid are almost in the same plane; they are only distinguished by a very low ridge, and there is no indentation separating them. The McII facet is flat. The trapezoid facet is large and widely connected to the proximal magnum facet.

Cuboid. The cuboid NMB-QE-362 is perfectly preserved (Fig. 13T–X). In proximal view, the posterior apophysis is almost not visible. The proximal articulation is oval-shaped, and the two surfaces for the astragalus and calcaneus are very poorly distinguished. It is very concave anteroposteriorly and very high at the posterior end. The proximal border of the anterior side is oblique, the distal one is slightly convex while the medial and lateral borders are irregular and are crossed by median grooves. The lateral one is much wider than the medial one and isolates the posterior apophysis. On the medial side, the anterodistal facet for the ectocuneiform is large and anteroposteriorly elongated. The postero-proximal facet for the navicular is very large, concave and bears a thin anterior extension below the proximal articulation. The small and rectangular posterior surface for the ectocuneiform is located almost perpendicular to the postero-distal border of this navicular surface. The distal articulation for the MtIV is a triangular-shaped lozenge and is deeper than wide.

Remark

Ronzotherium filholi is also known from other localities, notably in Villebramar and Bournoncle-Saint-Pierre, where specimens are rather well-preserved. It is found at several localities of South-Germany (e.g., Möhren, Burgmagerbein or Ronheim; Uhlig 1999a), but only by scarce remains. We also consider *R. kochi* from Cluj-Napoca (Fig. 14) as a junior synonym of *R. filholi*. All the material from Villebramar has already been fully described by Brunet (1979) so it will not be described again here. The locality of Villebramar provided by far the broadest sample for *R. filholi*, including a complete skull, several hemimandibles and numerous postcranial remains.

Ronzotherium romani Kretzoi, 1940
Figs 15–21

Ronzotherium romani Kretzoi, 1940: 91.
Hypsolophiodon csobánkanus Kretzoi, 1940: 94–95, fig. 6.
? *Praeaceratherium kerschneri* Spillmann, 1969: 241–253, figs 4 (bottom), 6, 13 (left), 15, pls XX–XXII.
Diaceratherium massiliae Ménouret & Guérin, 2009: 314–323, figs 10, 12a, 13a, b?, c–e, 14a?, 15a, 16a.

Acerotherium filholi – Roman 1910: 1559 (from La Ferté Aleps = La Ferté-Alais, La Comberatière and Marseille); 1912a: 55–56, fig. 17, pl. V–3.
Ronzotherium filholi – Bonis 1969: 1–8, pls 1–2. — Ginsburg 1969: 1267.
Ronzotherium velaunum – Heissig 1969: 20–36, figs 5, 6d, 7, 8d–g, 9c, 10c–d (from St-André, St-Henri, Marseille and Les Milles).
? *Ronzotherium filholi elongatum* – Heissig 1969: 47, 53, 82 (from Cournon).
Ronzotherium filholi romani – Heissig 1969: 55–90, figs 20–24, 26c–d, pls 1–3, 4(13).
Ronzotherium romani – Brunet 1979: 155, figs 7a, 9b, d, 10b, pls XVIb–n, XIXg–l, o–p (from Ferté-Alais, Etampes, Gaimersheim). — Brunet *et al*. 1981: 349. — Ginsburg & Hugueney 1987. — Ménouret & Guérin 2009: 306–314, figs 2, 7–9. — Mennecart *et al*. 2012: 166–169, fig. 3(3, 4?, 5–7, 8?, 9?) (partim). — Ménouret *et al*. 2015: 245–248, figs 4–5a–d.
Diaceratherium lamilloquense – Mennecart *et al*. 2012: 169, figs 3(10–11, 16), 4 (NMB-UM-2565) (partim).
Diaceratherium massiliae – Antoine & Becker 2013: 140. — Jame *et al*. 2019: 21.
"*Diaceratherium*" *massiliae* – Becker *et al*. 2018: 401.
"*Diaceratherium massiliae*" – Blanchon *et al*. 2018: 219.

Non *Ronzotherium filholi* – Lavocat 1951: 116, pl. 19 fig. 3, pl. 26 fig. 1 (from Vendèze).
Non *Ronzotherium romani* – Brunet 1979: 154, fig. 15, pls XVII–XVIII (from Vendèze).
Non *Ronzotherium romani* – Mennecart *et al*. 2012: fig. 4 (NMO-K3/13, NMOI10/103) (partim).

Historical diagnosis

Kretzoi (1940) did not provide any proper diagnosis when he named the species in a footnote. The only mentioned characters are that "the molars have higher crown and less forward inclined, more vertically-standing lophs" than *Ronzotherium filholi* (translated by the authors).

Emended diagnosis

The I1 is oval in cross-section and the crochet and crista are sometimes present on the upper molars. The lingual cingulum of the upper cheek teeth is usually absent. The protoloph of P2 is mostly interrupted and disconnected from the ectoloph. The posterior valley of d2 is usually open. The lingual cingulum of the lower premolars is usually absent. The radius and ulna are in contact or fused and there is a single distal contact facet. The gutter for the musculus extensor carpi is weak on the radius and the proximal ulna facets are not always separated. The trapezium facet is small on the scaphoid. The transverse diameter/height ratio of the astragalus is above 1.2 and the posterior stop on the cuboid facet is absent. The Cc1 facet of the astragalus is nearly flat. The proximal border of the anterior side of the MtIII is concave.

It differs from *R. velaunum* by the deep median constriction of the distal humeral articulation and from *R. filholi* by the absence of i1, the single-rooted d/p1, the reduced paraconid on p2 and the high posterior expansion of the scaphoid facet on the radius.

Type material

   Lectotype (designated by Heissig 1969)
FRANCE • right lower i2; Essone, La Ferté-Alais; MNHN.F.OBP63.

   Paralectotypes (designated by Brunet 1979)
FRANCE • 4 lower molars; same collection data as for lectotype; MNHN.F.OBP72, MNHN.F.OBP76, MNHN.F.OBP78, MNHN.F.OBP79.

   Additional material
FRANCE – **La Ferté-Alais, Essone** • 1 P2; same collection data as for holotype; MNHN.F.OBP55 • 1 P4; same collection data as for holotype; MNHN.F.OBP56 • 1 lingual fragment of P4; same collection data as for holotype; MNH.F.OBP57 • 1 M1; same collection data as for holotype; MNHN.F.OBP59 • 3 M2; same collection data as for holotype; MNHN.F.OBP58, MNHN.F.OBP60, MNHN.F.OBP61 • 1 M3; same collection data as for holotype; MNHN.F.OBP62 • 1 d1; same collection data as for holotype; MNHN.F.OBP86 • 1 p2; same collection data as for holotype; MNHN.F.OBP65 • 2 p3; same collection data as for holotype; MNHN.F.OBP66, MNHN.F.OBP67 • 2 p4; same collection data as for holotype; MNHN.F.OBP68, MNHN.F.OBP69 • 6 additional lower molars excluding the paralectotypes; same collection data as for holotype; MNHN.F.OBP70, MNHN.F.OBP71, MNHN.F.OBP73, MNHN.F.OBP74, MNHN.F.OBP75, MNHN.F.OBP77. – **St-Henri/St-André/Les-Milles** • 1 complete maxilla P1-M2 (left) and P1-M3 (right) with subcomplete mandible with p2–m3 (left) and p3-m3 (right); FSL-8547 • 1 fragment of right maxilla with P1–3; FSL-520275 (not found in collection) • 1 left I1; FSL-8835 • 2 right I2 and 1 left I2, with the same inventory number; NMB-Mar-354a (not found in collection) • 1 left i2; FSL-9445 (not found in collection) • 2 right I2; FSL-9524 (not found in collection) and FSL-9448 • 1 right P1; FSL-9519 • 1 right D3; FSL-8557 • 1 left D4; FSL-9530 • 1 right P2; FSL-8834 • 1 left P2; FSL-8833 • 1 left P3; FSL-8832 • 1 right P4; NMB-Mar-844 • 2 left M3; FSL-8828, NMB-Mar-862 • 2 right M3; FSL-520290 (not found in collection), NMB-Mar-862 • 1 subcomplete mandible with p3–m3 (right) and p2–4 and m2–3 (left); FSL-8545 • 1 right hemimandible with p3–m3; NMB-Mar-843, NMB-Mar-861 • 3 i2; NMB-Mar-862 (right and left), FSL-9524 • 1 d1; FSL-9521 • 2 rows with d2–3; FSL-9520, FSL-9518 (right), FSL-9517, unnumbered specimen (possibly FSL-9519?) (left) • 1 left p3; FSL-8831 • 1 right P4; FSL-520277

37

(not found in collection) • 1 right m1/2; FSL-520277 (not found in collection) • 3 left m2; FSL-8827 (not found in collection), FSL-8829 (not found in collection), FSL-8830 • 1 right m2; FSL-520278 (not found in collection) • 1 right m3; NMB-Mar-1 • 1 left scapula; AIX.1979-2 • 1 distal humerus; FSL-9523 • 1 radius in two fragments; FSL-520279, FSL-520280 • 1 scaphoid; FSL-520285 • 2 trapezoids; FSL-9501, FSL-520283 • 2 unciforms; FSL-520289, FSL-520282 • 1 unciform; NMB-Mar-865 • 1 left McIII; UPM 13667 • 2 fragments of McIII; FSL-9505, FSL-520281 • 1 McIV; NMB-Mar-863 • 1 proximal fragment of McIV; NMB-Mar-864 • 1 McIV; FSL-520287 • 1 distal femur; NMB-Mar-828 • 1 navicular; NMB-Mar-847e • 1 cuboid; FSL-9528 • 1 cuboid; NMB-Mar-847d • 1 MtII, originally identified as a McII by Ménouret & Guérin (2009); NMB-Mar-847a • 1 MtIV; FSL-520286.

GERMANY – **Gaimersheim** • 1 axis and several fragments of vertebrae, 1 complete radius, 1 complete scaphoid and a fragmentary one, 1 partial magnum, 1 broken McIII in articulation with a well preserved McIV as well as an incomplete tibia, 1 almost complete astragalus, and all dental specimens already attributed to *R. romani* by Heissig (1969); BSPG (unnumbered) • 1 left MtIII; BSPG-1952-II.

SWITZERLAND – **Jura Canton, Poillat** • 1 fragment of squamosal; MJSN-POI-007-59 • 1 maxilla with P1–M3; MJSN-POI-007-3219 • 1 isolated I2; MJSN-POI-007-168 • 1 isolated P4; MJSN-POI-007-346 • 1 juvenile hemimandible with i2–p1–m1 and erupting m2; MJSN-POI-007-174 • 1 isolated i2; MJSN-POI-007-937 • 1 isolated p4; MJSN-POI-007-211 • 2 scapulae; MJSN-POI-007-306, MJSN-POI-007-222 • fragments of lumbar vertebra IV; MJSN-PRC-005-1 • 1 sacrum; MJSN-BEU-001-280 • 1 left femur; MJSN-POI-007-80. – **Zürich Canton, Rickenbach** • 1 D3/4; NMB-UM-971 • 1 P2; NMB-Ri-24 • 1 P4; NMO-H9-13 • 1 M1; NMB-UM-972 • 2 M1; NMO-K11/250, NMO-I12/13 • 1 M2; NMO-I12-24 • 1 M2; NMB-Ri27 • 1 maxilla fragment with P4–M1; NMB-UM-1840 • 1 maxilla fragment with M2–3 (unnumbered in SMNS collection); SMNS • 1 mandible with left and right p2–m3; NMB-UM-3832 • 1 p3; NMB-H.R.2 • 1 p4; NMO-L6/25 • 1 m1; NMB-UM-806 • 1 broken humerus; NMB-UM-973 • 1 scaphoid; NMO-I5-62 • 1 lunate; NMB-Ri-21 • 1 lunate; NMO-I7-115 • 1 pyramidal; NMO-I11-82 • 1 magnum; NMO-H10-110 • 1 McIV; NMO-I8-117 • 1 MtII; NMB-UM-2565.

The specimens from St-Henri/St-André/Les-Milles have previously been attributed to "*Diaceratherium*" *massiliae*.

Type horizon and locality

La Ferté-Alais (Essonne, France), MP24 (latest early Oligocene).

Stratigraphical distribution

?MP23 (early Oligocene) to MP30 (latest Oligocene).

Geographical distribution

France: Aubenas-les-Alpes, La Bénissons-Dieu, Brons, La Comberatière, Cournon, Étampes, Gannat?, Itteville, Pech Desse, Sainte-Quitterie, St-Henri/St-André/Les-Milles (= 'Marseille'), Vodable. Germany: Gaimersheim. Hungary: Csobánka. Switzerland: Poillat, Rickenbach, Rüfi bei Schänis.

Description

   Material from the type locality
Part of this material was already described (Heissig 1969; Brunet 1979) but we provide here some short updated descriptions. Only isolated teeth are preserved from La Ferté-Alais.

Anterior dentition. The lectotype right lower i2 (MNHN.F.OBP63) is large and tusk-like (Fig. 15L–M). The root and the tip of the crown are broken, and the enamel is thin. The wear facet for the upper I1 is probably absent, either because of the absence of contact between these two teeth or because the tooth was not completely erupted if it belonged to a young individual. The transverse outline of the crown is drop-shaped, whereas the root is oval-shaped. There is a sharp mesial crest on the mesial border of the crown as well as a weaker crest on the lateral border. There is also a distomesial cingulum.

UPPER CHEEK TEETH. Seven isolated upper cheek teeth are preserved in La Ferté-Alais (Fig. 15A–E), but no upper incisors.

UPPER PREMOLARS. Only P2 (MNHN.F.OBP55) and P4 (MNHN.F.OBP56) are preserved. A lingual fragment of P4 (MNH.F.OBP57) is also preserved but is not informative. The lingual cingulum is strong and continuous on upper premolars and is deeply rippled in lingual view. The labial cingulum is fainted between the paracone and metacone of P4 and completely absent on P2. Crochet and antecrochet are completely absent and there is no protocone constriction. On P2, the protocone and hypocone are separated, but they are united by a bridge at the base of the tooth. The protocone is as strong as the hypocone and the protoloph is separated from the ectoloph. The metaloph is transverse. The paracone and metacone folds are wide and strong, whereas the parastyle is rather weak. On P4, the protocone and hypocone are fused, there is no lingual groove separating them and the protoloph is L-shaped. It is only weakly connected to the ectoloph. The metaloph is weak, S-shaped, directed postero-lingually and does not join the protocone nor the metacone. It joins however the wide and shallow crista at the base of the paracone. The paracone and metacone folds are very strong and separated by a deep groove of the ectoloph. The parastyle is large and the metastyle short. The postfossette is long and narrow.

UPPER MOLARS. Five upper molars are preserved: one M1 (MNHN.F.OBP59), three M2 (MNHN.F.OBP58, MNHN.F.OBP60 and MNHN.F.OBP61) and one M3 (MNHN.F.OBP62). The upper molars have almost no lingual cingulum, except on one M2, where it is strong and continuous under the protocone. The labial cingulum is restricted to the posterior-most part of the ectoloph under the metacone. The antecrochet is strong on M1–2 but very weak on M3. There is a weak crochet on M1–2 that would disappear early with wear and the crista is always absent. There is no protocone constriction. The paracone fold is strong and the metacone fold and mesostyle are completely absent. The metaloph is long but the metastyle is quite short. There is a small hypostyle in the postfossette of M1, contiguous to the strong posterior cingulum. The posterior part of the ectoloph of M1–2 is very straight. The postfossette is deep, below the posterior cingulum. There is no lingual groove of the protocone. The ectoloph and metaloph of M3 are fused into an ectometaloph, and there is no posterior groove. It is quadrangular. The posterior cingulum is strong and continuous and the protocone is not constricted.

LOWER CHEEK TEETH. Sixteen lower cheek teeth are preserved in La Ferté-Alais, including six premolars and ten molars (Fig. 15F–K).

LOWER PREMOLARS. Only one left d1 is known (MNHN.F.OBP86). It is very simple and has two cuspids: a very large protoconid and a small posterior cusp, possibly the hypoconid. There is a small paralophid, weakly constricted, but no anterior valley. The posterior valley is more developed. There is only a very short anterior cingulum but no lingual or labial one. The root is broken. A left p2 (MNHN.F.OBP65) and a left p3 (MNHN.F.OBP66) could have belonged to the same individual, whereas the right p3 (MNHN.F.OBP67) and the right p4 (MNHN.F.OBP68) could have belonged to another. Another left p4 (MNHN.F.OBP69) cannot be attributed to any individual. The p2 and p3 bear labial vertical rugosities whereas p4 only has discontinuous cingulum. The lingual cingulum is weak and only present at the opening of the valleys. The ectolophid groove is angular on p4, but less developed on p2–3, and it always disappears before the neck. The metaconid is very slightly constricted. The entoconid is either completely absent or very weak. The posterior valley is wide and U-shaped on p4 but narrower on p2–3. The paralophid of p2 is not constricted and the anterior valley is absent. The paraconid is reduced. The posterior valley is narrowly open. The anterior branch of the paralophid is long on p3–4.

LOWER MOLARS. The isolated lower molars are difficult to differentiate from one another, so they will be discussed globally. The ectolophid groove is developed until the neck. The trigonid is angular, in right dihedron, while the talonid is rounded. The entoconid and metaconid are very slightly constricted. Lingual cingulum is only present in the posterior valley of one specimen, otherwise it is completely absent. However, the anterolingual cingulum is present in the opening of the anterior valley, though it is weak. The labial cingulum is usually present, anteriorly, labially and in the ectolophid groove, but it is always discontinuous and rather weak. The hypolophid and protolophid are slightly oblique. There is no lingual groove of the entoconid. The anterior branch of the paralophid is high and long. The opening

of the anterior valley is higher than the posterior one. The posterior cingulum is always present, strong and continuous.

Material from other localities

Maxilla and mandible from Poillat. A complete upper tooth row (MJSN-POI-007-3219) and a very well-preserved juvenile mandible (MJSN-POI-007-174) are preserved (Fig. 16) from the recently discovered locality of Poillat, near Delémont (Jura Canton, Switzerland), which also yielded a well-preserved skull of *Epiaceratherium delemontense* Becker & Antoine, 2013, another rhinocerotid (Becker *et al.* 2013). The upper teeth are very worn, indicating a very old individual, but some characters can nonetheless be observed. The P1 is quite large, with a well-developed parastyle, and a single large lingual cusp. The ectoloph is convex. The paracone and metacone folds are strong on P2–4. There is almost no labial cingulum, but the lingual is subcomplete (it slightly faints below the protocone) and waved. The protocone and hypocone of P2 are connected by a lingual bridge. The protoloph is very short and does not connect to the ectoloph while the metaloph is oblique and connects to the paracone. The protocone and hypocone of P3–4 were either fused or connected. The molars have neither lingual nor labial cingulum, except below the metacone and at the opening of the median valley of M3. There is a posterior groove on the ectometaloph of M3.

The juvenile mandible is subcomplete. The symphysis is slightly upraised compared with the corpus mandibulae and its posterior border was just in front of d1. The foramen mentale is below p1 and there is no lingual groove for the sulcus mylohyoideus. The base of the corpus is completely straight, and the ramus is vertical. The coronoid apophysis is large and well-developed. The foramen mandibulare was below the teeth neck.

The i2 is partly unerupted. The d1 is single rooted and very simple. The posterior valley is very small. Lingual and labial cingulum are completely absent on d1–4 and m1 and there are no vertical rugosities on the ectolophid. The protoconid fold is present and the metaconid is slightly constricted on d3–4, but not the entoconid. The paralophid of d2–3 is double and the ectolophid folds are absent. The anterior groove of the ectolophid is present on d2 and its posterior valley is open lingually.

Postcranial remains

Until now, the postcranial skeleton of *R. romani* was almost completely unknown. No remains are preserved in the type locality of La Ferté-Alais and only a few bones were described from St-Henri/St-André/Les-Milles (Ménouret & Guérin 2009) and Rickenbach (Mennecart *et al.* 2012): a scapula, a distal femur, a cuboid and an ectocuneiform from the former locality, and a distal humerus, two astragali and various metapods from the latter. However, after re-examination of the material from Gaimersheim, several postcranial remains can be assigned to *R. romani*: a complete radius, a complete scaphoid, a partial magnum, a broken McIII articulated with a well-preserved McIV as well as an almost complete astragalus and a MtIII. These specimens are of drastic importance because they can be confidently attributed to *Ronzotherium*, contrary to specimens from other localities such as Rickenbach

Fig. 15 (next page). *Ronzotherium romani* Kretzoi, 1940 from La Ferté-Alais (late early Oligocene, France). – **A**. Left P2 MNHN.F.OBP55. **A1**. Occlusal view. **A2**. Lingual view. **A3**. Labial view. – **B**. Left P4 MNHN.F.OBP56. **B1**. Occlusal view. **B2**. Lingual view. **B3**. Labial view. – **C**. Left M1 MNHN.F.OBP59. **C1**. Occlusal view**. C2**. Lingual view. **C3**. Labial view. – **D**. Left M2 MNHN.F.OBP60. **D1**. Occlusal view. **D2**. Lingual view. **D3**. Labial view. – **E**. Right M3 MNHN.F.OBP62. **E1**. Occlusal view. **E2**. Lingual view. **E3**. Labial view. – **F**. Left p2 MNHN.F.OBP65. **F1**. Occlusal view. **F2**. Labial view. **F3**. Lingual view. – **G**. Left p3 MNHN.F.OBP66. **G1**. Occlusal view. **G2**. Labial view. **G3**. Lingual view. – **H**. Left p4 MNHN.F.OBP69. **H1**. Occlusal view. **H2**. Labial view. **H3**. Lingual view. – **I**. Right m1? MNHN.F.OBP71. **I1**. Occlusal view. **I2**. Labial view. **I3**. Lingual view. – **J**. Paralectotype right m3? MNHN.F.OBP72. **J1**. Occlusal view. **J2**. Labial view. **J3**. Lingual view. – **K**. Paralectotype right m3? MNHN.F.OBP79. **K1**. Occlusal view. **K2**. Labial view. **K3**. Lingual view. – **L–M**. Lectotype right i2 MNHN.F.OBP63. **L**. Medial view. **M**. Anterior view. (Labial view towards the top). Scale bars: 2 cm.
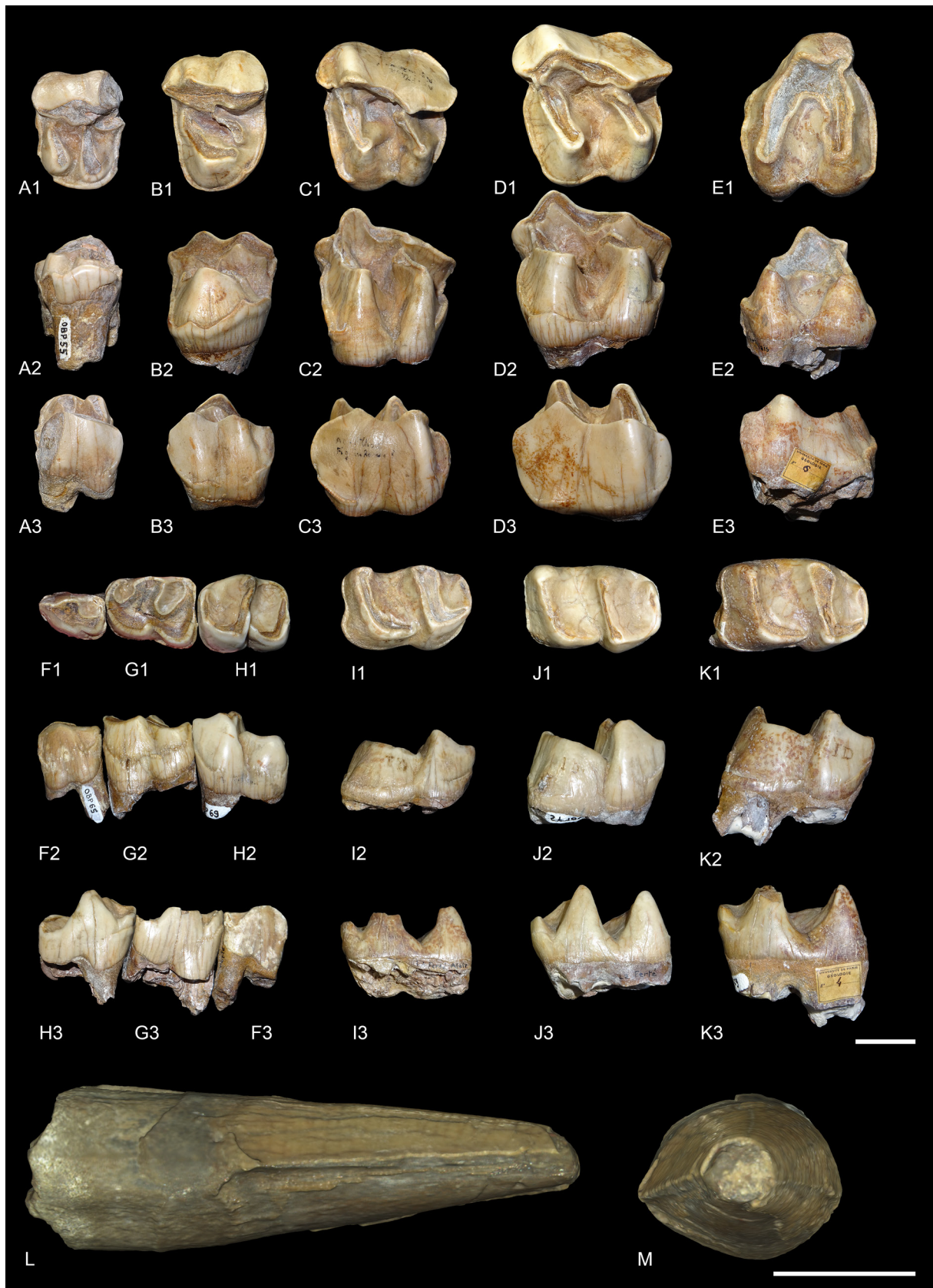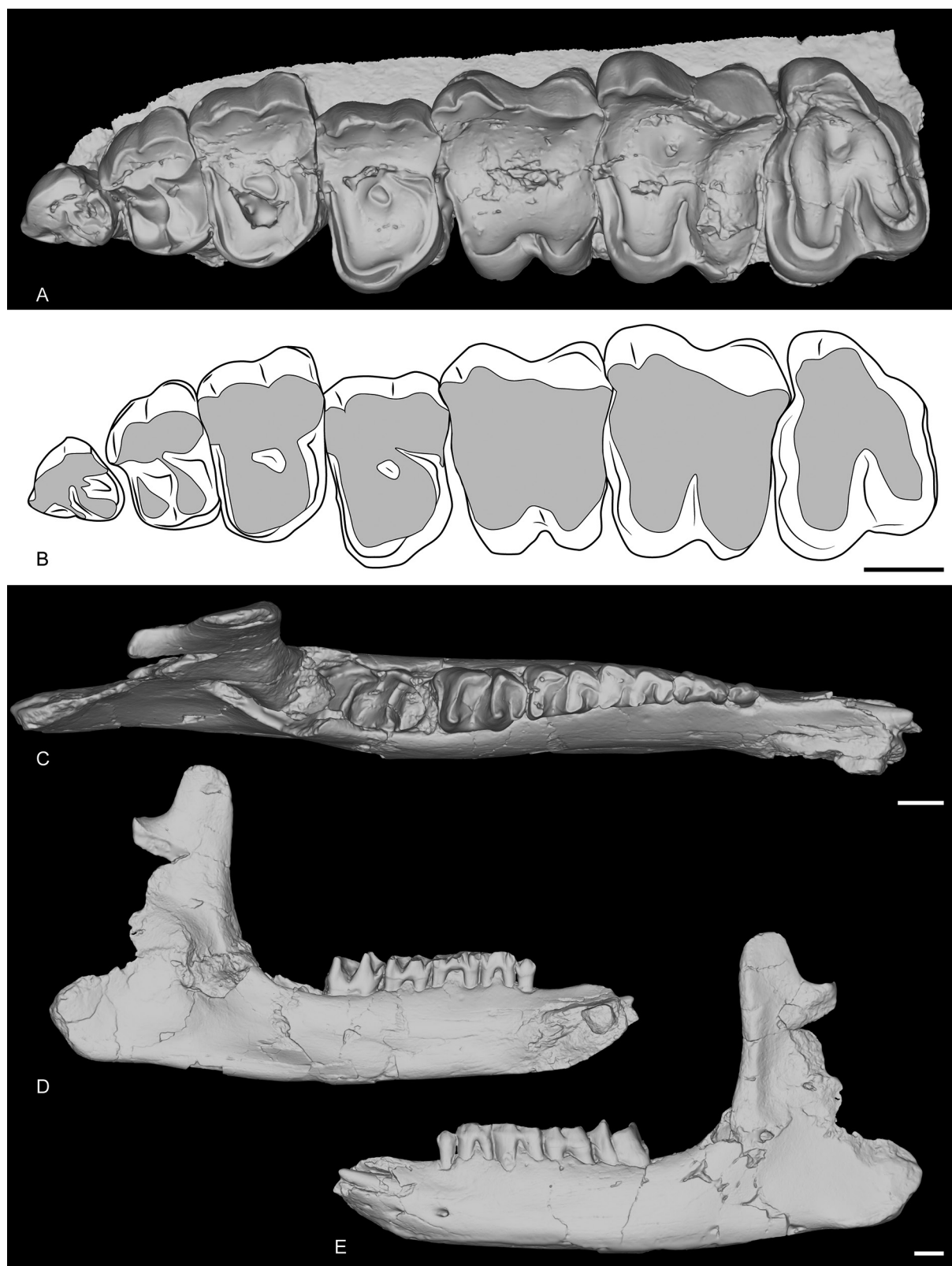
Fig. 16. *Ronzotherium romani* Kretzoi, 1940 from Poillat, near Delémont (late early Oligocene, Switzerland). – **A–B**. Left maxilla MJSN-POI-007-3219 with P1–M3. **A**. Occlusal view. **B**. Drawing of P1–M3. – **C–E**. Right juvenile hemimandible MJSN-POI-007-174 with erupting i2, d1–4, m1 and erupting m2. **C**. Occlusal view. **D**. Medial view. **E**. Lateral view. Scale bars: 2 cm.

or 'Marseille', that were previously partly referred to as the co-occurring *Diaceratherium*, mostly because of their dimensions. Yet, based on fine anatomical comparisons, we now refer most of the specimens from 'Marseille' (Figs 17–18), originally assigned to "*Diaceratherium*" *massiliae* (including the holotype McIV) by Ménouret & Guérin (2009), as well as new specimens from Poillat, Gaimersheim (Figs 19–20) and Rickenbach (Fig. 21), to *R. romani*. Furthermore, the two astragali previously identified as *R. romani* from Rickenbach (Mennecart *et al.* 2012) should in fact be referred to as *Diaceratherium*, while the metatarsals, also identified as *R. romani*, should be referred to as *Mesaceratherium* (Tissier *et al*. 2021). These new attributions show that *R. romani* had a larger size than previously thought and that it was less cursorial than other species of the genus. Throughout the description, comparisons will be made with other ronzothere species as well as with *Diaceratherium*, and in particular *D. tomerdingense*, the type species of the genus, to validate the synonymy of *R. romani* and "*D.*" *massiliae*.

SCAPULA. Two scapulae are preserved from Poillat (MJSN-POI-007-306 and MJSN-POI-007-222), and one from 'Marseille' (AIX.1979-2). The two scapulae from Poillat are complete, whereas the one from 'Marseille' is not. It is very wide, compared to its height (= spatula-shaped, sensu Antoine 2002). In distal view, the medial border of the articulation is straight. The posterior border of the scapula and the glenoid cavity are very concave.

COMPARISON. The scapula of *R. velaunum* is unknown but it is preserved in Villebramar for *R. filholi* (Brunet 1979) and it shares with *R. romani* the very concave posterior border of the scapula and glenoid cavity. The scapula of *Diaceratherium aginense* (Répelin, 1917) from Laugnac (Répelin 1917) widely differs by its reduced width compared to the height (being elongated, sensu Antoine 2002) and its slightly less concave distal border.

HUMERUS. It is known from 'Marseille' and Rickenbach (Fig. 17G–H). The distal fragment of humerus FSL-9523 from 'Marseille' is large-sized and incomplete. The fossa olecrani is low and wide in posterior view and the distal articulation is hourglass-shaped (or 'diabolo-shaped') in anterior view: there is a deep proximal incision between the two lips of the trochlea. However, there is no scar on the trochlea. The epicondylar crest is wide and laterally expanded. In anterior view, the articulation is oblique compared to the shaft of the humerus. The humerus NMB-UM-973 from Rickenbach is the most complete one but is very poorly preserved. The trochiter and the deltoid tuberosity are not preserved. The distal articulation is similar to that of other humeri from 'Marseille' in every aspect.

COMPARISON. The humerus of *R. velaunum* (PUY.2004.6.262.RON) differs by a smaller size and a higher fossa olecrani, as well as a distal articulation not medially constricted in anterior view. It further differs from the humerus from Rickenbach by a less developed lateral epicondyle. The largest humeri of *R. filholi* from Villebramar are more similar in size, in particular compared to the one from Rickenbach (NMB.UM-973). However, Ménouret & Guérin (2009) had referred the humerus from 'Marseille' FSL-9523 to *Diaceratherium massiliae* based on the size difference with *R. filholi*, as well as morphological differences, such as the wide coronoid and olecranon fossae. Yet, the humerus Vil.1970-225 of *R. filholi* from Villebramar (Brunet 1979: pl. XXI, fig. a) is very similar to FSL-9523: the two fossae are wide and the epicondylar crest and lateral epicondyle are equally developed. It only differs by less constricted condyles in anterior view. Furthermore, we believe that another very large humerus from 'Marseille' (FSL-8546; but see Ménouret & Guérin 2009: fig. 10a–b, which is indeed FSL-8546 and not FSL-9523, contrary to the legend of the figure) attributed to *D. massiliae* by Ménouret & Guérin (2009) could in fact come from another locality, based on its very different preservation. Finally, the humeri of *D. tomerdingense* (type species of the genus; SMNS-16154), *D. lamilloquense* Michel, 1987 (NMB-L.M.429) and even *D. aginense* (Répelin 1917: pl.VIII, fig. 1) all have a rather high fossa olecrani in posterior view, and unconstricted condyles in anterior view.

Fig. 17. *Ronzotherium romani* Kretzoi, 1940 from St-Henri/St-André/Les-Milles, near Marseille (late Oligocene, France). – **A–B**. Maxilla FSL-8547. **A**. Occlusal view. **B**. With left P1–M2 in lingual view. – **C, E–F**. Mandible FSL-8547 from the same individual. **C**. Occlusal view. **E**. With left p2–m3 in labial view. **F**. Right p3–m3 in lingual view. – **D**. Left i2 NMB-Mar-862, lingual view. – **G–H**. Left humerus FSL-9523. **G**. Anterior view. **H**. Posterior view. – **I–J**. Right radius FSL-520279+520280. **I**. Anterior view. **J**. Posterior view. Scale bar: 2 cm.

RADIUS. It is preserved from 'Marseille' and Gaimersheim. The radius from 'Marseille' FSL-520279+ 520280 (Fig. 17I–J) is subcomplete, but the distal articulation is poorly preserved. In proximal view, the anterior border of the articulation is straight. The proximal facets for the ulna are separated in posterior view. The lateral one is large and concave. The medial border of the diaphysis is straight in anterior view. In anterior view, the insertion for the m. biceps brachii is marked and deep. The gutter for the m. extensor carpi is very shallow on the distal articulation. The radius from Gaimersheim (BSPG collection, Fig. 19A–D) is complete and very well preserved. It shows that the radius was connected to the ulna over three quarters of the diaphyseal length. In proximal view, the medial articulation facet for the humerus is much larger than the lateral one and they are both concave. The medial articulation for the ulna is a thin lateromedially elongated band, whereas the lateral articulation is large and triangular. Distally, there are two poorly distinguished articulations: a large, medial one for the scaphoid and a smaller one, lateral, triangular and concave anteroposteriorly for the lunate. In posterior view, the extension of the distal articulation for the scaphoid is large and well developed, but wider than high. The distolateral contact area for the ulna is large.

COMPARISON. The radius of *R. velaunum* is unknown. The proximal facets for the ulna from the radii of *R. filholi* are like those of *R. romani*. The radius of *R. filholi* mostly differs from *R. romani* by its deep and wide gutter for the m. extensor carpi on the anterior side of the distal extremity, which is very shallow on the radii from 'Marseille' and Gaimersheim. This deep gutter is also present on a radius from Espenhain (BSPG-2008-I-44), also attributed to *R. filholi*, although the total length of the bone is much smaller than in Villebramar (around 30 cm versus 38 to 41 cm in Villebramar). However, a very deep gutter is also present on the radius of *Diaceratherium tomerdingense* (SMNS-16154), whereas it is shallow on a hand of *D. lemanense* (Pomel, 1853) from Gannat (MNHN-LIM-598). Therefore, there seems to be variation within this character, even among species of a same genus. Finally, Ménouret & Guérin (2009) referred the radius from 'Marseille' to *Diaceratherium massiliae* because they considered that in "*R. filholi* it is the external humeral facet that is the most developed (Brunet 1979: pl. 21)" [translated by the authors], which is actually incorrect. Brunet (1979: 138) in fact states in the description of the material from Villebramar that "[the proximal articulation surface] is composed of two glenoid cavities (a large internal one, long, weakly concave; a smaller external one, thinner and more concave, pl XXIc)" [translated by the authors], which is also the case in the radii described here. The radius of *D. lamilloquense* from Castelmaurou (UM CAM-22) differs by the very concave posterior border of the proximo-medial articulation surface in proximal view, whereas it is straight in *Ronzotherium*.

SCAPHOID. It is preserved in 'Marseille' (FSL-520285, Fig. 18A), Gaimersheim (BSPG collection, Fig. 19E–H) and Rickenbach (NMO-I5-62, Fig. 21G). All three specimens are very well preserved and almost identical. The proximal articulation for the radius is triangular, and concave anteroposteriorly. Posterodistal to the proximal articulation, there is a large lateromedially elongated tuberosity on which occurs an articulation for the lunate (the postero-proximal articulation for the lunate sensu Antoine (2002). This articulation for the lunate is fused with the anteroproximal facet for the lunate on the scaphoids from Gaimersheim and Rickenbach, but they are partly separated by a shallow groove on the specimen from 'Marseille'. The anteroproximal articulation for the lunate is band-shaped and separated from the anterodistal articulation for the lunate by a large and deep groove for ligaments, extending anteroposteriorly, below the proximal tuberosity. On the lateral side, the anterodistal articulation for the lunate is anteroposteriorly elongated, band-shaped and almost fused with the distal magnum facet. The distal articulations for the magnum (anteriorly) and the trapezoid (median) are concave and almost equal-sized. Posterior to these two facets, there is a small articulation facet for the trapezium on the specimens from 'Marseille' and Gaimersheim, that seems to be absent or fused with the trapezoid facet on the specimen from Rickenbach. The anterior and posterior heights of the scaphoid are equal. In medial view, the trapezoid facet is prominent and high, whereas the other facets are not visible.

Comparison. The scaphoid of *R. velaunum* shows many similarities with that of *R. romani*: the anterior and posterior heights are equal, the proximal articulation for the radius is triangular, the anterodistal facet for the magnum is very concave and the facet for the trapezoid is extended anteriorly. However, it differs by a smaller size, a better development of the trapezium facet and a less well developed tuberosity below the proximal articulation. The scaphoid of *R. filholi* is also similar to the scaphoid of *R. romani*, especially in its development of the distolateral apophysis (bearing the magnum facet). The scaphoid from Quercy attributed to ?*R. filholi* is almost identical, and also shows the typical fusion of the anteroproximal and postero-proximal facets for the lunate. The scaphoids of *Diaceratherium asphaltense* (Depéret & Douxami, 1902) from Pyrimont (FSL213008), *D. lamilloquense* (Michel 1983; Duranthon 1990), *D. aginense* from Laugnac (MHNM.1996.17.94) and *D. aurelianense* (Nouel, 1866) from Neuville-aux-Bois (MHNB41.2018.0.282, -.384 and -.866) differ from *R. romani* by a higher posterior height compared to the anterior, a more convex dorsal border in proximal view, a flattened articulation for the magnum, a much more concave articulation for the trapezoid and a larger articulation for the trapezium. Furthermore, *D. aurelianense* also greatly differs by the deep and wide groove separating the anteroproximal and postero-proximal facets for the lunate, as in *Pleuroceros blanfordi* (Antoine *et al*. 2010: fig. 6) or *Teleoceras aepysoma* (Short *et al*. 2019: fig. 45), whereas in *Ronzotherium* they are either completely fused or partly connected, although in *D. lamilloquense* from La Milloque and Castelmaurou they also seem to be fused (Michel 1983; Duranthon 1990). In *D. asphaltense*, this postero-proximal facet seems absent.

Lunate. It is only known from Rickenbach (NMO-I7/115 and NMB-Ri-27, Fig. 21H). One is complete (NMO-I7/115) but the other is broken. The proximal articulation for the radius is large and convex anteroposteriorly. It occupies the whole anteroproximal border, there is no articulation with the ulna. In proximal view, there is a drop-like posterior extension of the radius facet on the medial border. In anterior view, the proximal border is much wider than the distal part. The anterior side is deeply keeled. There are two medial articulations, two lateral and two distal. In lateral view, there is only one proximal articulation facet for the scaphoid, which occupies the whole proximal border, formed by the fusion of the anteroproximal and postero-proximal facets, as on the scaphoid. A shallow groove separates the proximal facet from the distal one. This distal facet for the scaphoid is high, almost triangular and restricted to the anterior portion of the lunate. In medial view, the proximal and distal articulations for the pyramidal are rather small, but they are not in the same plane, the proximal one is more medially displaced. The proximal one is a half oval, whereas the distal one is band-shaped and posteriorly displaced. In distal view, there are two large articulation facets: an anterior one for the unciform, and a distal one for the magnum, very concave, with a thin band-shaped anterior elongation separating the

Fig. 18 (next page). *Ronzotherium romani* Kretzoi, 1940 from St-Henri/St-André/Les-Milles, near Marseille (late Oligocene, France). – **A**. Left scaphoid FSL-520285. **A1**. Medial view. **A2**. Lateral view. **A3**. Proximal view. **A4**. Distal view. – **B**. Right trapezoid FSL-9501. **B1**. Anterior view. **B2**. Lateral view. **B3**. Medial view. **B4**. Proximal view. **B5**. Distal view. – **C**. Right unciform NMB-Mar-865. **C1**. Anterior view. **C2**. Medial view. **C3**. Lateral view. **C4**. Proximal view. **C5**. Distal view. – **D**. Left McIV FSL-520287. **D1**. Proximal view. **D2**. Anterior view. **D3**. Medial view. **D4**. Lateral view. – **E**. Right distal femur NMB-Mar-828. **E1**. Anterior view. **E2**. Distal view. – **F**. Right navicular NMB-Mar-847e. **F1**. Lateral view. **F2**. Proximal view. **F3**. Distal view. – **G**. Right cuboid NMB-Mar-847d. **G1**. Anterior view. **G2**. Proximal view. **G3**. Distal view. **G4**. Medial view. **G5**. Lateral view. – **H**. Left ectocuneiform NMB-Mar-735. **H1**. Proximal view. **H2**. Anterior view. **H3**. Lateral view. **H4**. Medial view. – **I**. Right MtII NMB-Mar-847a. **I1**. Anterior view. **I2**. Lateral view. – **J**. Left MtIV FSL-520286. **J1**. Proximal view. **J2**. Anterior view. **J3**. Medial view. Abbreviations: a = astragal; adl = anterodistal facet for the lunate; apl = anteroproximal facet for the lunate; c = cuboid; ca = calcaneus; ec = ectocuneiform; en = entocuneiform; l = lunate; m = magnum; mc = mesocuneiform; n = navicular; p = pyramidal; ppl = postero-proximal facet for the lunate; r = radius; s = scaphoid; td = trapezoid; tm = trapezium; un = unciform. Scale bar: 2 cm.
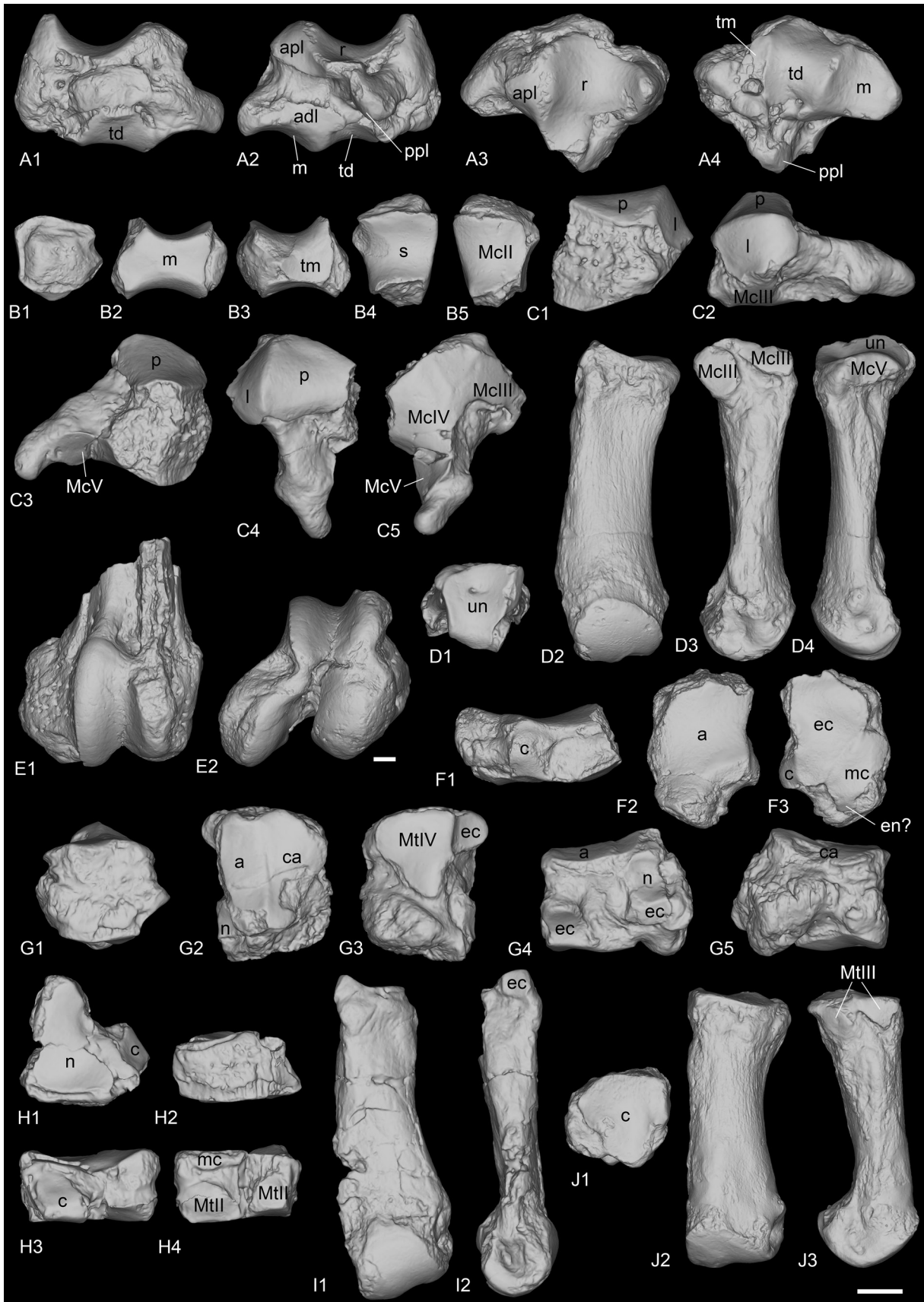
scaphoid facet from the unciform facet. The unciform facet occupies almost all of the distal border of the bone in anterior view and is nearly horizontal. The magnum facet is very small in anterior view and makes a very weak angle with the distal scaphoid facet.

Comparison. Although the lunate of *R. velaunum* from Ronzon is not fully extracted from the sediment, the visible part of the bone is similar to the lunate from Rickenbach. The proximal articulation for the radius is very wide and has a posterior extension. The posterior tuberosity is larger and wider than in Rickenbach. On the medial side, the two facets for the pyramidal are not in the same plane either, though on the specimen from Ronzon, the distal facet is much larger. These characters are also found in the lunate of *R. filholi* from Villebramar (Brunet 1979). However, the lunates of *R. velaunum* and *R. filholi* (both from Villebramar and Quercy) differ by the presence of a shallow groove separating the anteroproximal facet for the scaphoid from the postero-proximal one. The lunates of *Diaceratherium tomerdingense* (SMNS-16157c), *D. aurelianense* (Cerdeño 1993), *D. aginense* (MHNM.1996.17.21) and *D. asphaltense* (FSL-213008) differ by their reduced posterior tuberosity in proximal view, the reduced or absent posterior extension of the proximal facet for the radius and the much more proximo-distally compressed anterior side. They also mostly differ by the wide groove separating the anteroproximal facet for the scaphoid from the postero-proximal one as well as the larger anterior portion of the facet for the magnum (it is almost as large as the distal pyramidal facet). In *D. lamilloquense* from Castelmaurou (TLM.PAL.2014.0.2571), this postero-proximal facet for the scaphoid is either absent or separated from the anterior by a large groove, as in other diaceratheres, and the magnum facet is also rather large anteriorly. On the preserved hand of *D. lemanense* from Gannat (MNHN-LIM-598), the anterior portion of the magnum facet is also very large, as in other diaceratheres but the scaphoid facets are not visible.

Pyramidal. It is only known from Rickenbach (NMO-I11-82, Fig. 21I) and almost complete. The proximal ulna facet is large, saddle-shaped, concave anteroposteriorly, transversally convex and medially elongated. It contacts the long band-shaped postero-proximal pisiform facet. There are two lateral facets for the lunate: the proximal one is half-oval, and the distal one is asymmetrical. They are separated by a wide and shallow groove, and are not exactly in the same plane, in the same way as the two corresponding facets on the lunate. Furthermore, their size, shape and position also fit with it. The distal articulation for the unciform is triangular in distal view and concave anteroposteriorly.

Comparison. This specimen is almost identical to the pyramidal of *R. velaunum* MNHN.F.RZN.502, both in size and morphology. It only differs by a larger distal facet for the lunate, and a deeper groove between the two facets for the lunate. The pyramidal of *R. filholi* is overall also very similar but shows a deeper groove between the two lunate facets, as well as a tubercle on the posterior side, below the unciform facet, which is absent in *R. romani*. The pyramidals of *D. tomerdingense* (SMNS-16157d) and *D. aginense* (MHNM.1996.17.20) differ however by very different proportions: the anterior side is lower and more anteroposteriorly elongated, and the medial side, corresponding to the lunate, is extremely reduced proximo-dorsally. They also differ by their less elongated and drop-shaped facet for

---

Fig. 19 (next page). *Ronzotherium romani* Kretzoi, 1940 from Gaimersheim (late Oligocene, Germany). – **A–D**. Right radius. **A**. Anterior view. **B**. Disto-lateral view. **C**. Distal view. **D**. Proximal view. – **E–H**. Right scaphoid. **E**. Medial view. **F**. Lateral view. **G**. Proximal view. **H**. Distal view. – **I–L**. Left magnum. **I**. Anterior view. **J**. Lateral view. **K**. Medial view. **L**. Distal view. – **M, P–R, U**. Right McIII. **M**. Anterior view. **P**. Posterior view. **Q**. Proximo-medial view. **R**. Proximo-lateral view. **U**. Proximal view. – **N–O, S–T, V**. Right McIV. **N**. Anterior view. **O**. Posterior view. **S**. Proximo-lateral view. **T**. Proximo-medial view. **V**. Proximal view. Abbreviations: adl = anterodistal facet for the lunate; apl = anteroproximal facet for the lunate; h = humerus; im = insertion for the m. biceps brachii; l = lunate; m = magnum; ppl = postero-proximal facet for the lunate; pt = posterior tuberosity; r = radius; s = scaphoid; td = trapezoid; tm = trapezium; u = ulna; un = unciform. All specimens from BSPG collection. Scale bars: 2 cm.
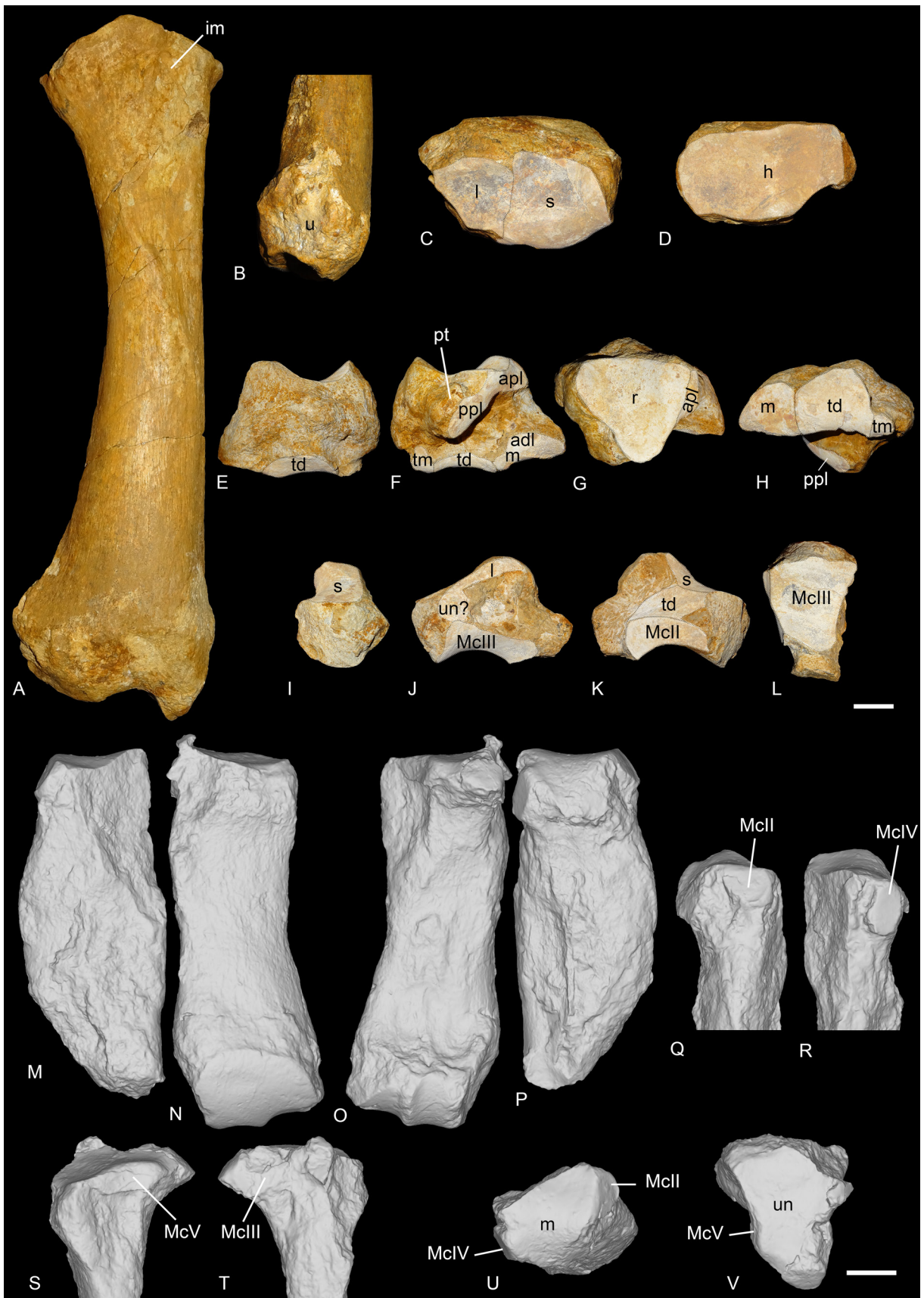
the pisiform and a laterally reduced facet for the ulna. On the medial side, the two facets for the lunate are very small, band-shaped and anteroposteriorly elongated, contrary to the pyramidal of *Ronzotherium*.

TRAPEZOID. Two trapezoids are preserved from 'Marseille' (FSL-9501 and FSL-520283, Fig. 18B). In anterior view, they are wider than high. The proximal border is sigmoid on the specimens from 'Marseille'. The magnum facet occupies the whole lateral side, while the medial side is partly occupied by the extension of the scaphoid facet, and by a subtriangular medio-distal articulation for the trapezium. The proximal side is fully occupied by the anteroposteriorly concave scaphoid facet. The distal articulation for the McII is anteroposteriorly concave.

Fig. 20. *Ronzotherium romani* Kretzoi, 1940 from Gaimersheim (late Oligocene, Germany). – **A–F**. Left astragalus (BSPG collection). **A**. Anterior view. **B**. Posterior view. **C**. Lateral view. **D**. Medial view. **E**. Distal view. **F**. Proximal view. – **G–K**. Left MtIII BSPG-1952-II. **G**. Anterior view. **H**. Posterior view. **I**. Lateral view. **J**. Medial view. **K**. Proximal view. Abbreviations: c = cuboid; Cc1 = calcaneus facet 1; Cc2 = calcaneus facet 2; Cc3 = calcaneus facet 3; ct = collum tali; ec = ectocuneiform; f = fibula; ll = lateral lip; ml = medial lip; n = navicular; t = tuberosity. Scale bar: 2 cm.

COMPARISON. The only other known trapezoid of *Ronzotherium* belongs to *R. filholi* from Villebramar (Brunet 1979). It differs by a flattened distal articulation for the McII and a concave proximal border in anterior view. This trapezoid is also smaller than those that we refer here to *R. romani*, especially anteroposteriorly. Because we lack comparative specimens, especially with the type species *R. velaunum*, we can only tentatively attribute these trapezoids to *R. romani*.

MAGNUM. It is preserved from Gaimersheim (BSPG collection, Fig. 19I–L) and Rickenbach (NMO-H10/110, Fig. 21J). The specimens are partly broken. In anterior view, the proximal border is straight. The anterior side is wider than high. The proximal apophysis is wide, high and very convex. This apophysis is laterally bordered by a long band-shaped articulation for the lunate, that completely fuses anteriorly with the small unciform facet. The proximomedial facet for the scaphoid is larger and concave anteroposteriorly. This facet is very poorly distinguished from the medial facet for the trapezoid. This latter facet is longer than high, and its morphology would fit the shape of the corresponding facet on the trapezoid from 'Marseille'. The trapezoid facet is separated from the medio-distal McII facet by a ridge and by a very short and shallow notch anteriorly. This facet is much longer than high, flat and its distal border is very concave in medial view. On the distal side, the McIII facet is large, trapezoidal, longer than wide and very concave anteroposteriorly. The posterior tuberosity of the magnum is short and straight in Rickenbach.

COMPARISON. The magnum of *R. velaunum* PUY.2004.6.263.RON differs from the specimens from Rickenbach and Gaimersheim by its narrower proximal apophysis. The magnum of *R. filholi* also differs from *R. romani* by its higher and narrower anterior side. The magnum of *Diaceratherium asphaltense* (FSL-213008) only differs by a slightly longer and straighter posterior tuberosity, and by a shorter proximal contact between the trapezoid and scaphoid facets.

UNCIFORM. Three unciforms (FSL-520289, FSL-520282 and NMB-Mar-865, Fig. 18C) are preserved from 'Marseille' according to Ménouret & Guérin (2009) but we only could recover the specimen NMB-Mar-865. It is almost complete, only a small part of the anterolateral side is missing. In anterior view, the two proximal facets for the pyramidal and the lunate are visible. In proximal view, the posterior expansion of the pyramidal facet was probably absent, and the pyramidal and McV facets were probably separated. The McV facet is large, very concave and located posteriorly. The posterior apophysis is thin, curved and 'hook-shaped'. In distal view, the McIII and McIV facets are almost undistinguishable, forming a single large convex facet.

COMPARISON. Only one other unciform of *Ronzotherium* is known, from Ronzon, but it is very incomplete. However, from the remaining part, the dimensions are very similar to those of *R. romani*, and no characters permit to distinguish them. In contrast, the unciform of *Diaceratherium tomerdingense* (SMNS-16157e) strongly differs from that of *R. romani* by its very wide and flattened posterior apophysis, its larger McV facet contacting the pyramidal facet, the much thinner and elongated McIII facet that is well distinguished from the McIV facet and the anteroposteriorly concave McIV facet. The unciform of *D. lemanense* (MNHN-LIM-598) also has a very wide posterior apophysis and a connection between the McV and pyramidal facets. The unciform of *D. aginense* (MHNM.1996.17.98) shows a similar wide posterior apophysis, but the contact between the pyramidal and the McV facets is absent.

McIII. The McIII is overall very badly preserved. In 'Marseille', UPM-13667 is incomplete and poorly preserved, whereas FSL-9505 and FSL-520281 are two proximal extremities (none found in collection). In Gaimersheim (BSPG collection, Fig. 19M, P–R, U), it is very broken and incomplete. The anterior McII facet is large and semi-circular. The posterior McII facet seems absent. The magnum facet is convex anteroposteriorly. On the lateral side, only the posterior McIV facet is preserved, but it was separated from the anterior by a shallow groove.

COMPARISON. The McIII of *R. velaunum* is unknown. One McIII of *R. filholi* is preserved in Möhren 7 (BSPG-1969-XXIV) and differs by the much smaller anterior McII facet. However, the posterior McIV facet is similar and also separated by a shallow groove from the anterior. This groove is larger in Villebramar (Brunet 1979). The McIII of *Diaceratherium* cannot be distinguished based on these characters.

McIV. It is preserved from 'Marseille' (FSL-520287, NMB-Mar-863 and NMB-Mar-864, Fig. 18D), Gaimersheim (BSPG collection, Fig. 19N–O, S–T, V) and Rickenbach (NMO-I8/117, Fig. 21K). In proximal view, the proximal side is lozenge to triangular-shaped. The articulation for the unciform is almost flat anteroposteriorly, but slightly concave lateromedially. On the lateral side, the articulation for the McV is long and low, except on the specimen from Rickenbach where it is reduced and circular. The rugosity of the contact surface for the McV on the lateral border occupies almost half of the diaphysis proximally. On the medial side, two large facets articulate with the McIII (broken on the specimen from Gaimersheim): one is band-shaped and anteroposteriorly elongated on the anteroproximal border, and the other oval-shaped, posterior and separated from it by a groove. These two facets are almost in the same vertical plane. In posterior view, the specimen from Rickenbach differs from the others by its very deep fossa, just above the distal articulation.

COMPARISON. The McIV of *Diaceratherium tomerdingense* (SMNS-16155b) strongly differs by its reduced length (only 9.5 cm), its convex medial border of the diaphysis with a prominent rugose tuberosity on the anteroproximal part of the diaphysis, the anterior McIII facet contacting the posterior one and the deep incision of the posterior border of the unciform facet in proximal view. The McIV of *D. asphaltense* (FSL-213012) also differs by its convex medial border of the diaphysis with a prominent rugose tuberosity on the anteroproximal part of the diaphysis, but the two McIII facets are separated, and the unciform facet is not incised.

SACRUM. A sacrum is preserved from Poillat (MJSN-BEU-001-280). It is quite well preserved and is formed by the fusion of five sacral vertebrae. The neural spines are not fused together and there are four dorsal and ventral sacral foramina on each side.

COMPARISON. Because of the rarity of the preservation of the sacrum, no comparison can be made, either with other ronzotheres or with *Diaceratherium*.

Fig. 21 (next page). *Ronzotherium romani* Kretzoi, 1940 from Rickenbach (late Oligocene, Switzerland). – **A**. Mandible NMB-UM-3832. **A1**. Occlusal view. **A2**. Lateral view. **A3**. Lingual view. – **B**. Left P2 NMB-Ri-24. **B1**. Occlusal view. **B2**. Lingual view. – **C**. Left P4 NMO-H9-13. **C1**. Occlusal view. **C2**. Lingual view. – **D**. Right P4–M1 NMB-UM-1840. **D1**. Occlusal view. **D2**. Lingual view. – **E**. Left M2 NMB-Ri-27. **E1**. Occlusal view. – **F**. Left M2–3 (SMNS collection). **F1**. Occlusal view. – **G**. Left scaphoid NMO-I5-62. **G1**. Medial view. **G2**. Proximal view. **G3.** Lateral view. **G4**. Distal view. – **H**. Right lunate NMO-I7-115. **H1**. Anterior view. **H2**. Proximal view. **H3**. Distal view. **H4**. Lateral view. **H5**. Medial view. – **I**. Right pyramidal NMO-I11-82. **I1**. Anterior view. **I2**. Medial view. **I3**. Proximal view. **I4**. Distal view. – **J**. Left magnum NMO-H10-110. **J1**. Anterior view. **J2**. Medial view. **J3**. Distal view. **J4**. Lateral view. – **K**. Right McIV NMO-I8-117. **K1**. Anterior view. **K2**. Medial view. **K3**. Lateral view. **K4**. Proximal view. – **L**. Left MtII NMB-UM-2565. **L1**. Proximal view. **L2**. Anterior view. **L3**. Lateral view. Abbreviations: adl = anterodistal facet for the lunate; apl = anteroproximal facet for the lunate; ec = ectocuneiform; l = lunate; m = magnum; mc = mesocuneiform; p = pyramidal; pi = pisiform; ppl = postero-proximal facet for the lunate; r = radius; s = scaphoid; td = trapezoid; tm = trapezium; ul = ulna; un = unciform. Scale bar: 2 cm.
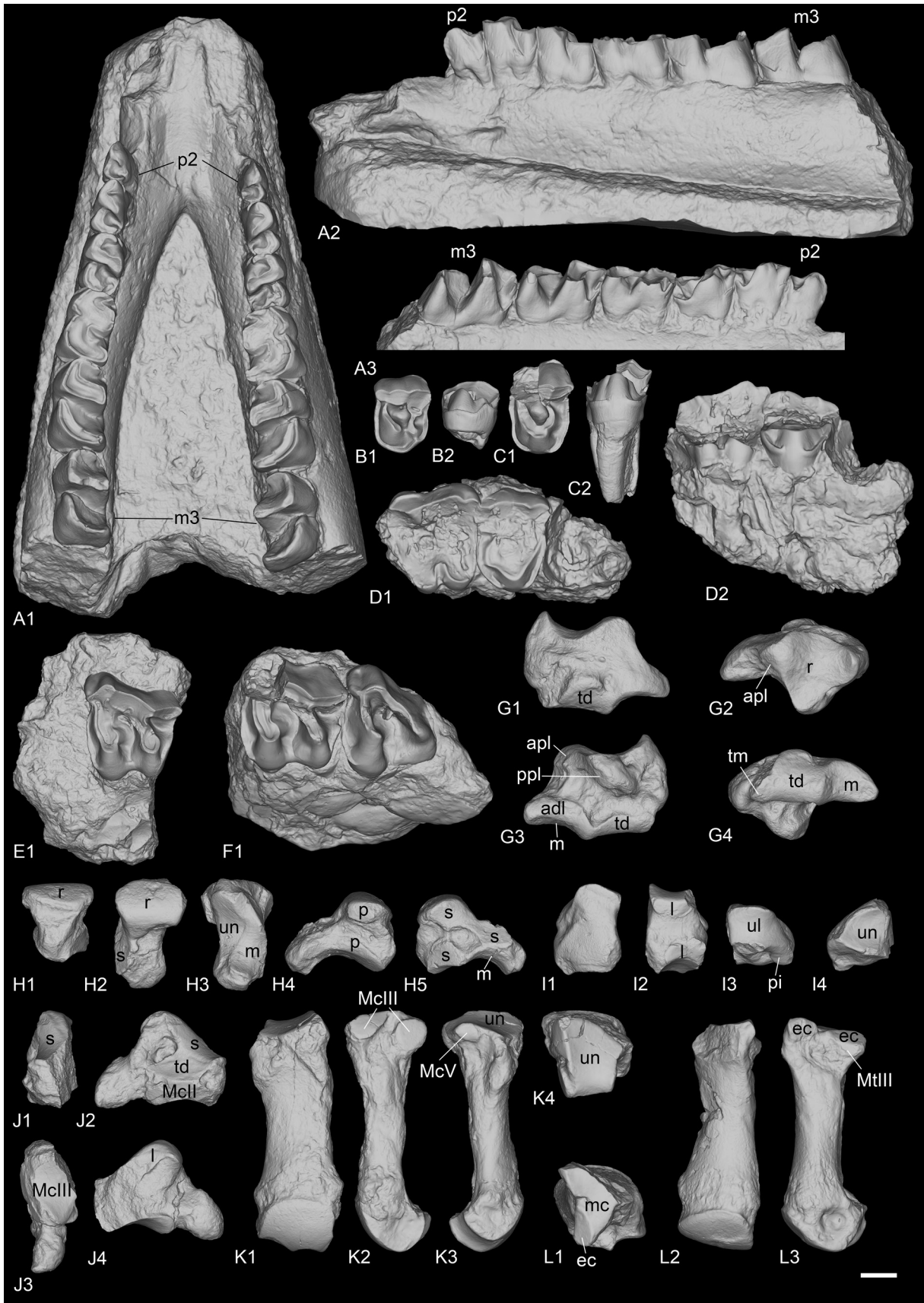
FEMUR. Only a very poorly preserved but subcomplete femur is known from the locality of Poillat (MJSN-POI007-80). The distal articulation is only known in 'Marseille' (NMB-Mar-828, Fig. 18E). The head of the femur is rounded, and the fovea capitis is deep. The smaller trochanter is only preserved on the specimen from Poillat, and it is very small. The third trochanter, the medial condyle and the medial lip of the trochlea are not preserved. The lateral condyle is protruding posteriorly, far behind the diaphysis and the lateral epicondyle is present but not very developed laterally.

COMPARISON. There are almost no characters preserved that permit to distinguish the femur of *R. romani* from other ronzotheres, or from *Diaceratherium* but it is overall very similar to the femur of *R. velaunum* from Ronzon.

TIBIA. It is only known from Gaimersheim (BSPG collection), and only its medial half is preserved. The medial articulation surface is circular and concave in proximal view and the medial intercondylar tubercle is present. The medial border of the diaphysis is slightly concave. In the distal part, the mediodistal gutter is not preserved and the posterior apophysis is broken. The ridge delimitating the two distal condyles is wide and low. The fibula is unknown.

COMPARISON. Based on what is left from this tibia, it only seems to differ from *Ronzotherium velaunum* (PUY.2004.6.260.RON and PUY.2004.6.261.RON) in having a larger size. However, it is slightly shorter than the tibiae of *R. filholi* from Villebramar. There are too few characters visible on the tibia from Gaimersheim to compare it with those of *Diaceratherium*, which also have a very similar size.

ASTRAGALUS. It is preserved from Gaimersheim only (BSPG collection, Fig. 20A–F) and slightly eroded but complete. It is wider than high (TD>H) and its APD/H ratio is high (around 0.78). On the lateral side, the fibula facet is large, flat and vertical. In anterior view, the lateral lip is larger than the medial one, and the groove between the two lips is wide. The collum tali is very high, the two lips of the trochlea do not contact the distal articulation at all. The distal articulation for the navicular is concave in anterior view. In distal view, this articulation is a parallelogram, and it bears a proximal extension on the posterior side of the astragalus. Lateral to the articulation for the navicular, there is a smaller, almost flat and anteroposteriorly elongated facet for the cuboid. This facet is posteriorly broken, and the posterior stop is thus not preserved. In distal view, the trochlea is oblique compared to the distal articulation. In proximal view, the posterior border of the trochlea is sinuous. In posterior view, the three facets for the calcaneum, Cc1, Cc2 and Cc3, are distinct. The Cc1 facet is the largest and it bears a low and wide distal extension on the lateral side. It is rather triangular, and almost flat in lateral view. It is separated from the Cc2 by a deep proximal fossa, and from the Cc3 facet by a wide groove. The Cc2 facet is almost contacting the Cc3 facet by a very thin bridge and it is oval-shaped and slightly proximodistally elongated. There is a strong, rounded tuberosity medial to this Cc2 facet and separated by a large and deep proximodistal groove. Distally, the Cc3 facet is low and band-shaped, but partly eroded. The medio-distal tubercle of the astragalus is broken.

COMPARISON. The astragalus of *R. velaunum* (PUY.2004.6.1770.RON) shares with the astragalus of *R. romani* the very high collum tali and the absence of contact between the trochlea and the distal border, the large lateral lip compared to the medial one, the wide groove between the two lips of the trochlea, the large and flat fibula facet, the transversally concave distal navicular facet and the oblique trochlea compared with the distal articulation, in distal view. These same characters are also found on the astragalus of *R. filholi* from Villebramar. Unfortunately, the posterior side of the astragalus of *R. velaunum* is still in sediment. Another astragalus (MNHN.LIM7) attributed to *R. filholi* from Bournoncle-Saint-Pierre is also very similar but it shows an even more laterally offset lateral lip of the trochlea. It shares, however, the deep proximal fossa separating the Cc1 and Cc2 facets, the oval-shaped and proximodistally elongated Cc2 facet, and the band-shaped Cc3 facet. However, on this specimen, the Cc1 facet is very concave in

lateral view and the Cc2 facet is connected to the Cc3 by a very wide band, contrary to the specimens from Gaimersheim and Villebramar (flattened sagittally). Also, the distal extension of the Cc1 facet is long, thin and drop-shaped. The astragalus of *Diaceratherium lemanense* from Gannat (NMB-Gn-158), as well as the astragali of *D. aginense* from Laugnac (MHNM.1996.17.41, -.55 and -.77) differ from the astragalus of *R. romani* in having a more visible and more concave facet for the navicular in anterior view, a lower height, a lower collum tali, more rounded lips of the trochlea, a larger and circular Cc2 facet, completely independent Cc2 and Cc3 facets, a concave Cc1 facet in lateral view and a reduced distal extension of the Cc1 facet.

The calcaneum, meso- and entocuneiform remain unknown for *R. romani*.

NAVICULAR. It is only preserved in 'Marseille' (NMB-Mar-847e, Fig. 18F). It is quite large, longer than wide and pretty high. The proximal articulation for the astragal is slightly anteroposteriorly concave and occupies the whole anterior side. The distal side is occupied by two poorly distinguished facets: a large, anterolateral and almost triangular one for the ectocuneiform, and a smaller one, rectangular and located postero-medially, for the mesocuneiform. There is possibly a third very small facet for the entocuneiform, but it cannot be distinguished from the mesocuneiform facet. On the lateral side, there is a single posterior and convex articulation for the cuboid. The cross-section of the navicular is lozenge-shaped.

COMPARISON. The navicular of *Ronzotherium velaunum* is not preserved from Ronzon, but one specimen is known in Haag 2 (unnumbered in BSPG collection). It shares a very similar shape in proximal view, with a distinct posterior notch, as well as the absence of an anterior cuboid facet and a similar concavity in lateral view. The only other known navicular of *Ronzotherium* belongs to *R. filholi* from Villebramar (Brunet 1979). Its morphology is very similar and it basically only differs by its slightly smaller size. The navicular of *D. lamilloquense* (Michel 1983) differs by its shape, it is as long as wide, and by the presence of an anterolateral facet for the cuboid. It also differs by its distal facets: the mesocuneiform facet is triangular and slightly convex, the entocuneiform facet is oblique, and the three cuneiform facets are distinguishable and separated. The navicular of *D. aginense* is also as wide as long and differs by its distal articulation surfaces. The navicular of *D. aurelianense* (Cerdeño 1993) also differs by its overall shape, by the two facets for the cuboid, and by a strong angle between the distal ento- and mesocuneiform facets.

ECTOCUNEIFORM. Only one ectocuneiform is known for *R. romani*, from 'Marseille' (NMB-Mar-735, Fig. 18H). The proximal articulation for the navicular is roughly triangular, concave and longer than wide. The postero-lateral process is absent. The lateral side bears two facets for the cuboid, a large and oblique anterodistal one, and a smaller postero-proximal one. The groove separating these two is rather deep. On the medial side, the mesocuneiform facet is thin, low, elongated and located postero-proximally whereas the two distal articulations for the MtII are rather large. The anterior one is concave whereas the posterior one is larger and convex. The distal articulation for the MtIII is triangular. In anterior view, the distal border is sinusoidal.

COMPARISON. The ectocuneiform of *R. velaunum* (PUY.2004.6.577.RON) slightly differs by its smaller and vertical anterodistal facet for the cuboid and its smaller posterior facet for the MtII. The ectocuneiform of *R. filholi* from Villebramar (Brunet 1979) only differs by its slightly smaller size. The ectocuneiform of *Diaceratherium* greatly differs from *Ronzotherium*. The ectocuneiform of *D. lamilloquense* from La Milloque (Michel 1983) differs by the presence of a facet for the MtIV below the anterior facet for the cuboid and by a less elongated and triangular facet for the mesocuneiform, that is located more anteriorly than in *Ronzotherium*. The ectocuneiform of *D. lamilloquense* from Castelmaurou (Duranthon 1990)

differs by the presence of a third articulation facet for the cuboid. The one of *D. aurelianense* from Artenay differs by the fusion of the two distal facets for the MtII (Cerdeño 1993).

Cuboid. It is preserved in 'Marseille' (FSL-9528 and NMB-Mar-847d, Fig. 18G). The anterior side is approximately as high as wide. In anterior view, the proximal articulation is posteriorly elevated. In proximal view, the posterior apophysis is almost not visible, the proximal side is occupied almost exclusively by the two articulation surfaces, for the astragalus on the medial side, and for the calcaneus laterally. The proximal side is trapezoid and the astragalus and calcaneal facets are almost equal-sized. On the medial side, the postero-proximal and elongated facet for the navicular is concave and contacts the small, square and postero-mesial facet for the ectocuneiform. The navicular facet bears a thin extension up to the anterior border, bordering the astragalus facet. The small anterodistal facet for the ectocuneiform is separated from the posterior one by a wide groove. On one specimen (NMB-Mar-847d), this anterodistal facet is very developed and deeply concave, with a strong medial extension, that is not visible on the other specimen. There is no articulation facet on the lateral side, but a large and deep groove, obliquely and forward oriented, which serves as a 'slideway' for the tendon of the m. fibularis longus and isolates the posterior apophysis of the cuboid from the main body of the bone. In distal view, the distal articulation for the MtIV is almost flat and triangular.

Comparison. The cuboid of *R. velaunum* (PUY.2004.6.1309.RON and PUY.2004.6.268.RON) differs from that of *R. romani* by its smaller and oval-shaped distal articulation for the MtIV, by its shallow groove separating the proximal calcaneal facet from the astragalus one, and by its slightly shorter proximal articulation. All other characters are overall very similar to those of *R. romani*. The cuboid of *R. filholi* from Villebramar is poorly preserved, but it differs nonetheless by its slightly shorter posterior height, at the level of the posterior apophysis. The cuboid from the Quercy (NMB-QE-362) tentatively referred to ?*R. filholi* differs by its very different morphology of the anterior side, the absence of ridge separating the proximal astragalus and calcaneal facets and its more posteriorly elevated proximal articulation, but resembles *R. romani* by its very similar medial articulations for the ectocuneiform and navicular. The cuboid of *Diaceratherium asphaltense* (FSL-213014) from Pyrimont-Challonges greatly differs from *R. romani* by its proportions, dimensions and morphology (see Depéret & Douxami 1902: pl. XXIX, fig. 7). It differs by the presence of an isolated anteroproximal facet for the lunate. The height of the anterior side is much smaller than in *R. romani*, whereas its width is similar. However, it is much higher posteriorly than the cuboids of *R. romani*, because of the very high apophysis, and the strong posterior elevation of the proximal surface. The proximal articulation is rectangular in proximal view and the posterior apophysis is very visible posterior to this articulation. The distal articulation for the MtIV is transversally convex and concave anteroposteriorly. The lateral groove for the tendons is very shallow. Another cuboid from Castelmaurou (TLM.PAL.2014.0.2563) attributed to *D. lamilloquense* (Duranthon 1990) also shares the same characters as *D. asphaltense*, and especially the isolated anteroproximal facet for the lunate, which is always absent in ronzotheres. The presence of this facet thus seems to be a diagnostic character differentiating *Diaceratherium* from *Ronzotherium*.

MtII. One MtII of *R. romani* is preserved from 'Marseille' (NMB-Mar-847a, Fig. 18I) but was originally attributed to a McII of "*Diaceratherium*" *massiliae* and another from Rickenbach (NMB-UM-2565, Fig. 21L). It is partly broken proximally. In anterior view, the proximal articulation for the mesocuneiform is concave. The diaphysis is curved towards the medial side and is very widened distally. Antero-laterally, there is no anterior articulation for the MtIII, only a single small facet for the ectocuneiform. A groove separates this facet from the two posterior facets (not preserved on the specimen from 'Marseille'): one is for the ectocuneiform, the other below, is for the MtIII. The ectocuneiform facet is large and oblique, whereas the MtIII facet is thin and elongated.

COMPARISON. The MtII of *R. filholi* from Villebramar (Brunet 1979) and Möhren 7 (BSPG-1969-XXIV-73) differ by the presence of an anterior facet for the MtIII, below the ectocuneiform facet, and by their gracility. The MtII of *D. lemanense* from Wischberg (Jame *et al.* 2019) differs in being more gracile, but also in having a very large posterior facet for the ectocuneiform, an anterior facet for the MtIII and an elongated posteromedial entocuneiform facet.

MTIII. It is only preserved from Gaimersheim (BSPG-1952-II, Fig. 20G–K). It differs drastically from MtIII of *R. filholi* from Villebramar by its robustness. The proximal part is slightly broken medially and laterally. The proximal articulation for the ectocuneiform is roughly trapezoid, with a lateral notch separating the two facets for the MtIV, and it is as wide as long. It is slightly bulged at the level of this notch. There is no facet for the cuboid. In anterior view, the proximal border is straight and oblique and there is a marked distal widening of the diaphysis towards the distal articulation. In medial view, the anterior articulation for the MtII is broken but may have been absent, and the posterior is small and poorly differentiated from the proximal articulation. In lateral view, the anterior articulation for the MtIV is large and triangular, whereas the posterior is poorly preserved. They are separated by a deep groove. The distal keel is quite smooth but still visible in anterior view, and there is no distal tubercle on the posterior side. The insertions of the m. interossei are long on the medial and lateral sides (they extend beyond the middle of the diaphysis).

COMPARISON. The MtIII of *R. velaunum* is poorly preserved, and it differs from that of *R. romani* by its greater length, even though its width is quite similar. It also shares with *R. romani* a distal widening of the diaphysis and a smooth distal keel of the articulation. The MtIII of *R. filholi* from Villebramar differs from that of *R. romani* by its higher gracility, but it shows a similar distal widening of the diaphysis. As in *R. romani*, the proximal border is straight and oblique in anterior view and the distal keel is smooth. Another MtIII from Möhren 7 (BSPG-1969-XXIV-156) is quite similar to that of *R. romani*, as it shares the distal widening of the diaphysis, the absence of a posterior facet for the MtII, the presence of a posterior articulation for the MtII and the similar shape of the proximal side. Although their length is almost equal, the MtIII of *R. romani* is much wider. The MtIII of *Diaceratherium asphaltense* (FSL-213016) differs by its smaller size and its reduced width, compared to the MtIII of *R. romani*. The shape of the proximal side in anterior view is also quite different, it is triangular. It also differs by its shorter insertion for the m. interossei, the absence of a posterior facet for the MtII and the absence of distal widening of the diaphysis. In proximal view, the anterior border of the proximal articulation is straight, and it is also slightly less oblique in anterior view. The MtIII of *D. lamilloquense* from Castelmaurou (TLM.PAL.2014.0.2564) differs from that of *R. romani* by its much thinner diaphysis, its concave proximal articulation in anterior view, the absence of a posterior facet for the MtII, and its proximal side being much wider than long in proximal view.

MTIV. It is only preserved from 'Marseille' (FSL-520286, Fig. 18J), and it is complete. As for the MtIII, it is also more robust than the MtIV of *R. filholi* from Villebramar. The proximal articulation for the cuboid is roughly triangular, with a small notch on the medial side between the two facets for the MtIII. The postero-proximal tuberosity is pad-shaped and continuous. On the medial side, the two facets for the MtIII are rather large, and separated by a narrow groove, than runs from the proximal side to the anterior side. The anterior MtIII facet is triangular while the posterior one is less proximal, and oval-shaped. There is no posterior tubercle. The MtV facet is absent. By virtually articulating the 3D models of this MtIV to the MtIII from Gaimersheim, their morphologies would both match very well: the length of the anterior MtIII/MtIV facet is identical, and the groove is located at the same position; on the diaphysis, the insertions for the m. interossei extend up to the same level.

COMPARISON. The MtIV of *R. velaunum* from Ronzon is lost. The MtIV of *R. filholi* from Villebramar (Brunet 1979) differs by its dimensions, the concave proximal facet for the cuboid, and the much wider

groove separating the two MtIII facets. The MtIV of *Diaceratherium lamilloquense* (Duranthon 1990) also differs by its dimensions, by the concave proximal facet for the cuboid, by the much wider groove separating the two MtIII facets and by the 90° angle between these two. The MtIV of *D. aginense* from Laugnac (de Bonis 1973: fig. 34a) further differs by the presence of an anterior ectocuneiform facet, by a reduced postero-proximal tuberosity and by the very different shape (triangular) of the proximal side.

Final remarks. All these newly identified postcranial remains considerably change our view of the species *Ronzotherium romani*. Prior to this study, only scarce remains were identified, and this species was believed to resemble its closely-related species *R. filholi*, by being rather medium-sized, gracile and cursorial. Based on this wrong premise, large and robust postcranial rhinocerotid remains from 'Marseille' were not assigned to the co-occurring *R. romani*. Indeed, the species, "*Diaceratherium*" *massiliae* was named based on these short and robust postcranials, as it was not conceivable to consider they would document any representatives of *Ronzotherium* (Ménouret & Guérin 2009). Yet, by comparing postcranial remains to other remains of *Ronzotherium*, especially to those of *R. velaunum* for which the postcranial skeleton is well preserved, we show that all of them can be assigned to *Ronzotherium*, instead of *Diaceratherium*. In particular, the postcranial skeleton of *Ronzotherium romani* differs from *Diaceratherium* by:

- the lower fossa olecrani of the humerus in posterior view and the constricted condyles in anterior view;
- the equal posterior and anterior heights of the scaphoid, a less convex dorsal border in proximal view, a concave distal articulation for the magnum, a less concave articulation for the trapezoid and a smaller articulation for the trapezium;
- the large posterior tuberosity of the lunate in proximal view, the developed posterior extension of the proximal facet for the radius, the higher anterior side in anterior view, the shallower groove separating the anteroproximal facet for the scaphoid from the postero-proximal, as well as the reduced anterior portion of the facet for the magnum (it is almost as large as the distal pyramidal facet);
- the higher anterior side of the pyramidal, the more elongated facet for the pisiform, the developed facet for the ulna and the larger facets for the lunate;
- the shorter and straight posterior tuberosity of the magnum and a shorter proximal contact between the trapezoid and scaphoid facets;
- the thin, curved and 'hook-shaped' posterior apophysis of the unciform, the larger McIII facet, poorly distinguished from the McIV facet and the convex McIV facet;
- the absence of rugose tuberosity on the anteroproximal part of the diaphysis of the McIV, the straighter medial border of the diaphysis and its more reduced robustness;
- the less concave facet for the navicular on the atragalus, the higer collum tali, the smaller Cc2 facet, the contact between the Cc2 and Cc3 facets, a flatter Cc1 facet in lateral view and the large distal extension of the Cc1 facet;
- the global size and shape of the navicular, longer than wide, and its single posterior articulation for the cuboid;
- the disposition of the facets of the ectocuneiform;
- the absence of anteroproximal facet for the lunate on the cuboid and the trapezoid proximal side;
- the more robust MtII, without anterior facet for the MtIII;
- the wider diaphysis of the MtIII and the different shape of its proximal articulation;
- the dimensions of the MtIV and the shallower groove separating the two MtIII facets.

Accordingly, *Diaceratherium massiliae* Ménouret & Guérin, 2009 should be considered as a junior synonym of *Ronzotherium romani* Kretzoi, 1940.

Ronzotherium heissigi sp. nov.

urn:lsid:zoobank.org:act:D1CFA5AE-6BC9-479B-AE43-F46EB9D86A49

Figs 22–26

Acerotherium lemanense – Roman 1912a: 61–62, pl. VII (from Lamothe-Capdeville).
Aceratherium filholi – Stehlin 1914: 183, 85 (Bumbach).
Ronzotherium filholi – Lavocat 1951: 116, pl. 19 fig. 3, pl. 26 fig. 1 (from Vendèze). — Brunet 1979: 105 (from Bumbach). — Becker 2003: 213–214.
Ronzotherium velaunum – Heissig 1969: 20–36, 77, fig. 8b (from Vendèze).
Ronzotherium filholi elongatum – Heissig 1969: 46–55, 71, 75–77, 82–83 (from Bumbach).
Ronzotherium filholi romani – Heissig 1969: 63 (from Lamothe-Capdeville).
Ronzotherium romani – Brunet 1979: 135–136, fig. 15, pls XVII–XVIII (from Vendèze).
Diaceratherium lemanense – Antoine & Becker 2013: 140 (from Lamothe-Capdeville).

Diagnosis

Differs from *R. romani* by the mandibular ramus inclined forward, the P1 sometimes absent and without anterolingual cingulum, the angular and V-shaped external groove of the lower cheek teeth, the lower premolars without lingual cingulum, the d/p1 always absent in the adult, the deep and wide gutter for the m. extensor carpi on the radius, the concave proximal border of the anterior side of the magnum, the salient insertion of the m. extensor carpalis of the metacarpals and the oval proximal side of the cuboid.

Differs from *R. velaunum* by the presence of a lingual groove on the corpus mandibulae, the curved and not constricted paralophid on p2 and the deep median constriction of the distal humeral articulation.

Differs from *R. filholi* by a foramen infraorbitalis above P3, a zygomatic width/frontal width ratio above 1.5, a concave occipital crest, the reduced paraconid on p2, the high posterior expansion of the scaphoid facet on the radius, the open angle between the diaphysis of the ulna and the olecranon and the curved magnum facet on the McII.

Differs from *R. elongatum* by the absence of processus lacrymalis, the reduction of the postorbital process on the zygomatic arch, its poorly developed processus posttympanicus and by the metaloph of P2 directed postero-lingually.

Further differs from *R. filholi* and *R. elongatum* by a convex processus postglenoidalis of the squamosal and by a narrow and V-shaped lingual opening of the lower premolars.

Etymology

The specific epithet honours Prof. Dr Kurt Heissig for his major and imperishable contributions on the study of the Rhinocerotidae, and for providing the first systematic revision on *Ronzotherium* more than 40 years ago.

Type material

Holotype

FRANCE • complete skull and associated mandible; Auvergne-Rhône-Alpes, Cantal, Vendèze near St-Flour; 45°02′36.8″ N, 3°06′13.1″ E; MNHN.F.LIM181.

According to the MNHN registry, it was discovered by M. Lauby (possibly Antoine Lauby), but sold to the MNHN by M. Hugon, from St-Flour on the 19th of June 1909. It bears the old MNHN inventory number MNHN.F.1909-25.

Additional material

SWITZERLAND – **Bumbach (MP25)** • 1 very poorly preserved and incomplete skull; NMB-UM-200 • 1 fragment of parietal bone with occipital crest; NMBE-5035820 • 1 P1; NMB-UM-463 • 1 P2; NMB-UM-126a • 1 P2; NMBE-5014494 • 1 P3; NMBE-5035822 • 1 P3; MGL-4264 • 2 P4; MGL-5265, MGL-5266 • 1 M2; NMBE-5014495 • 1 subcomplete mandible; NMB-UM-6132 • 1 d2; MGL-5275 • 1 d4; NMB-UM-13 • 1 p2; NMBE-5035824 • 1 p3; MGL-5274 • 1 fragment of mandible with p3–4; NMBE-5035825 • 2 p4; NMBE-5035826, NMBE-5035827 • 1 p4; NMB-UM-6133 • 1 m1; NMB-UM-806 • 1 m1; NMBE-5035828 • 1 m2; NMB-6278 • 3 m2; NMBE-5035829, NMBE-5035830, NMBE-5035831 • 1 m3; NMBE-5035832 • 2 incomplete   humeri; NMB-UM-132, NMB-UM-129a • 1 radius; NMB-UM127a • 1 ulna; NMB-UM-131b, NMB-UM-131c • 1 lunate; NMBE-5035833 • 2 trapezoids; NMB-UM-6136b, NMB-UM-6 • 1 magnum; NMB-UM-6136c • 1 McII; NMB-UM-6136a • 1 McII; NMB-UM-121 • 1 proximal fragment of femur; NMBE-5035835 • 1 cuboid; NMBE-5035834.

Type horizon and locality

Vendèze near St-Flour, Cantal, Auvergne-Rhône-Alpes, France (MP24, late early Oligocene), approximative coordinates: 45°02′36.8″ N, 3°06′13.1″ E.

Stratigraphical distribution

MP24–MP25.

Geographical distribution

France: 'Auvergne' (without precision, which could possibly correspond to Vendèze), Lamothe-Capdeville, Vendèze. Switzerland: Bumbach.

Description

Holotype

Sᴋᴜʟʟ. The skull MNHN.F.LIM181 is quite well preserved but the nasals are broken (Figs 22–23). The premaxillae are long and contact each other only at their anterior extremity. The nasal notch extends up to P2 and the foramen infraorbitalis is located above P3. The nasal septum is not ossified. The suture between the nasals and the lacrimal is not visible and the lacrimal process is absent. The orbit is large and its anterior border is above the anterior side of M1. The processus postrobitalis of the frontal is large. The anterior base of the zygomatic process is high above the teeth neck. The zygomatic arch is high in lateral view, it is almost reaching the dorsal border of the skull. The postorbital process of the zygomatic arch is almost absent and very poorly distinguishable. The dorsal profile of the skull is overall concave in lateral view. The external auditory pseudomeatus is partially closed and the occipital side is inclined forward. The nuchal tubercle is developed. The back of the teeth row is in the posterior half of the skull in lateral view. In dorsal view, the skull is brachycephalic and it is hornless. The orbit is not laterally projected. The zygomatic width/frontal width ratio is above 1.5. A very thin sagittal crest is present, and the occipital crest is not preserved. In ventral view, the anterior tip of the zygomatic arch diverges progressively from the maxilla, without a sharp angle. The vomer and most of the basicranium are not preserved. The articular tubercle of the squamosal is rather smooth and its transverse profile is straight. The anterolateral sides of the processus postglenoidalis form a right dihedron. There is no posterior groove on the zygomatic process. The processus posttympanicus and paraoccipitalis are fused at their base. The processus post-tympanicus is poorly developed while the paraoccipitalis is developed. The foramen magnum is circular and there are no median ridges on the condyles, neither medial truncation.

Mᴀɴᴅɪʙʟᴇ. The mandibular symphysis (Fig. 24A–B) is slightly upraised and it is long and massive in dorsal view. Its posterior margin is at the level of p2. There are two mental foramen, one bellow p2 and one below the root of i2. The lingual groove of the sulcus mylohyoideus is slightly marked on the lingual

Fig. 22. *Ronzotherium heissigi* sp. nov. from Vendèze (late early Oligocene, France). Skull MNHN.F.LIM181. **A**. Dorsal view. **B**. Left lateral view. **C**. Ventral view. Scale bar: 2 cm.
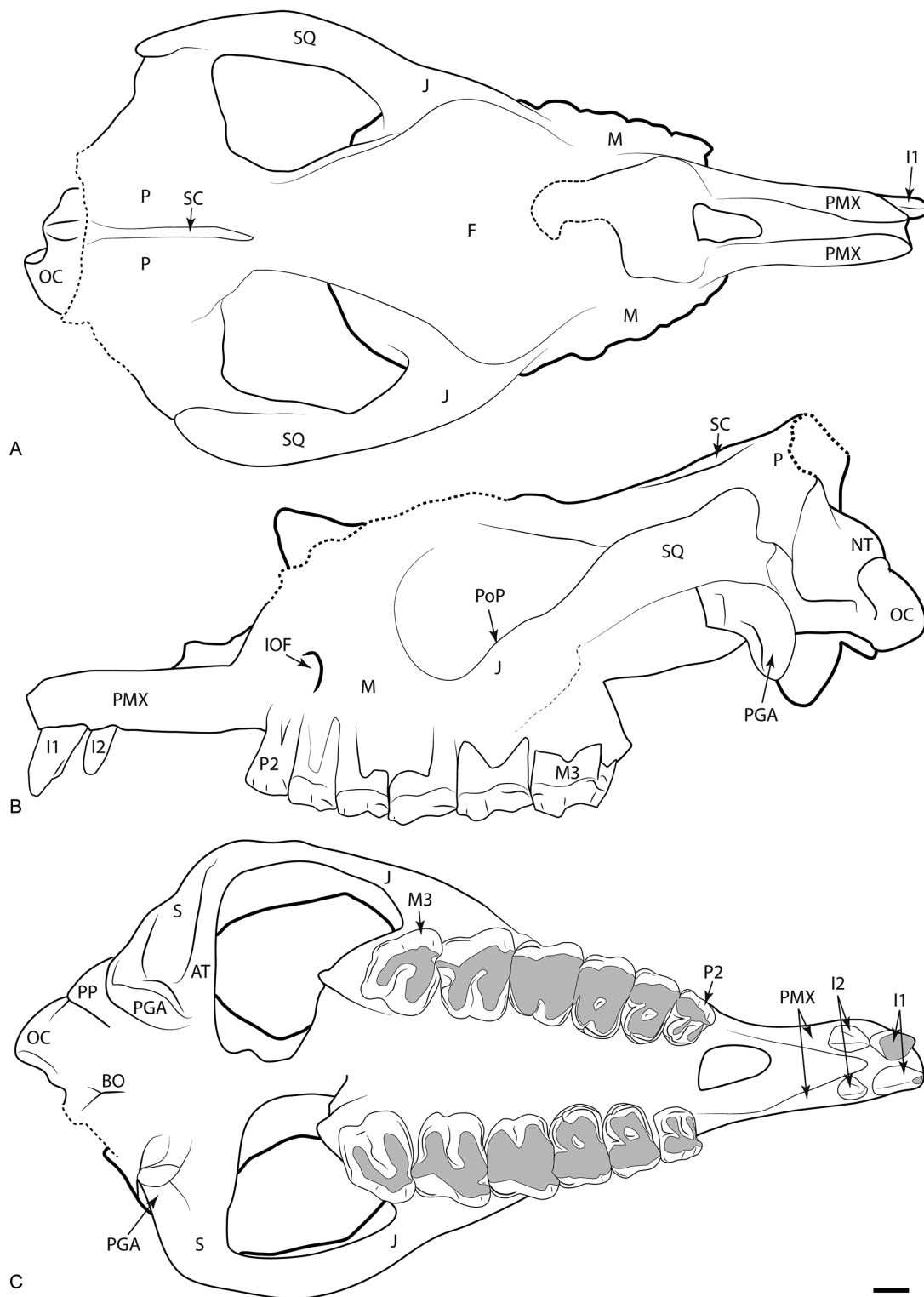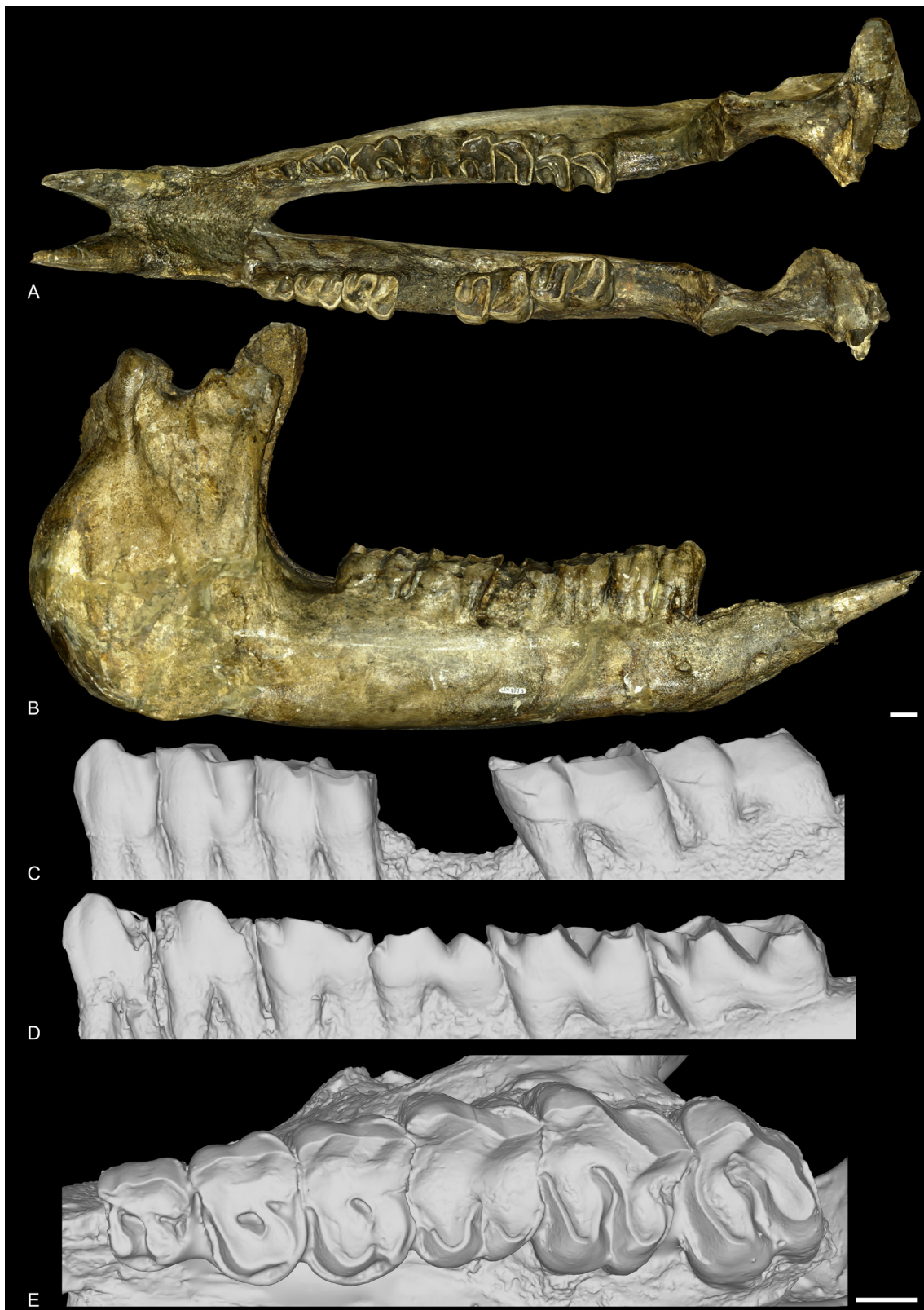
Fig. 23. *Ronzotherium heissigi* sp. nov. from Vendèze (late early Oligocene, France). Drawing of the skull MNHN.F.LIM181. **A**. Dorsal view. **B**. Left lateral view. **C**. Ventral view. Abbreviations: AT = articular tubercle; BO = basioccipital; F = frontal; IOF = infraorbital foramen; J = jugal; M = maxilla; NT = nuchal tubercle; OC = occipital condyle; P = parietal; PGA = postglenoid apophysis; PMX = premaxilla; PoP = postorbital process; PP = paraoccipital process; SC = sagittal crest; SQ = squamosal. Scale bar: 2 cm.

Fig. 24. *Ronzotherium* heissigi sp. nov. from Vendèze (late early Oligocene, France). **A–D**. Mandible MNHN.F.LIM181. **A**. Occlusal view. **B**. Lateral view. **C**. With left p2–p4 and m2–3 in labial view. View. **D**. Right p2–m3 in lingual view. – **E**. Skull MNHN.F.LIM181, belonging to the same individual as the mandible, close-up view of P2–M3 in occlusal view. Scale bars: 2 cm.

border of the corpus. The ventral base of the corpus is completely straight. The ramus is inclined forward in lateral view, and the coronoid process is well developed. In medial view, the foramen mandibulare is located below the teeth neck.

DENTITION. The complete dental formula is I1–2, P2–M3 / i2, p2–m3. The Length(P3–4)/Length(M1–3) ratio is between 0.42 and 0.5. The cement is absent and the crowns are very low (Figs 22–24).

I1 is oval in cross-section, pointed and not chisel-shaped. It is directed downwards, and it bears two crests, one anterior and one posterior. There was no contact with the lower incisor (no visible wear on any of them). It is separated from I2 by a very short diastema. I2 overall has the same shape as I1 but is smaller and less pointed. The diastema between I2 and P2 is very long. The i1 is absent, and the space between the two i2 is very short. The i2 are large, tusk-shaped and parallel.

The labial cingulum of the upper premolars is always present, posteriorly, below the metastyle. The lingual one is always present, continuous and undulating in lingual view: it is high below the protocone, very low at the level of the median valley, and very high at the level of the hypocone. The crochet is always absent. The hypocone is connected to the ectoloph. The postfossette is narrow and the antecrochet is always absent. The P1 is absent. The protocone and hypocone of P2 are separated and the hypocone is posterior to the metacone. The metacone fold is strong. The protocone is same sized as the hypocone. The protoloph of P2 is joined to the ectoloph. The medifossette is always absent on the premolars and the protocone is never constricted. On P3–4, the protocone and hypocone are connected by a lingual wall. The metacone fold is strong. The hypocone is posterior to the metacone as on P2. The protoloph of P3 is joined to the ectoloph and the crista and pseudometaloph are absent. The antecrochet is always absent on P3–4. The metaloph of P4 is continuous.

The labial cingulum of the upper molars is always present, as on the premolars, below the metastyle. The antecrochet is present on M2, absent on M3 and not visible on M1. The crochet, crista, cristella and medifossette are always absent. The lingual cingulum is always absent. The protocone is never constricted. The paracone fold is strong and the metacone fold absent. The metastyle is long, but the parastyle is rather short. The metaloph is long. The posterior part of the ectoloph is straight. The posterior cingulum is continuous. There is no lingual groove on the protocone of M2 and the mesostyle is absent. The antecrochet and hypocone are well separated. The ectoloph and metaloph of M3 are fused into an ectometaloph, and it is quadrangular. The protocone is not constricted and the protoloph is transverse. The posterior groove of the ectometaloph is present.

The lower p2–3 do not bear vertical external rugosities. The external groove of the lower cheek teeth is angular and is developed until the neck. The trigonid is angular and forms an acute dihedron. The metaconid and entoconid are always joined to the hypolophid. The lingual opening of the lower premolars is V-shaped. The lingual cingulum is always absent on all lower cheek teeth and the labial one is basically absent, except anteriorly below the paralophid. The d/p1 is always absent. The paralophid of p2 is curved, without constriction and the paraconid is quite reduced. The posterior valley is lingually open. The lingual branch of the paralophid of p3 is long and developed. The anterolingual cingulum does not reach the metaconid. The hypolophid of the lower molar is transverse and there is no lingual groove of the entoconid.

Fig. 25 (next page). *Ronzotherium heissigi* sp. nov. from Bumbach, Bern Canton (early late Oligocene; Switzerland). – **A–D**. Mandible NMB-UM-6132. **A**. Occlusal view. **B**. Left lateral view. **C**. With right p3–m3 in labial view. **D**. With right p3–m3 in lingual view. – **E–F**. Right humerus NMB-UM-129a. **E**. Anterior view. **F**. Posterior view. – **G–H**. Left humerus NMB-UM-132. **G**. Anterior view. **H**. Posterior view. – **I–J**. Right radius NMB-UM-127a. **I**. Anterior view. **J**. Posterior view. – **K–M**. Right ulna NMB-UM-131b. **K**. Anterior view. **L**. Posterior view. **M**. Distal view. Abbreviation: im = insertion for the m. biceps brachii. Scale bars: 2 cm.
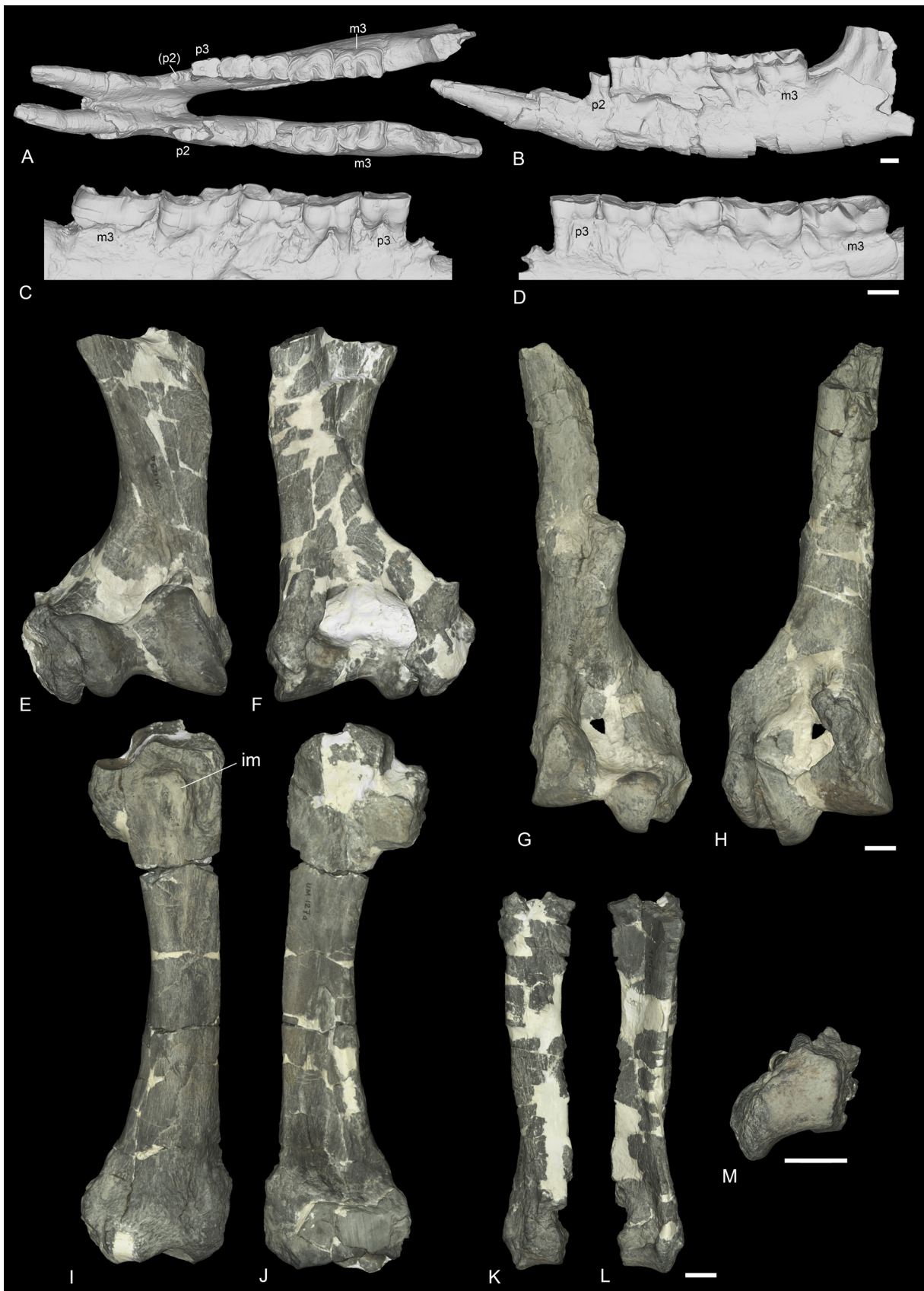
Material from Bumbach

Newly prepared specimens are referred to as *Ronzotherium heissigi* sp. nov. and they document the only known postcranial remains of this species.

HUMERUS. The two humeri from Bumbach are proximally broken (Fig. 25E–H). In posterior view, the fossa olecrani is high on NMB-UM-132, but lower on the other humerus, NMB-UM-6132, possibly due to taphonomical deformation. The lateral epicondyle is very prominent, and distally elongated. The distal articulation is hourglass-shaped in anterior view, with a deep proximal incision between the two lips of the trochlea and the articulation is oblique. The epicondylar crest is high. The distal gutter on the epicondyle is strong in posterior view.

RADIUS. The radius from Bumbach (NMB-UM-127a, Fig. 25I–J) belongs to the same individual as the humerus NMB-UM-132. The anterior border of the proximal articulation is straight. The medial border of the diaphysis is straight. The insertion of the m. biceps brachii is deep and the gutter for the m. extensor carpi is deep and wide. The posterior expansion of the scaphoid facet is high and there is no secondary distal articulation for the ulna.

ULNA. The ulna NMB-UM-131b-c (Fig. 25K–M) belongs to the same individual as the radius (NMB-UM-127a) and the humerus (NMB-UM-132). It is very poorly preserved. The olecranon of the ulna is rather long and makes an open angle with the diaphysis. The distal end is large, the anterior tubercle and the lunate facet are absent, and the pyramidal facet is concave.

LUNATE. The lunate NMBE-5035833 is complete and very well preserved (Fig. 26A–E). The proximal articulation for the radius is very large and convex anteroposteriorly. There is no articulation with the ulna. In proximal view, there is a long drop-like posterior extension of the radius facet on the medial side. The anterior side is deeply keeled, and the distal border is acute in anterior view. Medially, the two proximal articulations for the scaphoid are fused in a single facet. It is separated from the distal scaphoid facet by a deep groove. The distal facet for the scaphoid is large. In lateral view, the proximal and distal articulations for the pyramidal are large and the proximal one is medially displaced. In distal view, there are three articulation facets: a large anterior one for the unciform, and two for the magnum, one of which is distal and very concave and the other thin, flat and elongated is anterior, and located between the scaphoid and unciform facets.

TRAPEZOID. Two trapezoids are preserved from Bumbach (NMB-UM-6 and NMB-UM-6136b, Fig. 26F–J). The latter is slightly different from the former, and it articulates with the magnum NMB-UM-6136c and the McII NMB-UM-6136a. In anterior view, they are both wider than high. The proximal border is sigmoid on NMB-UM-6136b, whereas it is symmetric on NMB-UM-6. The magnum facet occupies most of the lateral side, while the medial side is occupied by the medio-distal articulation

---

Fig. 26 (next page). *Ronzotherium heissigi* sp. nov. from Bumbach, Bern Canton (early late Oligocene; Switzerland). – **A–E**. Left lunate NMBE-5035833. **A**. Anterior view. **B**. Proximal view. **C**. Distal view. **D**. Lateral view. **E**. Medial view. – **F–J**. Right trapezoid NMB-UM-6136b. **F**. Anterior view. **G**. Lateral view. **H**. Medial view. **I**. Proximal view. **J**. Distal view. – **K–N**. Right magnum NMB-UM-6136c. **K**. Anterior view. **L**. Distal view. **M**. Lateral view. **N**. Medial view. – **O–Q**. Right McII NMB-UM-121. **O**. Anterior view. **P**. Lateral view. **Q**. Proximal view. – **R–T**. Right McII NMB-UM-6136a. **R**. Proximal view. **S**. Anterior view. **T**. Lateral view. – **U–Y**. Right cuboid NMBE-5035834. **U**. Anterior view. **V**. Proximal view. **W**. Distal view. **X**. Medial view. **Y**. Lateral view. Abbreviations: a = astragalus; ca = calcaneus; e = ectocuneiform; l = lunate; m = magnum; n = navicular; p = pyramidal; r = radius; s = scaphoid; td = trapezoid; tm = trapezium; un = unciform. Scale bar: 2 cm.

for the trapezium. The proximal side is fully occupied by the anteroposteriorly concave scaphoid facet. The distal articulation for the McII is also anteroposteriorly concave.

MAGNUM. The magnum NMB-UM-6136c is complete (Fig. 26K–N). In anterior view, the proximal border of the anterior side is concave and the anterior face is wider than high. The proximal apophysis is very high, very convex and narrow. The lunate facet on this apophysis is very long and contacts the small unciform facet. On the other side of the proximal apophysis, the facet for the scaphoid is also long and is very poorly distinguished from the medial facet for the trapezoid. This latter facet is longer than high. The medio-distal McII facet is flat and its distal border is very concave in medial view. On the distal side, the McIII facet is very large, quadrate, as long as wide and very concave anteroposteriorly. The posterior tuberosity of the magnum is short and curved.

McII. There are two McII preserved from Bumbach (NMB-UM-121 and McII NMB-6136a, Fig. 26R–T). The outline of the proximal side is trapezoidal. The articulation for the trapezoid is concave lateromedially and slightly convex anteroposteriorly. On the lateral side, the magnum facet is curved and band-shaped. The anterior facet for the McIII is present but the posterior is absent. There is no trapezium facet. The insertion for the m. extensor carpalis is salient.

FEMUR. Only a proximal fragment is preserved in Bumbach (NMBE-5035835). The head is hemispheric and the fovea capitis is high and narrow. The major trochanter is lower than the head and separated from it by a short neck. It is nearly triangular in proximal view and in lateral view the posterior part is higher than the anterior. The trochanteric fossa is deep on the posterior side, with a well-marked intertrochanteric crest. A fossa is also present on the anterior side, overhung by the major trochanter.

CUBOID. The cuboid NMBE-5035834 is complete (Fig. 26U–Y). The anterior side is approximately as high as wide. In lateral view, the posterior side is higher than the anterior and the posterior apophysis of the cuboid is slightly lower than the distal articulation. In proximal view, the posterior apophysis is almost not visible. The proximal side is oval and the astragalus and calcaneal facets are almost equal-sized. On the medial side, the postero-proximal and elongated facet for the navicular is concave and contacts the small, square and postero-mesial facet for the ectocuneiform. The navicular facet bears a thin extension up to the anterior border, bordering the astragalus facet. The small anterodistal facet for the ectocuneiform is separated from the posterior one by a wide groove. On the lateral side, the groove for the tendon of the m. fibularis longus is very large and deep. The distal articulation for the MtIV is flat and triangular.

Discussion

An exhaustive list of occurrences is given in Supp. file 4. These occurrences are represented on palaeogeographical reconstructions of Europe (Fig. 27), from the earliest Oligocene (MP21) to the latest Oligocene (MP30).

Body mass evolution

The body masses of specimens of *Ronzotherium* have been estimated based on the regression equations provided by Fortelius & Kappelman (1993) for Rhinocerotidae (Supp. file 5). These equations allow estimations based on different measurement from the skull, upper dentition, humerus, radius, femur and tibia. We also used equations provided by Tsubamoto (2014) to estimate the body mass based on measurements on the astragalus. The results show a very large variation, even based on a single bone, especially for the astragalus, which ranges from approximately 400 kg to 1100 kg for the astragalus PUY.2004.6.1770.RON, for example. However, one equation does not necessarily always give higher or lower estimations than another. For example, on the tibia 1970-158 from Villebramar, the T2 estimator (tibia proximal width) gives a smaller estimate than the T5 (tibia distal anteroposterior diameter)

(740 kg vs 1060 kg, respectively), whereas on the tibia 1973-221, it is the T5 estimator that gives a smaller estimate than the T2 (840 kg vs 1300 kg, respectively). These differences are probably due to deformations or bad preservations of specimens. Thus, these estimated body masses should be taken with a lot of caution, and they probably do not reflect a realistic body mass for these animals. Yet, they can provide a base for comparisons, since equivalent equations are used for all specimens.

The average body mass for each population is represented in Fig. 27 and is placed on palaeogeographical maps. From this figure, we clearly observe the very large intraspecific and interspecific variation of the estimated body mass of *Ronzotherium*, and no clear trend through time can be detected. However, all
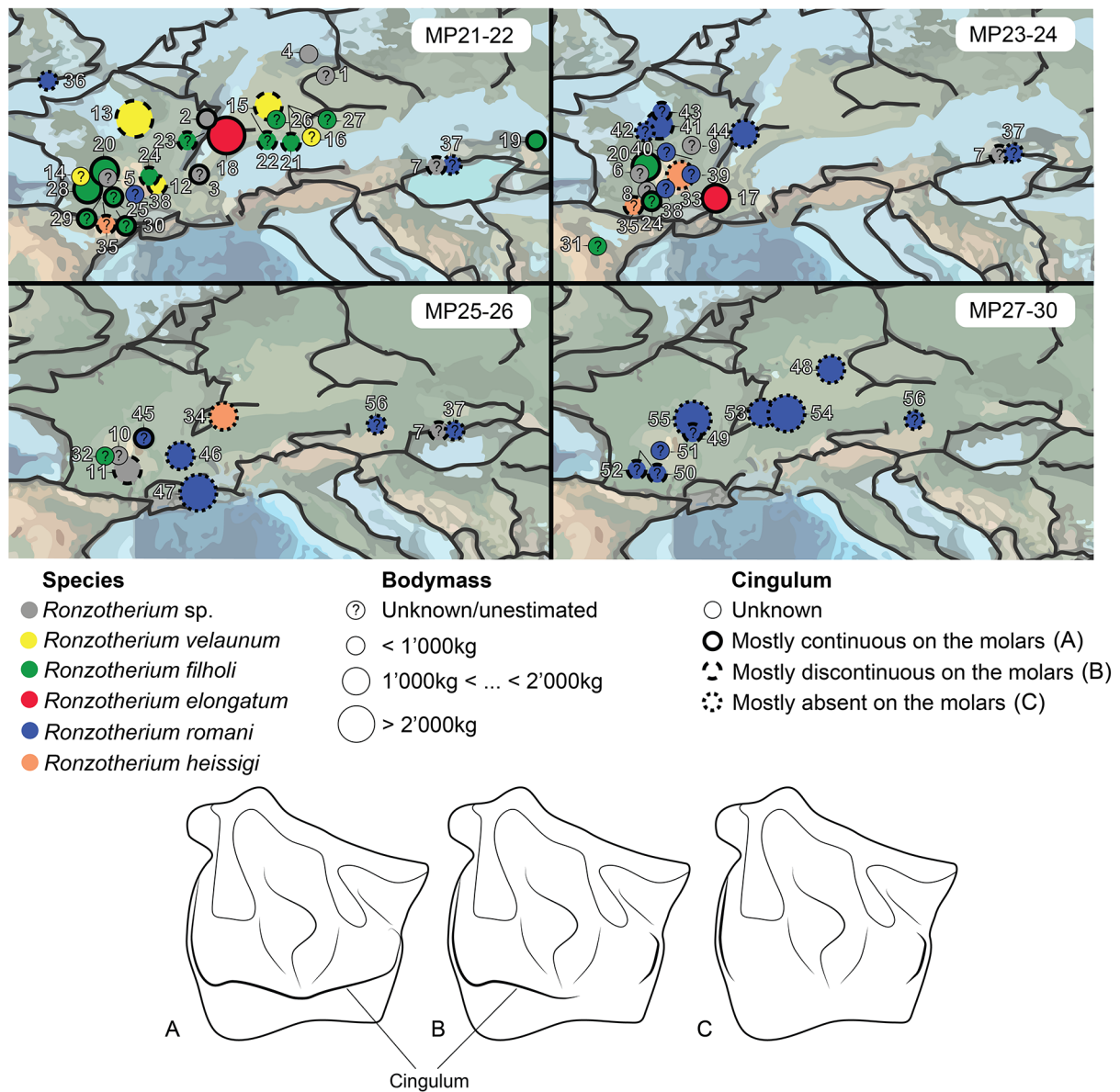
Fig. 27. Occurrences of *Ronzotherium* Aymard, 1854 in Europe, from MP21 (earliest Oligocene) to MP30 (latest Oligocene) with palaeogeographical reconstructions, modified from PALEOMAP (Scotese 2016). The diameter of the circles is proportional to the body mass of the specimens in each locality, and the thickness and shape of the outline refer to the shape of their cingulum. Numbers of circles refer to the number of the locality in Supp. file 4.

69

body masses below 1000 kg are found during the early Oligocene, with *Ronzotherium velaunum* in Ronzon (n° 11), *R.* cf. *romani* in Bouldnor (n° 35), *R.* sp. in Pechelbronn (n° 2) and Espenhain (n° 3) and *R. filholi* in Cluj-Napoca (n° 18), Möhren (n° 20) and Bournoncle (n° 23). *Ronzotherium velaunum* shows the highest variation of body mass, ranging from less than 1000 kg in Ronzon (n° 11), to more than 2000 kg in Lagny-Thorigny (n° 12). However, for this latter locality, only one estimator could be used to estimate its body mass (length of M2) and should thus be taken with even more caution. Finally, there does not seem to be any obvious correlation between the strength of the cingulum and the body mass, since large masses are found in species having complete cingulum (*R. elongatum*) as well as those having extremely reduced cingulum (*R. romani*).

Cingulum

Interestingly, the shape, strength and size of the cingulum of the cheek teeth seem to follow a trend of reduction through time. Furthermore, *Ronzotherium romani* and *R. heissigi* sp. nov. are the two species
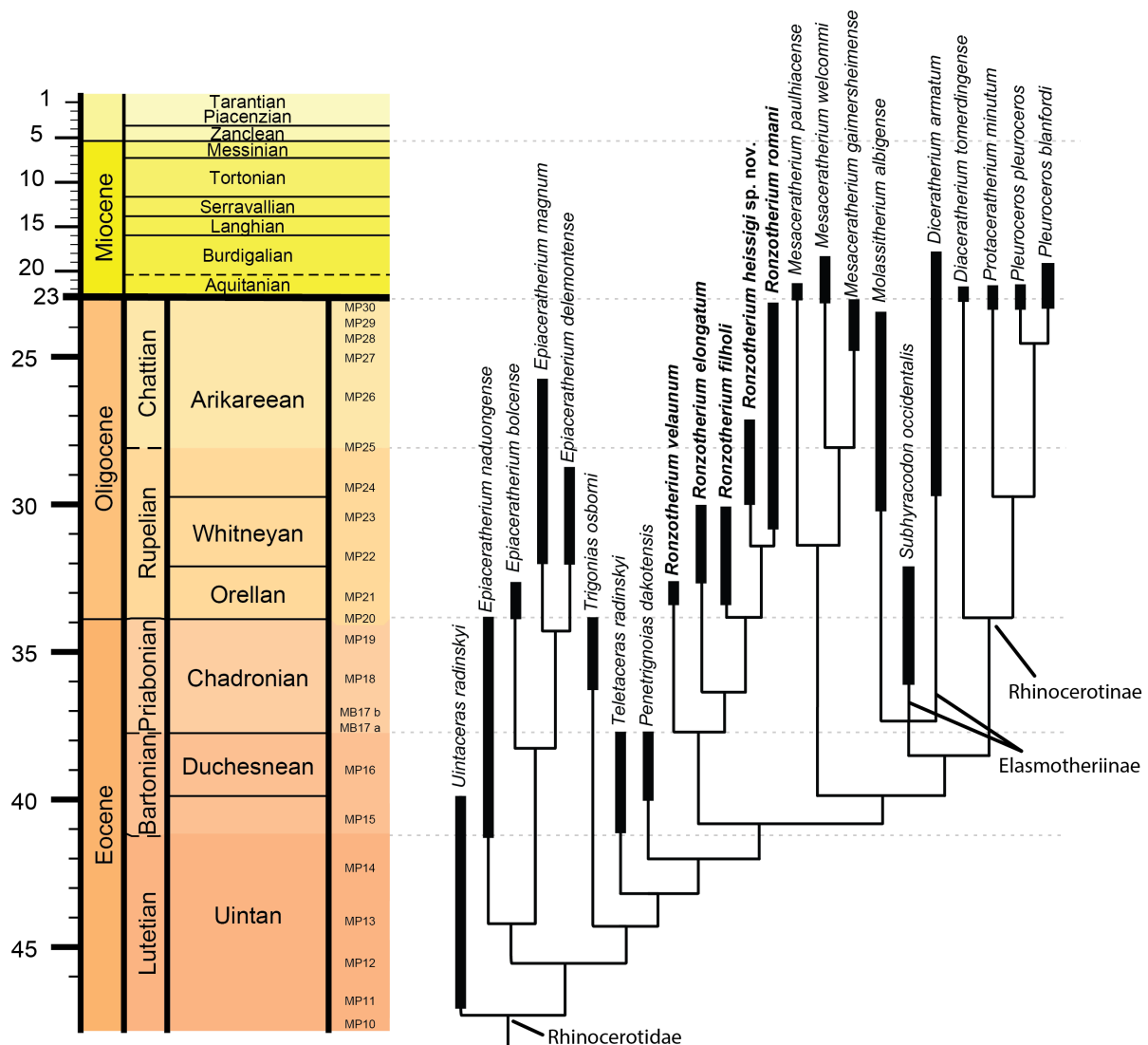
Fig. 28. Cladogram of Rhinocerotidae Owen, 1845 calibrated in time. Bold lines indicate the temporal range of each terminal. Temporal scale for the Miocene and younger periods has been compressed and differs from the Eocene and Oligocene.

that show the most discontinuous cingulum while *R. romani* is the only one that survived until the end of the Oligocene (Fig. 28).

It was first suggested that the biological role of the cingulum was to provide protection to the gums and the periodontal membrane (Mills 1967), but Lucas *et al*. (2008) recently proposed another hypothesis. According to them, and after testing their hypothesis with finite elements analyses, the cingulum could also protect from enamel cracks or fractures, by strengthening the crown base, especially during the mastication of soft food. More recently, Anderson *et al*. (2011) further tested this hypothesis by controlling the influence of several factors (hard vs soft food, symmetrical vs asymmetrical loads, size and shape of cingulum, etc.), and showed that, most of the time, having a cingulum could indeed protect from enamel fractures caused by mastication. Based on their results, having a complete cingulum (i.e., which surrounds the whole neck of the tooth) is only efficient if it is formed by actually creating more enamel around the tooth, which leads to additional enamel surface and volume. However, this hypothesis supposes that the generation of this additional enamel would be more costly during the development of the tooth, which could thus imply a trade-off. Yet, having even just a partial cingulum (i.e., a cingulum which is interrupted lingually or labially, for example) is almost as efficient as having a complete cingulum under a soft load (15 % crack reduction vs 18 % reduction with complete standard cingulum; see Anderson *et al*. 2011: table 1), but is also less costly. Furthermore, if the cingulum is not generated by adding enamel, but by restructuring the shape of the crown enamel (i.e., no additional enamel is needed for the formation of this cingulum, and thus no additional cost), then having a complete cingulum leads in fact to more fractures than without a cingulum, whereas having a partial cingulum still slightly reduces the number of fractures. Thus, considering the possible trade-off related to the developmental cost of the cingulum, and considering that complete cingulum is actually inefficient if it is not actually adding enamel surface, it would seem credible that the individuals of *Ronzotherium* having partial cingulum had been naturally selected and survived longer than the individuals having a complete cingulum. Perhaps this could explain the reduction trend observed in the cingulum size in this genus, though it would need further quantitative investigation. If this hypothesis were validated, it could partially explain the early disappearance of most species of *Ronzotherium*, while only *R. romani*, which has the most reduced cingulum, would have passed natural selection.

Conclusion

Ronzotherium is the most characteristic rhinocerotid from the Oligocene of Europe. Appearing from the earliest Oligocene and lasting to the latest Oligocene, it also had the longest timespan of all the European Oligocene Rhinocerotidae. Yet, and even though it was quite commonly found at numerous European localities, it remained under-investigated and its phylogeny had never been elucidated. This absence of well-defined systematics for this taxon had led to several contradictions in its taxonomy, which we hope are now partly enlightened. Five species can be distinguished and characterised, including a new species: *Ronzotherium heissigi* sp. nov. The postcranial skeleton of *Ronzotherium romani*, which was very poorly known, is now identified and described from several localities for the first time. A comprehensive map of the distribution of *Ronzotherium* is proposed and shows that only *R. romani* remained during the latest Oligocene. We finally discussed the evolution of the body mass and cingulum of this genus through time and suggest that the long survival of *R. romani* may have been linked to the reduction of the cingulum.

Acknowledgements

Contribution statement

All authors contributed to the study conception and design. Material study and analysis were performed by all authors. The first draft of the manuscript was written by Jérémy Tissier and all authors read and approved the final manuscript.

Funding

Conflict of Interest

The authors declare that they have no conflict of interest.

Data availability

All data generated or analysed during this study are included in this published article (and its supplementary information files). 3D models are available from the corresponding author upon request.

References

Abel O. 1910. Kritische Untersuchungen über die paläogenen Rhinocerotiden Europas. *Abhandlungen der geologischen Reichsanstalt, Wien* 20 (3): 1–52.

Adrover R., Feist M., Ginsburg L., Guerin C., Hugueney M. & Moissenet E. 1983. Les formations continentales paléogènes de la Sierra Palomera (Province de Teruel, Espagne) et leur place dans la biostratigraphie tertiaire des chaines iberiques orientales. *Bulletin de la Société géologique de France Série 7* 25 (3): 421–432. https://doi.org/10.2113/gssgfbull.S7-XXV.3.421

Airaghi C. 1925. Considerazioni filogenetiche sui Rinoceronti d'Europa. *Rivista Italiana di Paleontologia* 31: 23–46.

Anderson P.S.L., Gill P.G. & Rayfield E.J. 2011. Modeling the effects of cingula structure on strain patterns and potential fracture in tooth enamel. *Journal of Morphology* 272 (1): 50–65. https://doi.org/10.1002/jmor.10896

Antoine P.-O. 2002. Phylogénie et évolution des Elasmotheriina (Mammalia, Rhinocerotidae). *Mémoires du Muséum national d'histoire naturelle* 188: 1–359.

Antoine P.-O. & Becker D. 2013. A brief review of Agenian rhinocerotids in Western Europe. *Swiss Journal of Geosciences* 106 (2): 135–146. https://doi.org/10.1007/s00015-013-0126-8

Antoine P.-O., Ducrocq S., Marivaux L., Chaimanee Y., Crochet J.-Y., Jaeger J.-J. & Welcomme J.-L. 2003. Early rhinocerotids (Mammalia: Perissodactyla) from South Asia and a review of the Holarctic Paleogene rhinocerotid record. *Canadian Journal of Earth Sciences* 40 (3): 365–374. https://doi.org/10.1139/e02-101

Antoine P.-O., Downing K.F., Crochet J.Y., Duranthon F., Flynn L.J., Marivaux L., Métais G., Rajpar A.R. & Roohi G. 2010. A revision of *Aceratherium blanfordi* Lydekker, 1884 (Mammalia: Rhinocerotidae) from the Early Miocene of Pakistan: Postcranials as a key. *Zoological Journal of the Linnean Society* 160 (1): 139–194. https://doi.org/10.1111/j.1096-3642.2009.00597.x

Aymard A. 1854. Des terrains fossilifères du bassin supérieur de la Loire. *Comptes rendus des Séances de l'Académie des Sciences, Paris* 38: 673–677.

Aymard A. 1856. Rapport sur les collections de M. Pichot-Dumazel. *Congrès scientifique de France* 22: 227–245.

Balme C. 2000. Découverte d'empreintes de pas de mammifères fossilisées dans la Carrière d'argile de Triclavel, Commune de Viens (Vaucluse). *Courrier scientifique du Parc naturel régional du Luberon* 4: 152–155.

Becker D. 2003. Paléoécologie et paléoclimat de la Molasse du Jura (Oligo–Miocène) : apport des Rhinocerotoidea (Mammalia) et des minéraux argileux. *GeoFocus* 9: 1–327.

Becker D. 2009. Earliest record of rhinocerotoids (Mammalia: Perissodactyla) from Switzerland: systematics and biostratigraphy. *Swiss Journal of Geosciences* 102 (3): 489–504. https://doi.org/10.1007/s00015-009-1330-4

Becker D., Antoine P.-O. & Maridet O. 2013. A new genus of Rhinocerotidae (Mammalia, Perissodactyla) from the Oligocene of Europe. *Journal of Systematic Palaeontology* 11 (8): 947–972. https://doi.org/10.1080/14772019.2012.699007

Becker D., Antoine P.-O., Mennecart B. & Tissier J. 2018. New rhinocerotid remains in the latest Oligocene–Early Miocene of the Swiss Molasse Basin. *Revue de Paléobiologie* 37 (2): 395–408.

Blainville H.M.D. 1846. *Ostéographie, ou, Description iconographique comparée du Squelette et du Système dentaire des Mammifères récents et fossiles pour servir de base à la Zoologie et à la Géologie. Tome III.* J.B. Baillière et fils, Paris. https://doi.org/10.5962/bhl.title.127351

Blanchon M., Antoine P.-O., Blondel C. & de Bonis L. 2018. Rhinocerotidae (Mammalia, Perissodactyla) from the latest Oligocene Thézels locality, SW France, with a special emphasis on *Mesaceratherium gaimersheimense* Heissig, 1969. *Annales de Paléontologie* 104 (3): 217–229. https://doi.org/10.1016/j.annpal.2018.06.001

Boada-Saña A., Hervet S. & Antoine P.-O. 2007. Nouvelles données sur les rhinocéros fossiles de Gannat (Allier, limite Oligocène–Miocène). *Revue des Sciences naturelles d'Auvergne* 71: 3–25.

Bonis L. de. 1969. Les vertébrés fossiles de Saint-Paul-des Landes. *Revue de la Haute Auvergne* 41: 1–8.

Bonis L. de. 1973. Contribution à l'étude des mammifères de l'Aquitanien de l'Agenais: rongeurs, carnivores, périssodactyles. *Mémoires du Muséum national d'histoire naturelle, Sér. C – Sciences de la Terre* 28: 1–192.

Bravard A. 1843. Considérations sur la distribution des mammifères terrestres fossiles dans le département du Puy-de-Dôme. *Annales scientifiques, littéraires et industrielles de l'Auvergne* 16: 402–439.

Breuning S. von 1924. Beiträge zur Stammesgeschichte der Rhinocerotidae. *Verhandlungen der Zoologisch-Botanischen Gesellschaft in Wien* 73: 5–46.

Brunet M. 1970. Villebramar (Lot-et-Garonne): très important gisement de vertébrés Stampien inférieur du Bassin d'Aquitaine. *Comptes rendus hebdomadaires des séances de l'Académie des sciences. Série D, Sciences naturelles* 270: 2535–2538.

Brunet M. 1977. Les mammifères et le problème de la limite Eocène–Oligocène en Europe. *Geobios* 10: 11–27. https://doi.org/10.1016/S0016-6995(77)80003-X

Brunet M. 1979. *Les grands mammifères chefs de file de l'immigration Oligocène et le problème de la limite Eocène–Oligocène en Europe*. Fondation Singer-Polignac, Paris.

Brunet M. & Guth C. 1968. Découverte d'un crâne de Rhinocérotidé, *Ronzotherium filholi*, dans le stampien inférieur de Villebramar (Lot-et-Garonne). *Comptes rendus hebdomadaires des séances de l'Académie des sciences. Série D, Sciences naturelles* 266: 573–575.

Brunet M., Jehenne Y. & Ringeade M. 1977. Note préliminaire concernant la découverte d'une faune et d'une flore du niveau de Ronzon dans l'Oligocène inférieur du Bassin d'Aquitaine. *Geobios* 10 (1): 109–112. https://doi.org/10.1016/S0016-6995(77)80057-0

Brunet M., Hugueney M. & Jehenne Y. 1981. Cournon-les Souméroux: Un nouveau site a vertébrés d'auvergne; Sa place parmi les faunes de l'Oligocène supérieur d'Europe. *Geobios* 14 (3): 323–359. https://doi.org/10.1016/S0016-6995(81)80179-9

Cerdeño E. 1993. Étude sur *Diaceratherium aurelianense* et *Brachypotherium brachypus* (Rhinocerotidae, Mammalia) du Miocene moyen de France. *Bulletin – Muséum national d'histoire naturelle Section C: Sciences de la Terre* 15 (1–4): 25–77.

Cerdeño E. 1995. Cladistic analysis of the family Rhinocerotidae (Perissodactyla). *American Museum Novitates* 3143: 1–25.

Codrea V. 2000. *Rinoceri și tapiri terțiari din România*. Presa Universitara Clujeana, Cluj-Napoca.

Codrea V. & Şuraru N. 1989. On '*Cadurcodon*' *zimborensis* sp. nov., an amynodontid from the Zimbor Strata at Zimbor, Salaj district (NW Transylvanian Basin). *In*: *The Oligocene from the Transylvanian Basin*: 319–338. (Univ. Cluj-Napoca).

Costeur L. & Guérin C. 2001. Les pistes et empreintes de mammifères de l'Oligocène ancien de Viens (Vaucluse). *Courrier scientifique du Parc naturel régional du Luberon* 5: 74–89.

Croizet J.B. 1841. Travaux et découvertes paléontologiques dans les terrains tertiaires lacustres de l'Auvergne. *Congrès scientifique de France* 9 (1): 78–82.

Crusafont Pairó M. 1967. Nuevos datos sobre la edad de los sedimentos terciarios de la zona de Utrillas-Montalbán. *Acta geológica hispánica* 2 (5): 115–116.

Dashzeveg D. 1991. Hyracodontids and Rhinocerotids (Mammalia, Perissodactyla, Rhinocerotoidea) from the Paleogene of Mongolia. *Palaeovertebrata* 21 (1–2): 1–84.

Deninger K. 1903. *Ronzotherium Reichenaui* aus dem Oligocän Ton Weinheim bei Alzey. *Zeitschrift der Deutschen Geologischen Gesellschaft* 55: 93–97.

Depéret C. & Douxami H. 1902. Les vertébrés Oligocènes de Pyrimont-Challonges (Savoie). *Mémoires de la Société paléontologique de la Suisse* 29: 11–90.

Duranthon F. 1990. *Étude paléontologique (Rongeurs, Anthracothéridés, Rhinocérotidés) de la Molasse toulousaine (Oligo–Miocène). Biostratigraphie et implications géodynamiques*. Ecole Pratique des Hautes Etudes, Paris.

Filhol H. 1877. Recherches sur les phosphorites du Quercy. *Annales des Sciences géologiques*. 8 (1): 1–340.

Filhol H. 1881. Etude des mammifères fossiles de Ronzon (Haute-Loire). *Annales des Sciences géologiques.* 12: 1–270.

Fortelius M. & Kappelman J. 1993. The largest land mammal ever imagined. *Zoological Journal of the Linnean Society* 108 (1): 85–101. https://doi.org/10.1111/j.1096-3642.1993.tb02560.x

Gignoux M. 1928. Sur la découverte d'un Rhinocéridé (*Acerotherium* cf. *filholi*, Osborn) dans les couches pétrolifères de Pechelbronn (Bas-Rhin). *Bulletin du Service de la carte géologique d'Alsace et de Lorraine* 1 (3): 145–152. https://doi.org/10.3406/sgeol.1928.1092

Ginsburg L. 1969. Une faune de Mammifères terrestres dans le Stampien marin d'Etampes (Essonne). *Comptes rendus hebdomadaires des séances de l'Académie des sciences. Série D, Sciences naturelles* 268: 1266–1268.

Ginsburg L. & Hugueney M. 1987. Les mammifères terrestres des sables stampiens du Bassin de Paris. *Annales de Paléontologie* 73 (2): 83–134.

Guérin C. 1989. La famille des Rhinocerotidae (Mammalia, Perissodactyla): systématique, histoire, évolution, paléoécologie. *Cranium* 6 (2): 3–13.

Heissig K. 1969. *Die Rhinocerotidae (Mammalia) aus der oberoligozänen Spaltenfüllung von Gaimersheim bei Ingolstadt in Bayern und ihre phylogenetische Stellung.* Abhandlungen der Bayerischen Akademie der Wissenschaften, Mathematisch-Naturwissenschaftliche Klasse 138. Bavarian Academy of Sciences, Munich.

Heissig K. 1978. Fossilführende Spaltenfüllungen Süddeutschlands und die Ökologie ihrer oligozänen Huftiere. *Mitteilungen der Bayerischen Staatssammlung für Paläontologie und historische Geologie* 18: 237–288.

Jame C., Tissier J., Maridet O. & Becker D. 2019. Early Agenian rhinocerotids from Wischberg (Canton Bern, Switzerland) and clarification of the systematics of the genus *Diaceratherium*. *PeerJ* 7: e7517. https://doi.org/10.7717/peerj.7517

Jehenne Y. & Brunet M. 1992. Intérêt biochronologique de quelques grands mammifères ongulés de l'Eocène supérieur et de l'Oligocène d'Europe. *Geobios* 25 (14): 201–206. https://doi.org/10.1016/S0016-6995(06)80329-3

Jenny F. 1905. Fossilreiche Oligocänablagerungen am Südhang des Blauen (Juragebirge). *Verhandlungen der Naturforschenden Gesellschaft in Basel* 18 (1): 119–130.

Kafka J. 1913. Rezente und Fossile Huftiere Böhmens. (Ungulata.). *Archiv für naturwissenschaftliche Landesdurchforschung von Böhmen* 14 (5): 1–85.

Koch A. 1911. Rhinoceriden-Reste aus den mitteloligocenen Schichten der Gegend von Kolozsvár. *Annales Historico-Naturales Musei Nationalis Hungarici* 9 (2): 371–387.

Kretzoi M. 1940. Alttertiäre Perissodactylen aus Ungarn. *Annales Musei Nationalis Hungarici* 33: 87–99.

Landesque 1888. Sur le Calcaire à *Palaeotherium* de l'Agenais et du Périgord. *Bulletin de la Societe géologique de France* 17: 16–37.

Lavocat R. 1951. *Révision de la Faune des Mammifères oligocènes d'Auvergne et du Velay*. Sciences et Avenir, Paris.

Lucas P., Constantino P., Wood B. & Lawn B. 2008. Dental enamel as a dietary indicator in mammals. *BioEssays* 30 (4): 374–385. https://doi.org/10.1002/bies.20729

Lydekker R. 1886. *Catalogue of the Fossil Mammalia in the British Museum (Natural History). Part III*. Printed by order of the Trustees, London.

Mayden R.L. 1997. A hierarchy of species concepts: the denouement in the saga of the species problem. *In*: Claridge M.F., Dawah H.A. & Wilson M.R. (eds) *Species. The Units of Biodiversity*: 381–424. Chapman and Hall, London.

McKitrick M.C. & Zink R.M. 1988. Species concepts in ornithology. *The Condor* 90 (1): 1–14. https://doi.org/10.2307/1368426

Mennecart B., Scherler L., Hiard F., Becker D. & Berger J.-P. 2012. Large mammals from Rickenbach (Switzerland, reference locality MP29, Late Oligocene): biostratigraphic and palaeoenvironmental implications. *Swiss Journal of Palaeontology* 131 (1): 161–181. https://doi.org/10.1007/s13358-011-0031-6

Ménouret B. & Guérin C. 2009. *Diaceratherium massiliae* nov. sp. des argiles oligocènes de Saint-André et Saint-Henri à Marseille et de Les Milles près d'Aix-en-Provence (SE de la France), premier grand Rhinocerotidae brachypode européen. *Geobios* 42 (3): 293–327. https://doi.org/10.1016/j.geobios.2008.10.009

Ménouret B., Châteauneuf J.-J., Nury D. & Peigné S. 2015. Aubenas-les-Alpes, a forgotten Oligocene mammalian site in Provence (S-E France). Part I – Carnivora, Perissodactyla and Microflora. *Annales de Paléontologie* 101: 241–250. https://doi.org/10.1016/j.annpal.2015.06.002

Mermier E. 1895. Sur la découverte d'une nouvelle espèce d'*Acerotherium* dans la mollasse burdigalienne du Royans. *Annales de la Société linnéenne de Lyon* 42 (1): 163–190. https://doi.org/10.3406/linly.1895.4058

Michel P. 1983. *Contribution à l'étude des rhinocérotidés oligocènes (La Milloque; Thézels; Puy de Vaurs)*. Université de Poitiers, Poitiers.

Mills J.R.E. 1967. Development of the protocone during the Mesozoic. *Journal of Dental Research* 46 (5): 787–791. https://doi.org/10.1177/00220345670460053101

Osborn H.F. 1900. Phylogeny of the rhinoceroses of Europe. *Bulletin of the American Museum of Natural History* 13: 229–267.

Pavlov M. 1892. Etudes sur l'histoire paléontologique des Ongulés. — VI. Les Rhinoceridae de la Russie et le développement des Rhinoceridae en général. (Avec 3 pl.). *Bulletin de la Société impériale des Naturalistes de Moscou* 6: 137–221.

Pictet F.J. 1853. *Traité de paléontologie, ou histoire naturelle des animaux fossiles considérés dans leurs rapports zoologiques et géologiques – Seconde édition – Tome Premier*. J.-B. Baillière, libraire de l'Académie royale de Médecine, Paris. https://doi.org/10.5962/bhl.title.13903

Prothero D.R. 2005. *The Evolution of North American Rhinoceroses*. Cambridge University Press, Cambridge, UK.

Queiroz K. de. 2005. A unified concept of species and its consequences for the future of taxonomy. *Proceedings of the California Academy of Sciences* 56 (18): 196–215.

Queiroz K. de. 2007. Species concepts and species delimitation. *Systematic Biology* 56 (6): 879–886. https://doi.org/10.1080/10635150701701083

Radulescu C. & Samson P. 1989. Oligocene mammals from Romania. *In*: *The Oligocene from the Transylvanian Basin, Romania*: 301–312. University of Cluj-Napoca, Cluj-Napoca.

Répelin J. 1917. Études paléontologiques dans le sud-ouest de la France (Mammiféres): les rhinocérotidés de l'aquitanien supérieur de l'Agenais (Laugnac). *Annales du Musée d'histoire naturelle de Marseille* 16: 1–45.

Roman F. 1910. Sur les Rhinocéridés de l'Oligocène d'Europe et leur filiation. *Comptes rendus hebdomadaires des séances de l'Académie des Sciences* 150: 1558–1560.

Roman F. 1912a. Les Rhinocéridés de l'Oligocène d'Europe. *Archives du Muséum d'histoire naturelle de Lyon* 11: 1–92.

Roman F 1912b. Sur un *Acerotherium* des Collections de l'Université de Grenoble et sur les Mammifères du Stampien des environs de l'Isle-sur-Sorgues (Vaucluse). *Annales de l'Université de Grenoble*: 359–368.

Russell D.E., Hartenberger J.-L., Pomerol C., Sen, S., Schmidt-Kittler N. & Vianey-Liaud M. 1982. Mammals and stratigraphy: the Paleogene of Europe. *Palaeovertebrata Mémoire extraordinaire 1982*: 1–77.

Santafé Llopis J. 1978. Revisión de los Rinocerótidos miocénicos del Vallès-Penedés. *Acta geológica hispánica* 13 (2): 43–45.

Schlosser M. 1902. Beiträge zur Kenntnis der Säugethierreste aus den süddeutschen Bohnerzen. *Geologische und Palæontologische Abhandlungen* 5 (9): 117–258.

Scotese C.R. 2016. PALEOMAP PaleoAtlas for GPlates and the PaleoData Plotter Program, PALEOMAP Project. https://doi.org/10.1130/abs/2016NC-275387

Short R.A., Wallace S.C. & Emmert L.G. 2019. A new species of *Teleoceras* (Mammalia, Rhinocerotidae) from the Late Hemphillian of Tennessee. *Florida Museum of Natural History Bulletin* 56 (5): 183–260.

Sorenson M.D. & Franzosan E.A. 2007. TreeRot, version 3. Available from http://people.bu.edu/msoren/TreeRot.html [accessed 5 May 2021].

Spillmann F. 1969. Neue Rhinocerothiden aus den Oligozänen Sanden des Linzer Beckens. *Jahrbuch des Oberösterreichischen Musealvereines* 114: 201–254.

Stehlin H.G. 1903. Ueber die Grenze zwischen Oligocaen und Miocaen in der Schweizer Molasse. *Eclogae Geologicae Helvetiae* 7 (4): 360–365.

Stehlin H.G. 1909. Remarques sur les faunules de Mammifères des couches éocènes et oligocènes du Bassin de Paris. *Bulletin de la Société géologique de France* 4 (9): 488–520.

Stehlin H.G. 1914. Übersicht über die Säugetiere der schweizerischen Molasseformation, ihre Fundorte und ihre stratigraphische Verbreitung. *Verhandlungen der Naturforschenden Gesellschaft in Basel* 25: 179–202.

Swofford D.L. 2002. PAUP*. Phylogenetic Analysis Using Parsimony (*and other methods). Version 4. Available from https://paup.phylosolutions.com [accessed 5 May 2021].

Thomas P. 1867. Note sur une mâchoire inférieure de *Rhinoceros* de l'Eocène supérieur du Tarn. *Bulletin de la Société géologique de France, Série 2* 24: 235–245.

Tissier J., Becker D., Codrea V., Costeur L., Fărcaş C., Solomon A., Venczel M. & Maridet O. 2018. New data on Amynodontidae (Mammalia, Perissodactyla) from Eastern Europe: Phylogenetic and palaeobiogeographic implications around the Eocene–Oligocene transition. *PLoS ONE* 13 (4): e0193774. https://doi.org/10.1371/journal.pone.0193774

Tissier J., Antoine P.-O. & Becker D. 2020. New material of *Epiaceratherium* and a new species of *Mesaceratherium* clear up the phylogeny of early Rhinocerotidae (Perissodactyla). *Royal Society Open Science* 7 (7): 200633. https://doi.org/10.1098/rsos.200633

Tissier J., Geiger-Schütz P., Flückiger P.F. & Becker D. 2021. Neue Erkenntnisse über die Nashorn-Funde von Rickenbach (SO) (Oberes Oligozän, Kanton Solothurn, Schweiz) aus der Sammlung des Naturmuseums Olten. *Naturforschende Gesellschaft des Kantons Solothurn* 44: 26–51.

Tsubamoto T. 2014. Estimating body mass from the astragalus in mammals. *Acta Palaeontologica Polonica* 59 (2): 259–265. https://doi.org/10.4202/app.2011.0067

Uhlig U. 1996. Erstfund eines juvenilen Unterkiefers von *Epiaceratherium bolcense* Abel, 1910 (Rhinocerotidae, Mammalia) aus dem Unteroligozän von Monteviale (Italien). *Mitteilungen der Bayerischen Staatssammlung für Paläontologie und historische Geologie* 36: 135–144.

Uhlig U. 1999a. Paleobiogeography of some Paleogene Rhinocerotoids (Mammalia) in Europe. *Acta Palaeontologica Romaniae* 2: 477–481.

Uhlig U. 1999b. *Die Rhinocerotoidea (Mammalia) aus der unteroligozänen Spaltenfüllung Möhren 13 bei Treuchtlingen in Bayern*. Abhandlungen der Bayerischen Akademie der Wissenschaften, Neue Folge 170. Bavarian Academy of Sciences, Munich.

Wang H., Bai B., Meng J. & Wang Y. 2016. Earliest known unequivocal rhinocerotoid sheds new light on the origin of Giant Rhinos and phylogeny of early rhinocerotoids. *Scientific Reports* 6: 39607. https://doi.org/10.1038/srep39607

Wood H.E. 1927. Some early Tertiary rhinoceroses and hyracodonts. *Bulletins of American Paleontology* 13 (50): 165–249. Available from https://www.biodiversitylibrary.org/page/30374668 [accessed 4 May 2021].

Wood H.E. 1929. *Prohyracodon orientale* Koch, the oldest known true rhinoceros. *American Museum Novitates* 395: 1–7.

Supp. file 1. Measurements in mm of dental specimens of *Ronzotherium* Aymard, 1854.
https://doi.org/10.5852/ejt.2021.753.1389.4387

Supp. file 2. Measurements in mm of postcranial specimens of *Ronzotherium* Aymard, 1854. https://doi.org/10.5852/ejt.2021.753.1389.4389

Supp. file 3. Data matrix of 288 morphological characters in NEXUS format for Mesquite with the two parsimonious trees. https://doi.org/10.5852/ejt.2021.753.1389.4391

Supp. file 4. List of occurrences of *Ronzotherium* Aymard, 1854, with their age and corresponding number for Fig. 27. https://doi.org/10.5852/ejt.2021.753.1389.4393

Supp. file 5. Body mass estimates of *Ronzotherium* Aymard, 1854 in kg, estimated from the equations for Rhinocerotidae Owen, 1845 of Fortelius & Kappelman (1993: appendix 1) based on cranial, dental, humeral, radial, femoral and tibial measurements, as well as equations for astragalar measurements (Li1, Ar1 and Ar3) of Tsubamoto (2014). https://doi.org/10.5852/ejt.2021.753.1389.4395

Appendix

Comparative material

Diaceratherium tomerdingense Dietrich, 1931
(5 specimens)

GERMANY – **Tomerdingen** • 1 humerus and radius; SMNS-16154 • 1 lunate; SMNS-16157c • 1 pyramidal; SMNS-16157d • 1 unciform; SMNS-16157e • 1 McIV; SMNS-16155b.

Diaceratherium lamilloquense Michel in Brunet, De Bonis & Michel, 1987
(5 specimens)

FRANCE – **La Milloque** • 1 humerus; NMB-L.M.429.

FRANCE – **Castelmaurou** • 1 radius; UM CAM-22 • 1 lunate; TLM.PAL.2014.0.2571 • 1 cuboid; TLM.PAL.2014.0.2563 • 1 MtIII; TLM.PAL.2014.0.2564.

Diaceratherium aginense (Répelin, 1917)
(7 specimens)

FRANCE – **Laugnac** • 1 scaphoid; MHNM.1996.17.94 • 1 lunate; MHNM.1996.17.21 • 1 pyramidal; MHNM.1996.17.20 • 1 unciform; MHNM.1996.17.98 • 3 astragali; MHNM.1996.17.41, MHNM.1996.17..55, MHNM.1996.17..77.

Diaceratherium aurelianense (Nouel, 1866)
(3 specimens)

FRANCE – **Neuville-aux-Bois** • 3 scaphoids; MHNB41.2018.0.282, -.384 and -.866.

Diaceratherium asphaltense (Depéret & Douxami, 1902)
(4 specimens)

FRANCE – **Pyrimont-Challonges** • 1 scaphoid, 1 lunate, 1 magnum; FSL-2130008 • McIV; FSL-213012 • 1 cuboid; FSL-213014 • 1 MtIII; FSL-213016.

Diaceratherium lemanense (Pomel, 1853)
(2 specimens)

FRANCE – **Gannat** • 1 hand; MNHN-LIM-598 • 1 astragalus; NMB-Gn-158.